2011

An Investigation of Surface Engineering Techniques to Minimize Wear of Thermoplastic Injection Mold Tooling

Tyler Skiba
Lehigh University

An Investigation of Surface Engineering Techniques to Minimize Wear of Thermoplastic Injection Mold Tooling

Tyler J. Skiba

Presented to the Graduate and Research Committee
of Lehigh University
in Candidacy for the Degree of
Master of Science
in
Mechanical Engineering and Mechanics

Lehigh University
Bethlehem, Pennsylvania
May 2011

CERTIFICATE OF APPROVAL

Thesis is accepted and approved in partial fulfillment of the requirements for the Master of Science in Mechanical Engineering and Mechanics.

An Investigation of Surface Engineering Techniques to Minimize Wear of Thermoplastic Injection Mold Tooling

Tyler J. Skiba

_____
Date Approved

_____

Dr. John P. Coulter, Dissertation Advisor and Committee Chairman
Associate Dean of P.C. Rossin College of Engineering Department of Mechanical Engineering and Mechanics

_____

Dr. Gary Harlow
Department Chair
Mechanical Engineering and Mechanics

Table of Figures

Table of Contents

Acknowledgments

First and foremost I would like to acknowledge my advisor John Coulter, Ph.D. for his valuable advice and insight into my research, as well as his continued support of me as graduate student. He is truly great advisor and mentor providing me with great insight into the world of research, graduate studies, career development, and life. I would also like to acknowledge the industrial partner in this research, TE Connectivity, and all of their staff that have been involved in my research, especially Aleksandar Angelov, Ph.D. who was with me every step of the way throughout the entire thesis providing excellent engineering insight and expertise.

Additionally, I would like to express my appreciation to the entire Manufacturing Science Laboratory at Lehigh University who continuously make every day enjoyable and generate fun working atmosphere. Burak Bekisli, Ph.D. who is the current postdoc in the Manufacturing Science Laboratory has been instrumental in the later work of my thesis and I owe him much gratitude. Other staff members at Lehigh University who contributed directly or indirectly to my research are Dick Towne, David Angstadt, Ph.D., and Herman Baader (R.I.P).

Sincere appreciation is extended to my family, especially my father, my grandparents, and my Aunt Lisa and Uncle Randy who have been a source of encouragement to me through my entire life and my graduate studies. Also, I want to express gratitude to my girlfriend, Randi, who always supports and

encourages me as well as tolerates me giving more attention at times to math equations and polymer processing than to her.

I would like to dedicate this work to my mother who passed away unexpectedly on April 13th, 2010. She is truly missed.

Abstract

Wear and corrosion are significant industrial issues resulting in high financial losses. With continuously increasing demands placed on thermoplastic injection molded products with regards to increased mechanical properties, leading to the incorporation of highly abrasive fillers and corrosive additives, and narrow dimensional tolerances, the surface engineering techniques to increase wear and corrosion resistance and improve the lifespan of mold tooling are of paramount concern. Proper surface engineering of expensive injection molds which can cost over 300,000 U.S.D. to fabricate is a technically challenging issue due to limitations imposed by the injection mold, coating deposition processes, the wide array of coating architectures, and coating suppliers available.

This study investigates three commercially supplied surface treatments for injection molding, electrodeposited chromium, and PVD TiAlN, and PVD/PACVD DLC containing an interfacial layer of chromium nitride. Testing methodologies for evaluation of the tribological performance of these surface treatments in the plastics processing environment have been developed and employed. Analysis of the pristine coatings is conducted to investigate porosity, surface roughness, inherent defects, frictional properties against nylon and polybutylene terephthalate, and elemental composition. Pin-on-plate wear testing is used to evaluate coating-metal sliding contact. Also, a novel test apparatus has been developed and fabricated to emulate the tribology of flowing polymer compounds

against mold tooling during the injection process. The dominant wear mechanisms of the chrome coating in exposure to the flowing polymer compound are micro-milling from the abrasive fillers in the compound and corrosive pitting, while the DLC coating exhibits localized delamination from the substrate material. TiAlN shows superior resistance to both corrosion and abrasion in addition to excellent adhesion to the substrate material. Results indicate that TiAlN is a promising candidate for replacement of electroplated chrome which has long been an industry standard.

Chapter 1 : Introduction

Injection molding is the dominant manufacturing process for high volume production of discrete, three-dimensional thermoplastic products. Sustainability in this industry requires the ability to produce enough products to generate the finances needed to cover the costs of the molding machine, overhead, personnel, and the mold tooling. Molds may actually be the largest upfront investment that a processing company must undergo, considering molds can cost anywhere from tens-of-thousands of dollars to hundreds-of-thousands of dollars depending on size and complexity. With increased throughput of polymers at elevated temperatures and high filler content, especially abrasive glass fibers, mold wear from abrasion, corrosion, and adhesion will continue to be a concern for the molding industry. This certainly applies to products with narrow dimensional tolerances because wear of the part forming cavities of a mold leads to unacceptable dimensional changes in the molded product. Such wear shortens the time interval for maintenance and retooling of worn components leading to increased downtime and reduced throughput and efficiency. Surface engineering of mold tooling with deposition of coatings possessing superior mechanical properties in comparison with the bulk mechanical properties of the mold steel shows much promise for reducing the overall wear and increasing the time intervals for mold maintenance. With the large variety of coatings and coating suppliers available, the decision of which coating will perform best for the given scenario is difficult to say the least. This

study examines appropriate test procedures to determine coating performance and evaluates three commercially available mold coatings.

1.1 Overview of Injection Molding Industry

The plastics industry accounts for one of the largest manufacturing sectors in the United States. According to the Society of the Plastics Industry, the plastics industry is the third largest manufacturing sector in the United States accounting for 374 billion dollars in annual shipments while directly employing over 1.1 million workers.[1] For thermoplastic resins, injection molding is a principal processing method. Thirty-three percent of all polymeric materials manufactured in the United States are processed via injection molding.[2] Injection molding is increasingly becoming the preferred processing method to fabricate complex, three-dimensional, value-added, thermoplastic parts.[3] Owing to the high initial capital investment in mold tooling, injection molding is typically reserved for high volume production of more than 10,000 parts per year, yet with ever-increasing mold capacities and relatively low cycle times, injection molding is a well suited process for mass production.

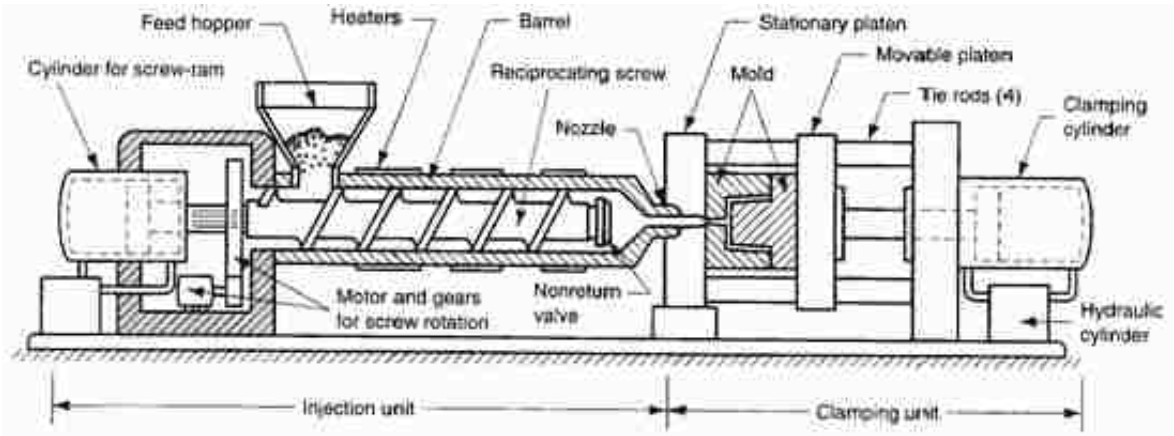

Figure 1-1: General Schematic of Injection Molding Machine [4]

Major components of a typical injection molding machine are presented in Figure 1-1. The injection molding process begins with material, usually in the form of small pellets, being fed into the hopper. When the material exits the hopper and enters the injection barrel, heat is acquired through two mechanisms: thermal conduction and shear heating. Thermal conduction occurs between the heater bands surrounding the injection barrel and the polymer inside. Shear heating is generated by the mechanical action of the screw compressing the material between flights of the screw. Both of these heating mechanisms serve to raise the polymer above its melting temperature changing the material from a visco-elastic solid to a visco-elastic fluid. A schematic of a typical reciprocating screw design is depicted in Figure 1-2. When material first enters the injection barrel, the resin is fed through the feed zone of the screw which has constant, relatively large flight depth. The purpose of this zone is to convey the material forward from the hopper and to begin the melting process. The next zone of the screw is a transition or compression zone in which the minor diameter gradually

increases, decreasing the feed depth. This zone compresses the material which removes air bubbles from the polymer and continues the melting process. Finally, the molten polymer flows into the metering zone which has the minimum feed depth with a constant, relatively large minor diameter. Since the flight depth is at a minimum, the polymer is forced into close proximity of the surrounding heater bands, which serves to complete the melting process as well as obtain a certain degree of homogeneity in the melt with regards to temperature distribution and, ultimately, viscosity. This homogeneity is desirable for consistency in the filling patterns during injection and in the molded part quality.

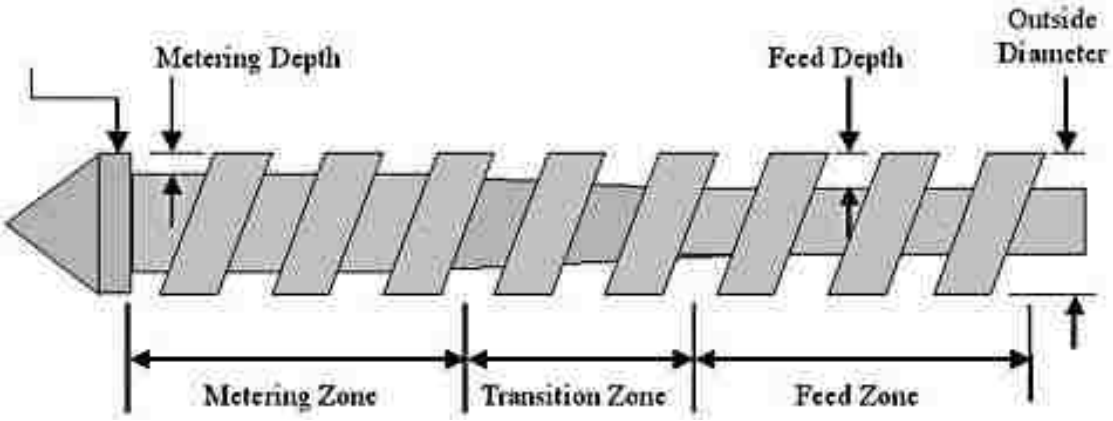

Figure 1-2: Typical configuration of reciprocating screw for injection molding [5]

As the polymer melt is conveyed forward in the injection barrel, the material passes through a check ring or a non-return valve and accumulates in front of the screw into a “shot”, refer to Figure 1-3. A “shot” refers to the amount of resin accumulated prior to injection which includes the material necessary to fill the mold cavity and melt delivery system, as well as, an additional cushion, which is held under pressure after injection to compensate for the volumetric

shrinkage that occurs inside the mold cavity as the material cools and solidifies. The check ring/non-return valve closes upon injection preventing back-flow of the shot into the screw flights, which enables a consistent volume of material to be injected each cycle. This again aids in cycle-to-cycle reproducibility.

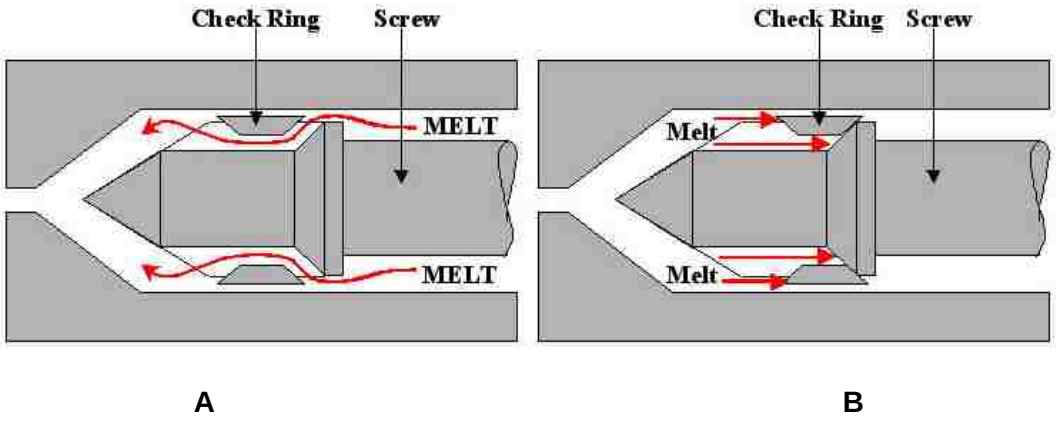

Figure 1-3: Check ring position (A) during shot accumulation and (B) during injection [5]

Hydraulic pressure is the most common method of developing the driving force necessary to force the viscous material into the mold cavity.[6] The hydraulic pressure is intensified to even greater pressures within the melt. The mechanism for this intensification is the sizing of the injection piston to screw diameter, known as an intensification ratio which typically range from 8:1 to 15:1.[7] Electromechanical driving forces can also be used to convey the molten resin.

Once the desired shot size has accumulated at the front of the screw, the injection cycle is ready to initiate. Typically, the injection phase fills the melt delivery system and approximately 95% of the mold cavities utilizing velocity

control, which can be either constant or profiled. While the mold cavities are filling, the air inside the mold cavities escapes through vents in the parting line of the mold, which is crucial to avoid dieseling or short shots due to trapped gas. 10%-15% of the shot volume remains as a cushion between the injection nozzle and the end of the screw, which is later utilized to compensate for volumetric shrinkage. As mentioned previously the injection phase is controlled by screw position and velocity, i.e. the screw translates from an initial position at a particular speed to another position, known as the transfer position, corresponding to the 95%-98% full cavities. When the screw reaches the transfer position, the injection phase terminates, and the machine transfers to pressure control.

Once the machine transfers to pressure control, also known as hold pressure or pack pressure, the packing phase initiates. The packing phase completes filling of the mold cavities. After the cavities are completely filled, the screw continues to apply pressure on the cushion to compensate for the volumetric shrinkage occurring within the cavities as the polymer cools. This prevents defects such as sink marks or voids in the final part. The desired pack pressure is specified as a machine parameter for an allotted period of time, known as hold time. The hold time normally corresponds to the gate freeze time. Gates are restrictive cavity entrances which introduce shear heat to the melt as it enters the cavity, effectively reducing viscosity and aiding filling. When the gate freezes, no more material can enter the cavity; thus, this is an appropriate time to terminate mold packing.

After the packing phase has ended, the screw rotates, acquiring the shot for the next cycle, and reciprocates to the specified shot size. During which time, the material remains in the mold cavity to solidify for a specified cooling time. Once the cooling time elapses, the mold opens, and ejector pins are driven forward to remove the part from the mold. Screw revolution speed should be set to a value which enables the screw to reciprocate to the shot size moments before the mold opens and ejects the part. This minimizes residence time of the polymer melt within the shot, which will provide more uniform thermal distributions, corresponding to more uniform viscosity, and prevents thermal degradation of material adjacent the barrel wall. Also, proper screw revolution speed insures that the next cycle is ready to initiate after part ejection which maximizes throughput and reduces cycle time.

The above process description applies to two-stage, velocity and pressure control, injection molding. Other process configurations exist, especially for specialized applications such as the molding of components with living hinges, but two-stage injection molding is a common method utilized.

1.2 Overview of Injection Molds for Polymer Processing

As previously noted, the molds for injection molding of polymer products are perhaps the largest upfront expense that a molding company must incur. These molds are nearly always custom designed and built.[7] A great variety of mold styles and designs exists. Molds can have a single part forming cavity or up to hundreds of part forming cavities. Family molds enable the molding of

different components simultaneously within a single cycle and mold. Modular designs are utilized to permit the exchange of different mold inserts to manufacture different parts within the same base mold. Most commonly, molds are custom designed and fabricated to produce single part geometries whether it is in single or multi-cavity tooling. [7]

Molds must be designed and built to perform a multitude of functions. The primary function of the mold is to shape the molten polymer into the desired size and shape via cavity and core geometry, but to accomplish this successfully many other factors need to be considered and addressed. Firstly, the polymer melt needs a passage to transport from the barrel of the injection molding machine to the part forming core and cavity. This is known as a melt delivery system which typically consists of four major components: sprue, cold slug well, runner, and gate. Figure 1-4 depicts a typical configuration for a two-plate cold runner mold with four part forming cavities producing disk shaped plastic parts. Upon injection, the molten polymer exits the nozzle of the injection barrel and enters the mold through the sprue. Flowing polymer then enters the primary or main runner and proceeds into the tertiary or branch runner. Restrictive gates are utilized as entrances to the part forming cavities, which aid in mold filling from high shear rates and separation of part from the melt delivery system. Often a cold slug of material will form in the nozzle between injection cycles. This cold slug is the first material to exit the injection cylinder. The cold slug well collects any cold slugs exiting the injection cylinder to prevent these from entering the

runner system eventually blocking the flow of polymer at the gate or entering the part forming cavity.

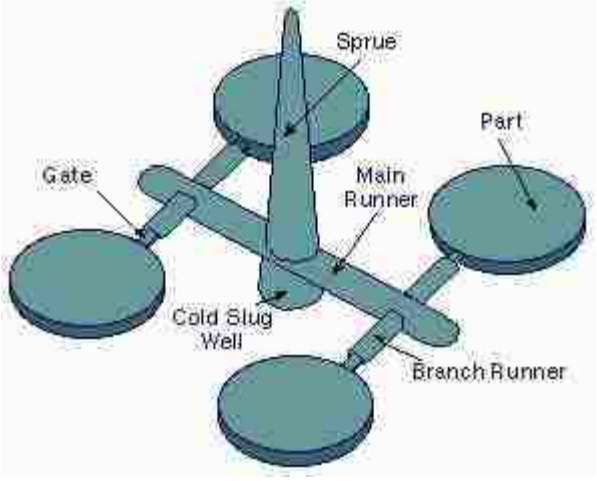

Figure 1-4: Typical Melt Delivery System for Two-Plate Cold Runner Mold with Four Cavities [8]

Generally, molds can be divided into two primary categories based on the melt delivery architecture. These categories are “cold runner” and “hot runner” molds. Cold runner molds are those in which the melt delivery system is cooled, solidified, and ejected along with the molded component each cycle.[7] Currently, approximately 70% of molds utilized in industry are cold runner type molds.[7] Hot runner mold are typically more complex and described by the principal components of their melt delivery system, namely their manifolds and drops.[7] In hot runner molds, the entire melt delivery system or certain components of the melt delivery system remain heated or insulated from cooling and solidification, which reduces scrap material. Classification of molds can further be categorized by the overall design configuration.

Cold runner molds are usually of either a two-plate or a three-plate configuration. These two configurations refer to the minimum number of mold

plates necessary to mold, solidify, and eject the part and melt delivery system.[6] Two-plate cold runner molds are the simplest and least costly molds to fabricate, as well as the easiest to operate. Usually in a two-plate mold, the primary and tertiary runners are positioned on the primary parting plane where the molded part is formed and ejected from the mold. The two-plate cold runner mold design presented in Figure 1-5 depicts a cavity offset from the sprue which permits the gate location to be at the outside perimeter of the part. If the single cavity were to be positioned centered with the sprue, the sprue could lead directly into the part forming cavity eliminating the need for a runner on the primary parting plane. With multi-cavity two plate cold runner molds, typically the cavities must be offset from the center line of the sprue and fed by primary/tertiary runners, with gating near the perimeter of the part. Limitations of two-plate cold runner molds include: limited gating options for multi-cavity tooling, which may cause core deflection, gas traps, or undesirable weld lines; waste material in the form of the melt delivery system which must be sold or reground; and potentially increased cycle time, if the cycle time is dictated by the cooling and solidification of the sprue and runner.[7]

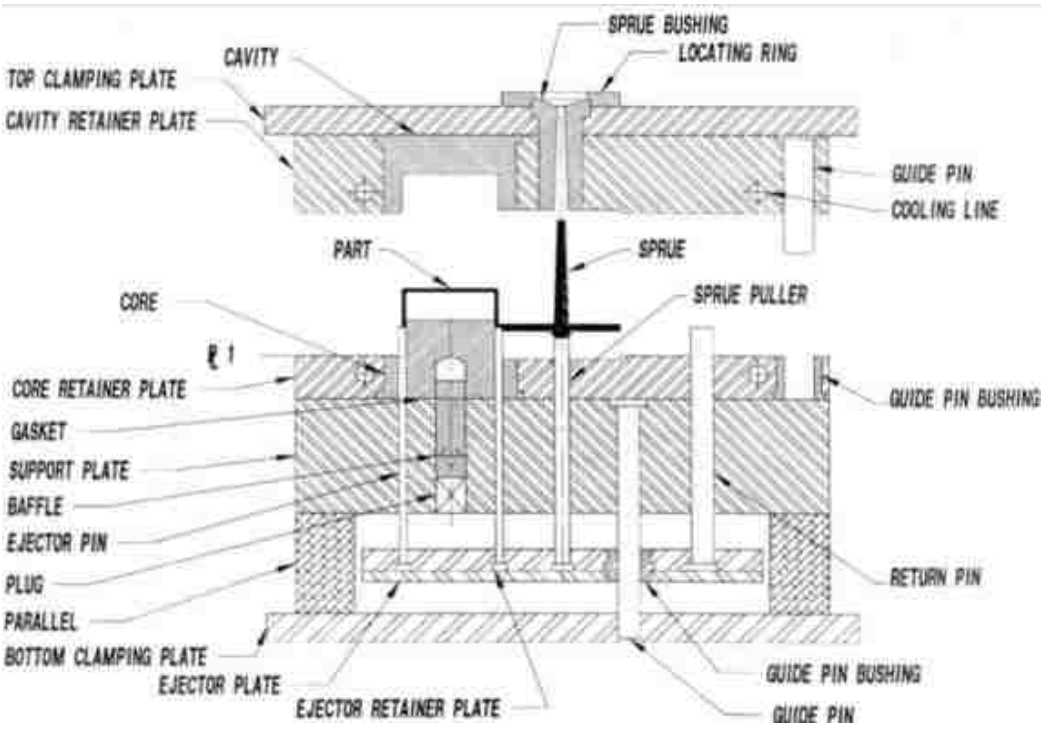

Figure 1-5: Cross-Sectional View of a Two-Plate Cold Runner Mold Design (Mold Open) [7][9]

Three-plate cold runner molds are more expensive to design and fabricate and more complex to operate than two-plate cold runner molds, yet the three-plate cold runner mold is generally cheaper to fabricate than hot runner molds. A general cross-sectional schematic of a three-plate cold runner mold is presented in Figure 1-6. The major advantage of the three-plate design is flexibility in choice of the gating location. Typically, two-plate designs are limited to gating around the perimeter the mold cavity on the parting plane; whereas, three-plate designs permit the freedom to gate the cavity nearly anywhere.

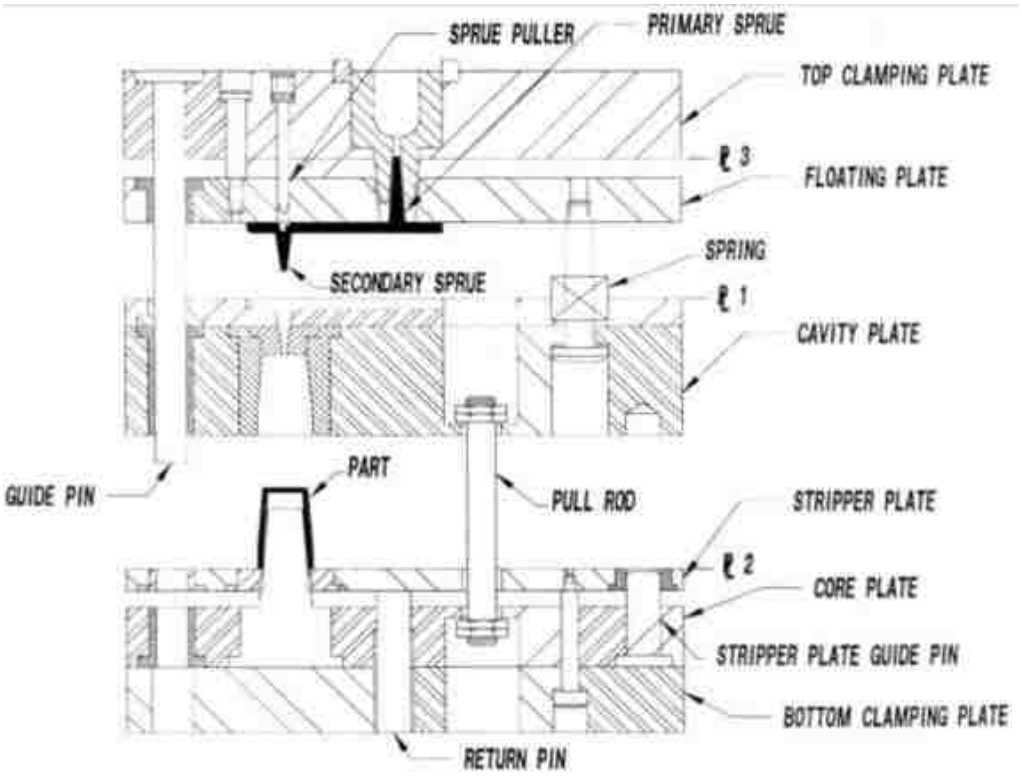

Figure 1-6: Cross-Sectional View of a Three-Plate Cold Runner Mold Design (Mold Open) [7] [9]

Hot-runner molds, as the name implies, are molds in which the melt delivery system remains in a molten state during processing. The key advantage of such a system is the elimination the scrap material considering that the melt delivery system does not have to be solidified and ejected each molding cycle, reducing material cost and eliminating the need for regrinding or disposing of the sprue and runners. Hot-runner molds are more costly to fabricate due to the costs associated with the design, fabrication, and control of the system needed to keep the runner at the melting temperature of the polymer. In general, hot runner molds are similar in design to three-plate cold runner molds. [7] The melt

delivery system consists of manifolds and drops which are either internally or externally heated or insulated from the mold cooling system.[7]

1.3 Surface Engineering of Mold Steel

Corrosion and wear caused by adhesion, abrasion, and erosion are major technical tribulations in modern industry resulting in significant financial losses.[10] These losses can effectively be reduced or eliminated through the use of various wear and corrosion resistant coatings, which provide improved mechanical properties at the surface compared to the bulk mechanical properties of the substrate. Since wear and corrosion typically occur on the surface of a given component or at the interface between moving components in contact, improving the surface properties is clearly advantageous.

Ever since the advent of injection molding, wear and corrosion on the surface of mold tooling and machine components exposed to the polymer melt has been observable. Additionally, components in sliding metal-to-metal contact such as the interface of ejector pins or pneumatic slides and the mold block result in adhesive/abrasive wear. As the demands on the mechanical properties of engineering polymers have become more stringent in recent decades, the use of heavily reinforced polymers has seen a dramatic increase. Such reinforced polymers often contain high volume percentages of high hardness fillers, such as glass fibers and natural or synthetic minerals. Certainly, these high hardness fillers induce accelerated abrasive wear on the surfaces of the mold tooling exposed polymer melt injected at high velocities, often completely filling an empty

mold in less than one second. Additionally, other types of additives induce corrosion from decomposition by-products.[11] Some polymers, like polyvinyl chloride (PVC) and polycarbonate (PC), are inherently corrosive when processed. In the case of a combination mechanical and thermal stresses, superposition of abrasive and corrosive affects escalates the resulting wear synergistically. [11][12]

Wear of injection mold tooling leads to dimensional shifts in molded components over the production period. For injection molded parts with narrow dimensional tolerances, such a shift is unacceptable. Once a critical degree of wear has occurred to the surface of an injection mold, parts can no longer be produced within the required specifications. This leads to production downtime in which the injection mold must be removed from the molding press and undergo costly and timely repairs. Such repairs greatly increase the manufacturing cost, diminishing financial gains.

Numerous commercially available surface treatments exist to improve wear resistance and extend the working life of an injection mold. Hard chrome electroplating has long been a trusted functional hard coating used to extend tool life. Electroplating is a simple, well-understood process able to be conducted at near ambient temperatures, yet as the science and technology of different coating systems are improving and maturing; those faced with the responsibility of specifying surface treatments are looking to alternative deposition techniques and chemical architectures for superior performance. Coating processes such as chemical vapor deposition (CVD) and physical vapor deposition (PVD) are

gaining attention in the injection molding industry. The classical versions of these processes, especially CVD, require excessive substrate temperatures during coating deposition, an impractical processing constraint due to possible distortion of the mold geometry. In recent decades, coating suppliers have realized the detriments of high deposition temperatures, and processes with lower temperatures are proliferating.

Titanium nitride (TiN), produced by PVD, has received the most attention and use as a functional hard coating. TiN is viewed as a relatively safe, low risk, all-purpose coating.[13] Possessing higher hardness and being chemically more inert than chrome and other bath plated materials, the benefits of TiN surface enhancements are clear.[13] TiN is also a rather lubricious coating providing superior release properties during demolding. Other PVD coatings receiving limited attention from the molding community are titanium carbonitride (TiCN), titanium aluminum nitride (TiAlN), chromium nitride (CrN), chromium carbide (CrC), zirconium nitride (ZrN), and diamond-like carbon (DLC) among others. Although many of these coatings have not attained wide-spread acceptance by the molding community, they are worthy of attention and indeed may be viable alternatives to the current coatings that industry is comfortable with employing. The coatings mentioned above certainly appear to be the dominant players in the world of functional hard PVD coatings, although an extremely large array of elemental designs is available, making proper coating selection a formidable challenge.

1.4 Purpose of Study

In essence, four factors dictate the degree of wear incurred during injection molding: the composition of the material being processed, the processing parameters, the design of the equipment and mold tooling, and lastly the selection of metals and surface treatments.[11][14] The last factor, surface treatments, is of concern for this study.

A significant amount of scientific research exists in the development of thin film deposition processes and parameters, coating characterization, and tribological evaluation of functional coatings for various applications, especially for the cutting tool industry. Unfortunately, research specifically directed toward the protection of mold tooling and the tribological evaluation of commercially available surface treatments subject to the rigors of the polymer processing environment is limited in scope. A well established fact is that wear mechanisms of a surface are a function of the tribological environment that surface is subjected to; hence, correlating results from one tribological environment to another, while expecting similar performance, is a recipe for failure. For example, a study conducted to evaluate the wear incurred by functional coatings on cutting tools in a milling process probably has limited relevance to the same coatings subject to flowing polymer compounds because the tribological environment is completely different. Armed with such limited knowledge on the tribological performance of surface treatments for injection molding, selection of the best mold coating is a considerable challenge. This challenge is further escalated by the overwhelming number of polymers, coating processes, coating

chemistries, and coating suppliers in addition to the limitations imposed by the injection mold itself.

The purpose of this study is to expand the scientific knowledge-base regarding surface engineering techniques applied to injection mold tooling. Additionally, practical testing methods have been developed to evaluate the tribological performance of coatings subject to the polymer processing environment. Evaluation includes three commercially supplied coatings; electrodeposited chrome, Oerlikon Balzers BALINIT® FUTURA NANO PVD TiAlN and Oerlikon Balzers BALINIT® DLC STAR, in their pristine and worn state. Additionally, key considerations and difficulties specific to surface treatments of thermoplastic injection molds are highlighted. The research included in this thesis constructs the groundwork for standard wear testing methods applicable to the injection molding industry and helps demystify the coating selection process.

Chapter 2 : Coating Processes for Increased Tool Life

2.1 Considerations for Surface Treatment of Injection Molds

Considering the high upfront capital investment in mold tooling, the financial feasibility of injection molding is directly related to the degree of tool wear incurred during the production period. Accordingly, the practice of depositing functional hard coatings on the surfaces of injection mold tooling has evolved into an industrial standard. In order to specify an adequate coating(s), mold designers need to consider many key factors.

Perhaps the most prominent consideration, depending on the dimensional requirements of the given mold, is the deposition temperature required for the given coating process. Most likely, surface treatment of the mold tooling is the final or near final step in the fabrication process prior to production. By the time the coating supplier receives the mold, the given corporation has already invested tens to hundreds of thousands of dollars in the associated fabrication costs. Deposition temperatures exceeding the tempering temperatures of the steel can result dimensional distortion as the crystal structure of the steel reorganizes and relieves internal stresses within the material. For molds with narrow dimensional specifications, distortion is intolerable. Moreover, as the steel undergoes heating the material hardness is permanently decreased, if heated above its original tempering temperature. Even with deposition of a high hardness coating, reducing the base material's hardness is undesirable because the surface properties have a dependence of the substrate's properties.

Considering the high compressive stresses the mold experiences during clamping and injection, a thin coating will likely crack and subsequently delaminate if the substrate possesses low hardness and deforms. Hence, deposition temperature and its potential implications should be carefully contemplated when specifying a surface treatment.

Another vital concern is the uniformity of the deposited coating. Some surface treatments provide a conformal coating with uniform thickness on complicated geometry, while others are line-of-sight processes, unable to uniformly coat complex three-dimensional geometry. Detailed areas like ribs, bosses, and blind holes are often problematic with line-of-sight processes because these features shadow areas of the substrate from the deposition source. Depending on the coating thickness, expected inhomogeneity, and dimensional tolerances of the mold; the mold may have to be specifically machined, prior to or after deposition, to account for the variance in coating thickness, especially with a relatively thick coating and a tightly toleranced mold.

Inevitably, mold coatings will not last forever; hence, mold coatings that are chemically strippable are preferred. Chemically strippable coatings can be removed in a relatively short period of time with little to no alteration to the substrate. Afterwards, the coating can be reapplied with minimal complications, yielding a mold in pristine condition; in contrast, mechanical stripping of coatings can be an invasive process which severely alters the substrate. Often mechanical stripping leads to timely and expensive operations to repair the mold to a condition conducive of quality, “in-specification” part production. Regular

monitoring of mold wear, especially areas prone to accelerated wear like gates and end of fill locations near mold vents, is recommended. The best approach is to remove the coating before the wear penetrates to the substrate because the substrate is less resistant to deterioration. Failure to cease production prior to substrate exposure can result in more extensive retooling operations with additional associated costs and production downtime.

Several other factors should be considered. Adhesion strength at the coating-substrate interface is also crucial. Some surface treatments inherently produce stronger adhesion than others. Without strong adhesion to the substrate the coating properties are irrelevant. Low friction coefficients against the polymeric compound of interest aid in demolding of the formed part and reduced wear during the demolding cycle. The coating needs to perform sufficiently well at the processing temperature of the polymer, retaining both corrosion and abrasion resistance. Also, depending on the tribological environment of a given mold component, realization of the optimal service life span for individual components can be obtained by individually selecting specific coatings for specific mold components; for example, cavity and core geometry (melt-polymer contact) likely will benefit more from certain coatings while cam actuated slides and guide pins (metal-metal contact) benefit more from other coatings

After considering all of the factors mentioned above, the two most perplexing issues are left to be addressed. The first issue is the number of available coating suppliers and which supplier should be selected. Unfortunately, sufficient comparative data does not exist to decipher which supplier provides the

best quality coating. Fortunately, the science of thin film deposition has matured to a point that numerous suppliers are able to produce thin films with reasonably comparable and repeatable properties. This decision is probably best determined from a corporate logistics point of view. The second issue is deciding the appropriate coating to use. Using the factors mentioned earlier in the chapter, at least the list of potential coatings and processes can be narrowed. Wear resistance in not a simple mechanical property. Rather, wear resistance is a function of the complex tribological environment for the specific application; for instance, superior tribological performance of “coating X” against “polymer compound Y” does not entail that “coating X” will also have superior performance against “polymer compound Z” because different polymers will have different wear mechanisms. Considering that more than 100,000 varieties of plastics exist [7] and the wide variety of surface treatments available, the likelihood of finding scientific data on the desired coating for the desired polymer compound is diminutive; therefore, it is beneficial for molding corporations to develop and implement coating evaluation procedures. Additionally, although the number of polymeric compounds is staggering, the scientific community, with continued investigation, hopefully can devise category schemes that begin to characteristically classify different groups of resin compounds based on their dominating wear mechanisms to stimulate more educated, science-based decisions in the surface treatment selection.

2.2 Electrodeposition

Electrodeposition, also known as electrochemical deposition and electroplating, is a well established process for altering the mechanical, chemical, and optical properties on the surface of a substrate by deposition of a thin layer of material, usually metallic. The driving force of this deposition process is an electrical current. During electrodeposition, the substrate to be plated is submerged in an electrolytic solution or bath. The substrate serves as the negatively charged cathode in an electrolytic cell, also containing a positively charged anode or multiple positively charged anodes. Anode(s) can either be composed of an inert material, permanent anode, or the material to be deposited onto the cathode, sacrificial anode.[15][16] In the case where the anode is chemically inert, the electrolytic solution contains positively charged ions of the metal to be deposited. Typically, the electrolytic solution also contains other additives to promote the deposition process and properties of the deposit.[17] When the power source or rectifier supplies current to the anode, the current is carried by the positively charged ions away from the anode to the cathode, causing a migration of positively charged metal ions to the free electrons on the surface of the cathode.[15] Electrolysis occurs at the cathode surface removing the metal ions from the electrolytic solution and depositing them onto the surface of the cathode.[15]

Deposition rate and thickness is typically dictated by exposure time in the bath and also by the applied potential to the anode which controls the flux of the metal ions. Electrodeposition can deposit coatings with virtually any desired

thickness, although typical thicknesses are under 100 μm. A major disadvantage of electrodeposition is that the geometric shape and contour of the cathode affects the thickness of the coating.[15] Ultimately for complex three-dimensional geometry like injection mold tooling, the coating thickness will be inhomogeneous. Variance in coating thickness results from different current densities based on the geometrical features. [15] For example, dc current will flow more densely to sharp exterior corners than less accessible recessed areas, resulting in thicker deposit on the sharp exterior corners. [15] Conformal anodes can be fabricated to aid in thickness uniformity, yet this increases lead time and cost of the coating process, proportional to the complexity of the mold.

Electrodeposited coatings are easily stripped from a substrate. Removal of the coating simply involves reversal of the electrolytic cell where the coated substrate becomes the anode. The ability to electrochemically strip the coating is extremely beneficial for injection mold tooling. When significant wear has accumulated on the surface of the injection mold, the mold coating can be stripped to its pre-coated condition. Afterwards, the mold can again undergo the electrodeposition process and be returned to a near pristine condition.

2.3 Autocatalytic Deposition

Autocatalytic deposition, more commonly known as electroless plating, is a purely chemical process for coating deposition that does not employ an electrical current. Like electroplating, autocatalytic plating is also a “wet” plating technique performed in electrolytic solution. Electroless plating involves an

autocatalytic redox reaction of metal ions on the surface of the substrate.[18] A full detail chemical description of this process is beyond the scope of this thesis, but is well documented in literature and books elsewhere. [19]

The use of autocatalytic deposition is especially relevant to this study because of the ability deposit a uniform coating thickness on a complex three-dimensional geometry. The thickness uniformity is derived from the purely chemical nature of the process as opposed to electrodeposition.[19] Homogenous thickness over complicated geometry makes this process a viable alternative in instances where the complexity of the substrate to be coated is not conducive to electroplating and physical vapor deposition. Chromium and nickel are two of the most widely applied coatings for enhanced tribological performance with autocatalytic deposition. Electroless nickel is superb corrosion barrier. This coating type is especially well suited for processing polymer compounds that are prone to corrosive out-gassing like PVC and compounds containing halogenated flame retardants. Electroless nickel could be used in conjunction with other deposition processes; for instance, the use of an electroless nickel undercoat and a Titanium Aluminum Nitride (TiAlN) overcoat would exploit both the high corrosion resistance of the nickel and the high abrasion resistance and hardness of the TiAlN provided that good adhesion strength exists between all interfaces. A drawback to electroless deposition is reduced hardness (i.e. reduced abrasion resistance) in comparison to many ceramic and metal nitride based coatings produced by physical and chemical

vapor deposition. Additionally the cost of producing these electroless coatings is five to ten times greater than their electroplated counterparts. [19]

2.4 Vapor Phase Techniques

Deposition of thin films via vapor phase techniques typically refers to one of two processes, chemical vapor deposition (CVD) or physical vapor deposition (PVD). Currently these deposition processes do not dominate the coating marketplace, yet in the past few decades, interest in using these vapor phase deposition techniques has significantly increased.[20] CVD and PVD processes have the ability to deposit a wide array of compound materials including: metallic, alloyed, ceramic, and some organic (PVD) coatings. The characteristic coating thickness, density, and surface finish of both PVD and CVD are quite similar.[21] The key difference between these two deposition processes is that CVD involves the reaction of gaseous chemicals on the surface of the substrate to be coated, while PVD utilizes physical mechanisms to vaporize atoms from a source material and transport these atoms onto the substrate surface where condensation into a thin film occurs.

2.4.1 Chemical Vapor Deposition (CVD)

CVD underwent major technological advances in the period from 1960-1990 and is indeed considered to be a mature technology.[22] The phrase CVD has evolved over the years to encompass a variety of technologies which

developed from the initial concept of vaporizing a metallic source and employing chemical reactions at the surface of a substrate material resulting in the deposition of a thin film coating.[21]

Depicted in Figure 2-1 is a basic schematic of the CVD process. In general the CVD process consists of four stages. The initial stage involves the formulation of a reactant vapor, which followed by mass transport of this vapor into the reactor containing the substrate material to be coated. Inside the reactor the substrate is heated, and upon introduction of the gaseous reactant chemicals, chemical reactions between the substrate material and vapor occur resulting in coating deposition. The final stage is essentially the removal of the reaction by-products. Within the reactor, air pressure is maintained at or below atmospheric pressure.[21] The coatings produced via CVD contain few pores/defects and are characteristically thicker, with thickness ranging from 10μm to 1 mm, than those produced by PVD.[21]

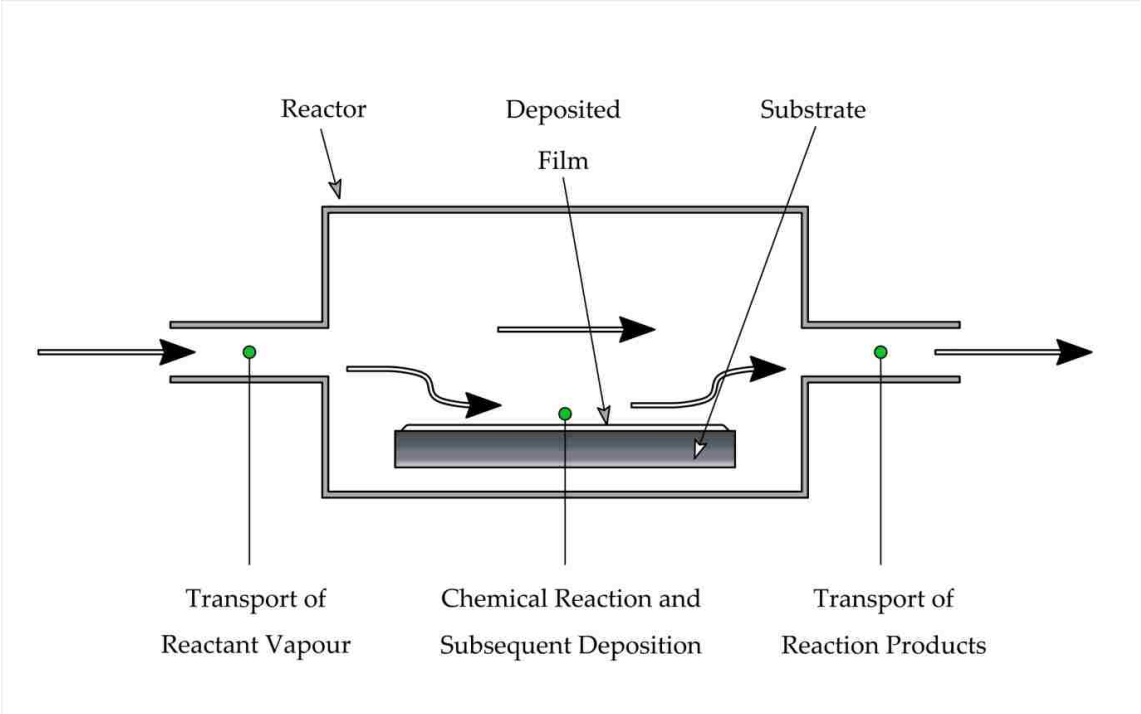

Figure 2-1: Schematic of CVD Process [21]

CVD has two principal advantages in comparison to PVD. The first advantage is that this coating process is conformal. Conformal coating processes can deposit coatings with uniform thickness even on complex three-dimensional geometry. Additionally, the chemical nature of this deposition technique necessitates chemical bonding to the substrate material granting greatly improved adhesive properties.

High temperatures within the reactor are necessary with classical CVD to facilitate reduction or decomposition of the reactant vapor, containing the desired deposition material.[20] CVD processes typically are conducted with temperatures in the range from 500-1200 °C, although higher temperatures are not uncommon.[23] For the application of interest, wear-resistant coatings, many nitrides, carbides, borides, silicides, and oxides are deposited with CVD, but

unfortunately the reactants normally require temperatures in excess of 1000 °C.[23] Such a thermal load is incompatible with many substrate materials; for example, 1000 °C exceeds the tempering/annealing temperature of H13 steel, a common tool steel used for fabrication of thermoplastic injection molds. For injection molded products with narrow dimensional tolerances, deposition temperatures above the annealing temperature of the tool steel is detrimental because dimensional integrity may be compromised yielding a mold incapable of producing parts within the dimensional specification window.

"The great improvements in PVD processes brought about by ionizing the reactive species prompted a similar approach in CVD where the introduction of a glow discharge further lowers reaction temperatures by many hundreds of degrees Celsius." [23] Plasma enhanced CVD (PECVD), also known as plasma assisted CVD (PACVD), is an adaption of classical CVD developed to reduce temperatures within the reactor, increasing the appeal of this deposition technique for substrates prone to dimensional distortion or other complications resulting from high thermal loads. The reduction in the required substrate temperature with PECVD is coupled with the need for significantly reduced operating pressure, consequently reducing the deposition rates [23] leading to increased batch processing times.

2.4.2 Physical Vapor Deposition (PVD)

Tool surface engineering via the use of PVD coatings has been an industrial reality since 1980.[10][24] The PVD process is a technique with the

capability to deposit a wide range of chemical compositions from the typical metallic coatings to ceramic and alloyed coatings.[25] Such flexibility in the chemical composition of PVD coatings is advantageous in that coating chemistries can be specifically tailored to provide the desired mechanical and wear/corrosion-resistant properties. For the application of wear and corrosion resistance, ceramic and metal nitride based PVD coatings are the most highly employed resulting from their high hardness and being relatively chemically inert.

PVD is a process in which a source material is vaporized and deposited onto a substrate material as a thin film. The basic sequence of steps in this process are as follows: 1) the source material (material to be deposited) is vaporized via physical means; 2) mass transport of the vaporized material occurs across a regions of low pressure within the deposition chamber; and 3) the vapor is condensed onto the substrate's surface in the form of a thin film. All of the PVD processes are reactive methods, in that the reactive species is vaporized subsequently reacted with a gas that is fed into the deposition chamber to form the desired compound.[24] Although many variations of the PVD process exist, all PVD processes can basically be classified into two categories based on the manner in which the source material is vaporized. In general, evaporation of the source material is either a thermal or non-thermal process.[26] Thermal vaporization techniques most commonly utilize resistive heating of the source material, heating with an electron-beam, or arc evaporation, while the method of non-thermal evaporation is accomplished via sputtering. Other subcategories of PVD processes are defined by the manner of plasma generation and also the

types of electrons, ions, or atom constituents of the plasma.[24] A diagram expressing the general classification of PVD techniques is shown below in Figure 2-2.

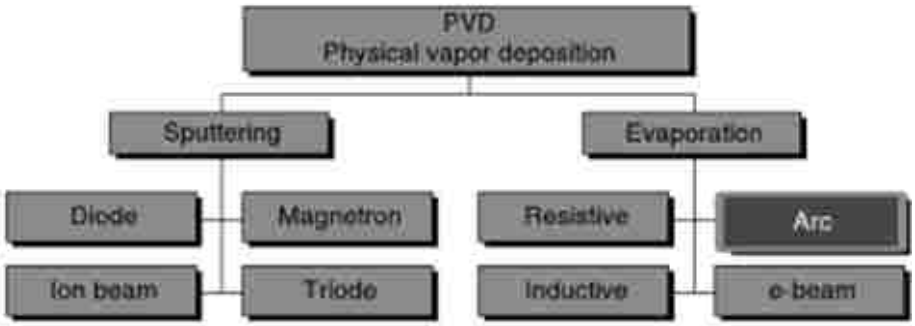

Figure 2-2: General Classification of PVD Techniques [27]

A major advantage of PVD over CVD is a much lower required substrate temperature during the deposition process. This is clearly advantageous for substrates sensitive to dimensional distortion at elevated temperatures, like expensive injection mold tooling.

PVD is a line-of-sight process. With line-of-sight coating deposition processes, achieving a uniform coating thickness on complex, three-dimensional geometry is generally not possible. Geometric shadowing effects of features blocking a direct line-of-sight to the source material lead to reduced coating thickness on such shadowed features such as the interior of a large aspect ratio blind-hole, where the hole depth is considerably larger than the hole diameter. Rotation of the substrate within the deposition chamber and the use of multiple vaporization sources can aid in homogenizing the thickness of a PVD coating.

2.4.2.1 Evaporation

Thermal evaporation of the source material to be deposited is predominantly realized by means of resistive heating, heating with an electron beam, or arc-evaporation. Vacuum evaporation using resistive heating is the most widely used and oldest method of thermal evaporation for PVD.[21]

Resistive heating is accomplished by passing and electrical current through the source material leading to evaporation of the source. Vacuum evaporation via resistive heating is the simplest PVD process, but certainly not the most versatile. Limitations exist on the solid precursor to be vaporized. Typically, evaporation of alloys can be problematic.[21] Considering that alloys are composed of two or more elements, the difficulties associated with resistive heating of alloyed materials stems from the different melting temperatures of the constituent elements. Additionally, source materials with high melting temperatures, above approximately 1000 °C, such as refractory metals and oxide compounds, require the use of a focused electron beam.[26] Resistive heating of such high melting temperature solid precursors results in undesired reactions between the melt and the resistance carrier, which has its own temperature limitations.[28] When using resistance heating, the vapor flux distribution has approximately a cosine(Θ) characteristic resulting in a inhomogeneous coating thickness on a planar substrate's surface, requiring either a relatively large distance between the substrate and source or suitable motion of the substrate. [28]

Electron-beam PVD (E-B PVD) uses a focused, high voltage electron beam as the heat source on the solid precursor to induce thermal evaporation. The source material is held in a water cooled crucible, and evaporation is again conducted in a high vacuum as with resistive heating. Virtually any material than can be vaporized through resistance heating can also be vaporized via electron-beam heating.[26] Relatively high deposition rates can be obtained using a high voltage electron beam, yet ionization of the evaporated reactive gases is limited due to the small ionization cross-section of a high voltage electron beam.[24] Additionally, multiple source materials can be simultaneously bombarded by focused electron beams, generating alloyed coatings from mixing vapor fluxes as depicted in Figure 2-3.[28] Motion of the substrate can be used to preferentially control the alloyed deposition composition in a multiple source system.[28]

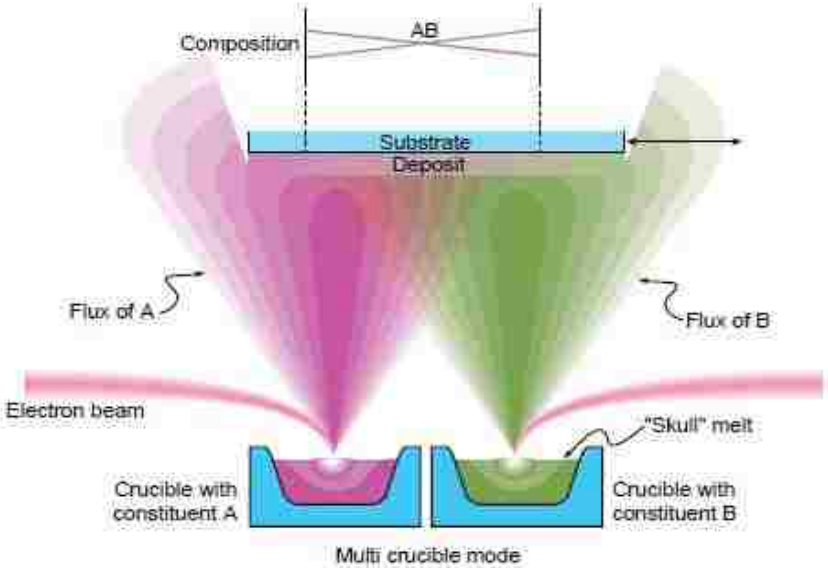

Figure 2-3: Schematic of Alloyed Coating Deposition by E-B PVD [28]

Another process for vaporizing the source material in PVD is known as arc evaporation. Cathodic arc evaporation is the dominant arc evaporation

technique. Cathodic arc evaporation utilizes a high-current density, low voltage electrical current generated between a cathode and an anode.[29] The electrical current can be applied continuously or pulsed. This process leads to localized surface heating of the cathode, known as a cathode spot, inducing melting, subsequent evaporation, and ionization of the cathode, which is the source material.[27] At the cathode spot, emission of ions of the cathode material and electrons transpires.[30] Cathodic arc evaporation generates high ionization and ion energy in the evaporated species, which is advantageous when introducing reactive gases. [29][31][32] A major disadvantage accompanying cathodic arc evaporation is the coemission of macro-droplets from the cathode spot.[30][32] These macro-droplets adhere to the coating that is being deposited, roughening the surface and deteriorating the coating uniformity and exfoliation.[32] Numerous methods have been developed to address this issue by either suppressing droplet generation and emission or using preventing the transport of the macro-droplet to the substrate.[32] Filtered cathodic arc deposition is of the later variety and seemingly is the most dominant method of controlling the macro-droplet phenomena.

2.4.2.2 Vaporization with Sputtering

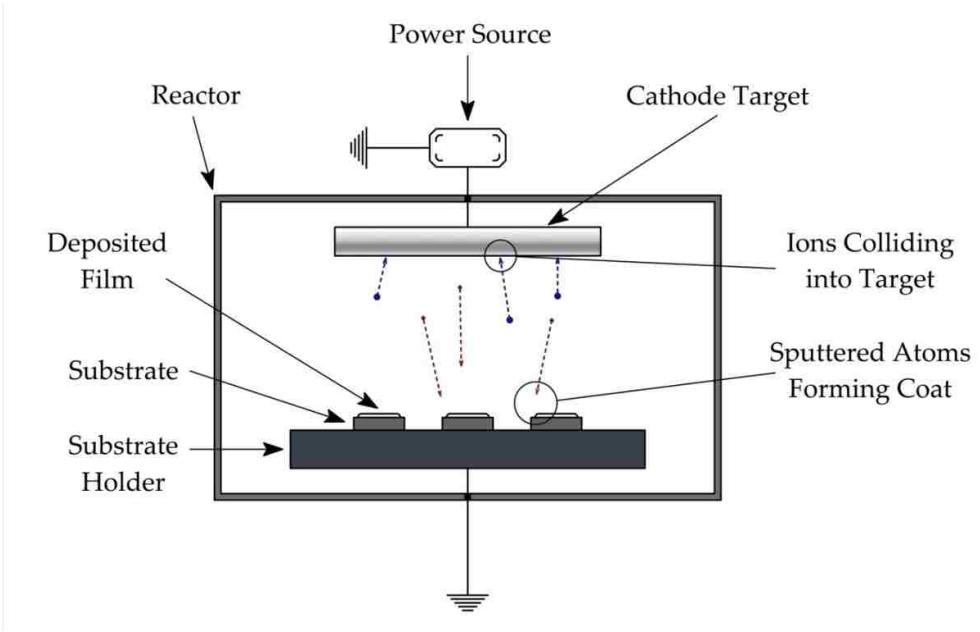

Figure 2-4: General Sputtering Schematic [21]

Sputtering is an adaption to the PVD process that vaporizes the source material by means of high velocity impact of ions, atoms, or other particles created in an energetic plasma where the kinetic energy of impact is in excess of the binding energy of the at the surface atoms of the source, liberating these atoms.[26] Once the atoms are liberated by means of ion bombardment from the target material, transport of these atoms to the substrate surface occurs across a region of reduced pressure where condensation into a thin film is then achieved on the substrate surface. Figure 2-4 visual depicts the general sputtering process. Although many variations to sputtering methods are regularly emerging, the basic sputtering techniques include DC diode, radio frequency, triode, and magnetron, which refer to the manner in which gas ionization within the reactor is realized.[21][26] A basic schematic of these sputtering deposition methods is presented in Figure 2-5. The principle behind all sputtering techniques is

basically the same, yet the major distinction between the different sputtering methods is derived from the manner in which ion bombardment is realized.[33] The most common sputtering technique is planar magnetron sputtering.[34] Magnetron sputtering utilizes a magnetic field to confine the plasma cloud in near proximity to the target material to be evaporated. Such use of concentrated magnetic fields provides increased deposition rates, in comparison to other sputtering techniques, due to increased plasma and power density on the target material.[26]

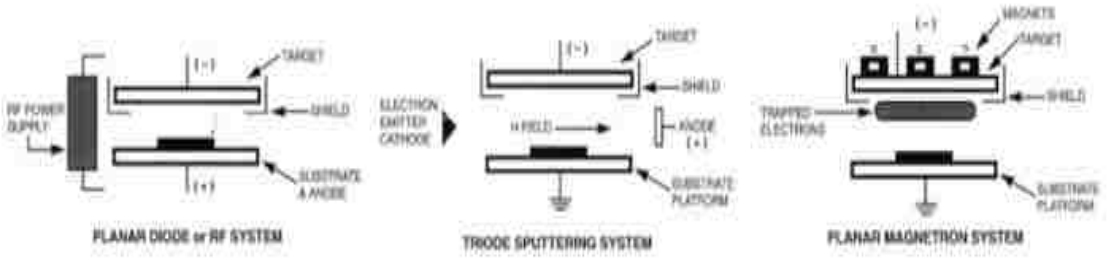

Figure 2-5: Schematic of Basic Sputtering Techniques [26]

Sputtering presents numerous advantages over the thermal evaporation processes. PVD films produced with sputtering are denser than those produced by thermal evaporation.[26] A side effect of the increased density in sputtered films is a notable increase in compressive residual stresses within the film.[26] High compressive residual stress in thin films can limit the coating thickness. Such residual stresses increase with thickness of the deposited film which can overcome the adhesion forces between the substrate and coating leading to spalling and delamination of the coating. Since sputtering is a non-thermal process, deposition temperatures tend be lower than those occurring with evaporation. Additionally, ion bombardment yields increased deposition rates

than those typically achieved via thermal evaporation processes. Within the sputtering PVD deposition chamber, the pressure is maintained at a level that is three orders of magnitude higher than in the thermal evaporation process.[26] The higher pressure leads to increased collision between the liberated atoms during transport to the substrate surface. Higher collision frequencies result in increased scatter [26], resulting in a more homogenous, conformal coating like in those produced by CVD, which is an especially important factor in the coating of complex, three-dimensional substrates.

2.5 Literature Review of Surface Engineering Research

Wear and corrosion resistant coatings are utilized in an extremely broad array of applications including: cutting and forming tools, mechanical components, thermal and electrical barriers, decoration, etc. These coatings also possess a great variety of elemental structures as well as industrial suppliers. The existence of such variety poses considerable challenge for engineers and scientists who need to specify the optimal coatings for certain applications. A significant amount of research has been conducted to evaluate the tribological behavior, mechanical properties, and physical structure of wear resistant coatings. Considering the broad array of elemental coating structures and end-use applications, the research in this field is extremely diverse in scope. The vast majority of research is directed toward cutting tools; whereas, research directed toward injection molding machines and mold tooling is limited.

The PVD process has reached a level of maturity that repeatable coating qualities can be guaranteed by an array of commercial suppliers. The most commonly employed PVD nitride coatings in industrial applications are TiN, CrN, TiCN, TiAlN, and ZrN.[35] Presently, no ceramic PVD coating universally satisfies the needs of the polymer injection molding industry.

Hard coatings, especially PVD coatings, are application specific. Wear resistance is not a mechanical property that is easily measured like modulus. Rather, wear is the property of a complex tribological system. Deductions of the wear properties of one tribological system cannot be accurately applied to a different tribological system because different interactions occur.

The wear resistance of a coating is not simply a function of its elemental design. A multitude of variables affect the overall performance of a coating as a wear resistor. One such variable is coating thickness. The overall surface microhardness which is the sum of the hardness of the substrate and the film is of primary concern from a mechanical point of view.[36] Y.L. Su, et al, found that the microhardness of a surface increases with increasing film thickness because the substrate effect is decreased.[36] Ultimately, an intrinsically softer coating deposited to a greater thickness can possess higher microhardness than an intrinsically harder coating.[36] This phenomena results from reduced substrate effect during hardness testing. CrN is inherently softer than TiCN, but as experimental evidence shows in Figure 2-6, a 7.5 μm layer of CrN possesses exactly the same surface microhardness as a 3 μm layer of TiCN deposited on

identical substrate materials because the substrate effect during microhardness testing is reduced.

Materials	Micro-hardness (Hv 50 g)
Uncoated WC	1774
2 μm TiN/WC	2094
3 μm TiN/WC	2395
5 μm TiN/WC	2756
3 μm TiCN/WC	2536
5 μm TiCN/WC	2854
7 μm TiCN/WC	3129
5 μm CrN/WC	2065
7.5 μm CrN/WC	2536
10 μm CrN/WC	3097

Figure 2-6: Surface Microhardness of Uncoated Tungsten Carbide (WC) and TiN-,TiCN-, and CrN-Coated Tungsten Carbide.[36]

Although microhardness is an important mechanical property for the wear resistance, higher microhardness does not guarantee superior performance as a wear resistant coating. The same study analyzed wear with an SRV reciprocating sliding wear test machine, with a cylinder-on-plate line-contact configuration between coated samples and 1045 steel.[36] As expected from the analyzed microhardness values, the thickness of the coating did indeed affect the coatings' performance, yet the results depicted in Figure 2-7 show variable trends. The wear resistance of TiN increased with coating thickness while an optimal thickness level existed for TiCN and CrN.[36] These results can be expected to vary under a different tribological environment; for instance, testing with lubrication or with a different contact material will most likely significantly impact the coating performance and optimal thickness.

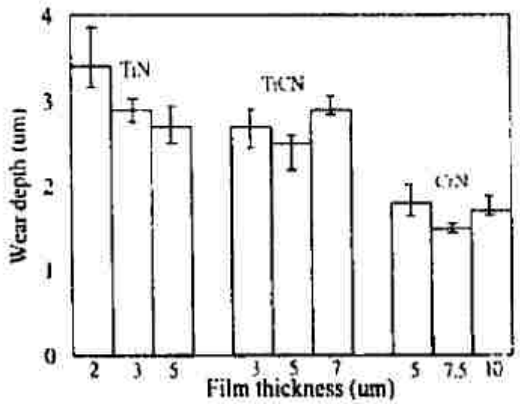

Figure 2-7: Effect of TiN, TiCN, and CrN coating thickness deposited on WC on wear resistance in sliding contact with 1045 steel.[36]

Compressive residual stresses are present in PVD coatings. As thickness increases, the magnitude of these residual stresses increases. If the residual stresses of a coating become too high, adhesion with the substrate material will be overcome causing delamination of the coating. These residual stresses are a limiting factor on coating thickness, and may explain the phenomena presented in Figure 2-7.

Of the nitride based coatings, TiN is the most widely studied and employed. TiN is often used as a reference for comparison. TiN is considered the most universal coating due to its effectiveness in many industrial applications considering that it represents about 90% of the PVD nitride coating market.[35] Conventionally, the thickness of TiN coatings is less than 10 μm. [36]

TiCN and TiAlN are solid solutions. At the substrate interface, a high concentration of TiN is present for good adhesion while C or Al concentrations increase at the coating surface which provides increased hardness and abrasion

resistance, and also for TiCN increased lubricity. A broad range of stoichiometric compositions of these multi-component coatings exist.

CrN is generally used in industry as coating for corrosion resistance. CrN can be grown much thicker than TiN.[36] Recent studies have shown CrN to be a viable replacement of certain nitride coatings. Rodriguez et al. [35] found CrN to possess a lower wear coefficient than TiCN, TiN, ZrN, and AlTiN under room temperature conditions. Su et al. [36] determined the wear resistance of CrN to be superior to TiN and TiCN under room temperatures. Other studies contradict this finding. Reiter et al. [37] found TiCN and TiAlN to show superior wear resistance to CrN. In the temperature interval 100-400 ˚C, Polcar et al. [38] determined the wear resistance of CrN coating is inferior to TiN and TiCN by a factor 20-80 (refer to Figure 2-8).

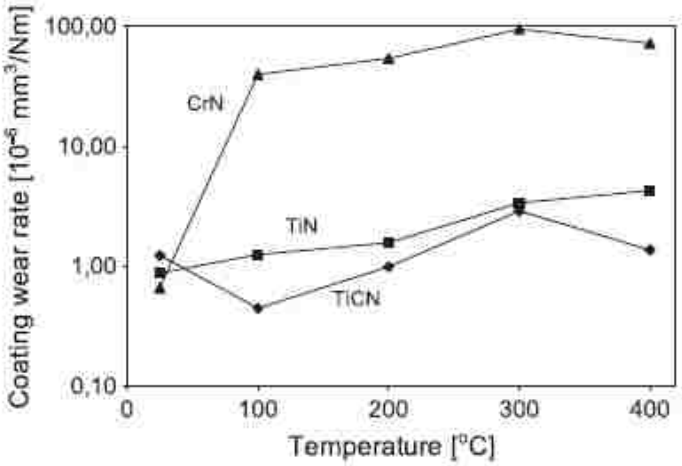

Figure 2-8: Influence of Temperature on Coating Wear Rate against Ceramic Ball. [38]

TiAlN has been proven to enhance the wear and corrosion resistance of dies, molds, and machining tools. Wear and high temperature oxidation resistance of TiAlN makes this PVD coating a suitable functional hard coating

which can overcome the shortcomings of TiN and TiCN.[39] TiAlN exhibits over a 300 ˚C increase in oxidation threshold in comparison to TiN. [39] TiAlN also provides increased hardness in comparison to TiN at temperatures up to 1000 ˚C, yet the hardness of TiAlN is less than that typical of TiCN in the up to approximately 750 ˚C (refer to Figure 2-9) .[40]

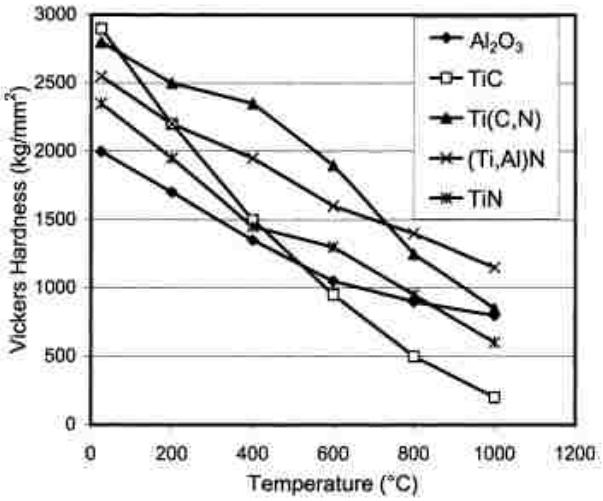

Figure 2-9: Temperature dependence on microhardness [40]

Studies comparing all numerous different families of coatings are few. One extremely relevant study characterized an array of Oerlikon Balzers' coatings.[37] Various properties of the Balzers' coatings are presented in Figure 2-10. The abrasive wear rates of the Balzers' coatings are presented in Figure 2-11. Oerlikon Balzers' diamond-like carbon (DLC) had the lowest abrasive wear rate of all the coatings. From the data in Figure 2-11, the abrasive wear rate of CrN is relatively poor, which is one of many contradictions found throughout the literature review (compare with Figure 2-7).

Coating	Deposition method	Hardness [HV] (mean values)	Friction (mean values)	Roughness Ra [µm] (mean values)	Thickness [µm] (mean values)
CrC	AIP	2200	0.49	0.24	2.8
CrN	AIP	1500	0.38	0.18	2.5
TiAlN	AIP	2800	0.52	0.20	4.1
TiCN	Ionitron	3100	0.29	0.08	3.5
WC/C	UBM	1200	0.10	0.03	2.4
DLC	PA-CVD	2700	0.08	0.03	2.1
TiCN+DLC	AIP+PA-CVD	–	–	–	3.4
TiCN+WCC	AIP+UBM	–	–	–	3.6
AlCrN(20/80)	AIP	2300	0.47	0.13	1.6
AlCrN(45/55)	AIP	2900	0.58	0.14	1.4
AlCrN(70/30)	AIP	2800	0.45	0.12	1.5

Figure 2-10: Selected Mechanical Properties of Investigated Oerlikon Balzers' Coatings.[37]

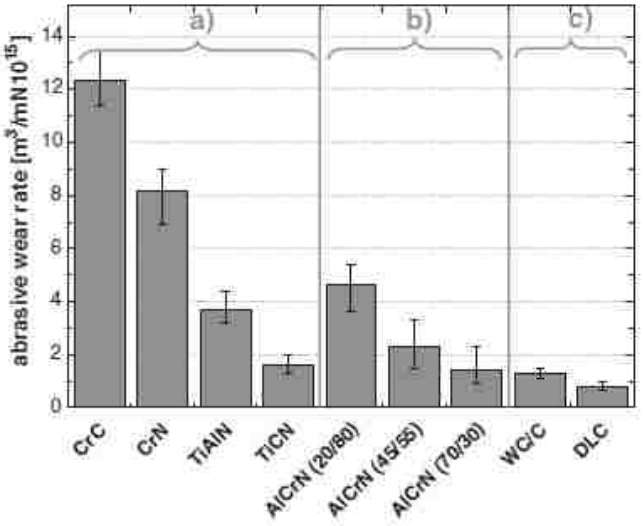

Figure 2-11: Abrasive Wear Rates of Select Oerlikon Balzers' Coatings [37]

To further illustrate discrepancies present in the literature review, Figure 2-12 presents the results of a different study.[41] This study showed TiCN to possess better wear resistance than the DLC coating which contrasts the results presented in Figure 2-11. Considering the coatings in this study were not obtained by Oerlikon Balzers, quality discrepancies may exist from supplier to supplier as well as testing procedures utilized in the studies.

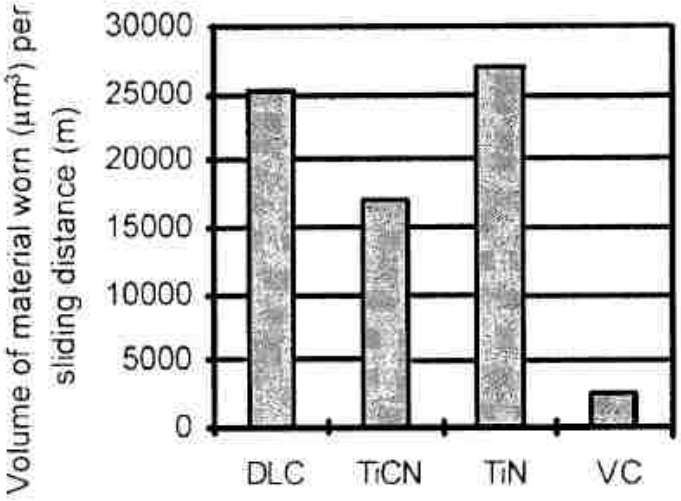

Figure 2-12: Pin-on-disc wear rates for the coatings investigated (Note: VC is a thermal diffusion coating) [41]

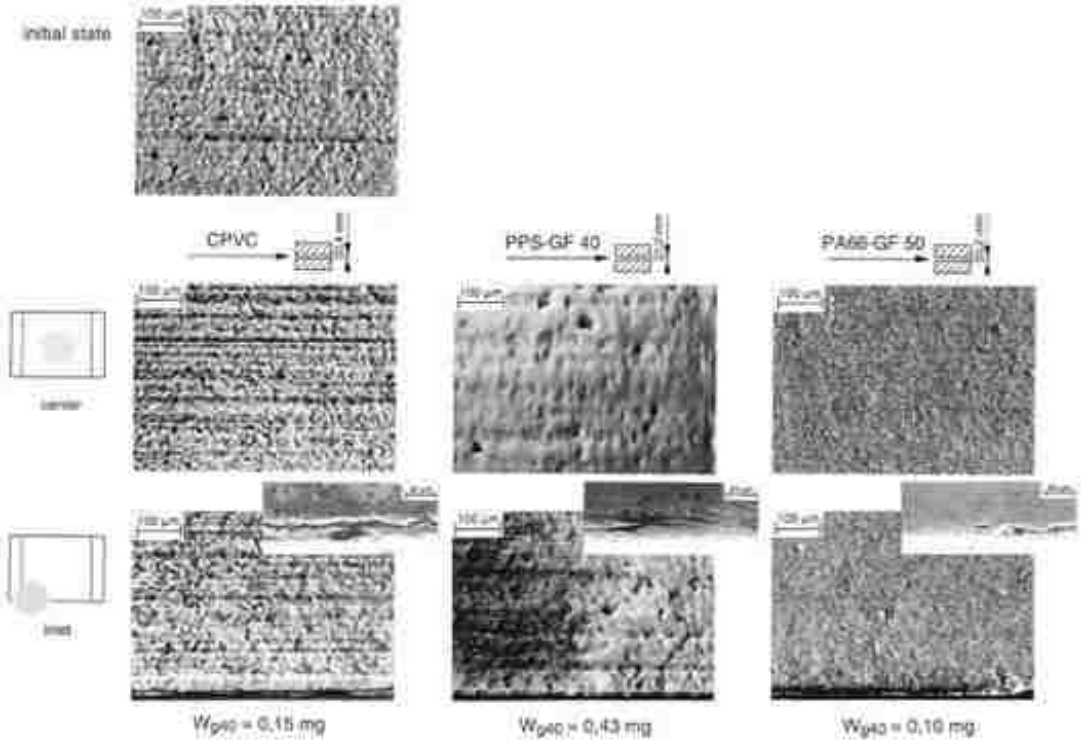

Figure 2-13: Surface of TiC-Coated Test Specimen after 40-kg Throughput by Different Raw Materials [42]

During injection molding, the type of polymer significantly impacts wear and corrosion performance. Figure 2-13 shows the SEM photographs and the gravimetric wear of TiC-coated specimens subjected to 40 kg throughput of different raw materials. Surprisingly, the lowest gravimetric values were observed for the processing of PA66-GF50 (i.e. the material with the highest glass fiber content). [42] The same study provided insight to the deposition temperature's affect on wear resistance of a TiCN coating. The results, presented in Figure 2-14, show a decrease in wear with increasing deposition temperatures. [42]

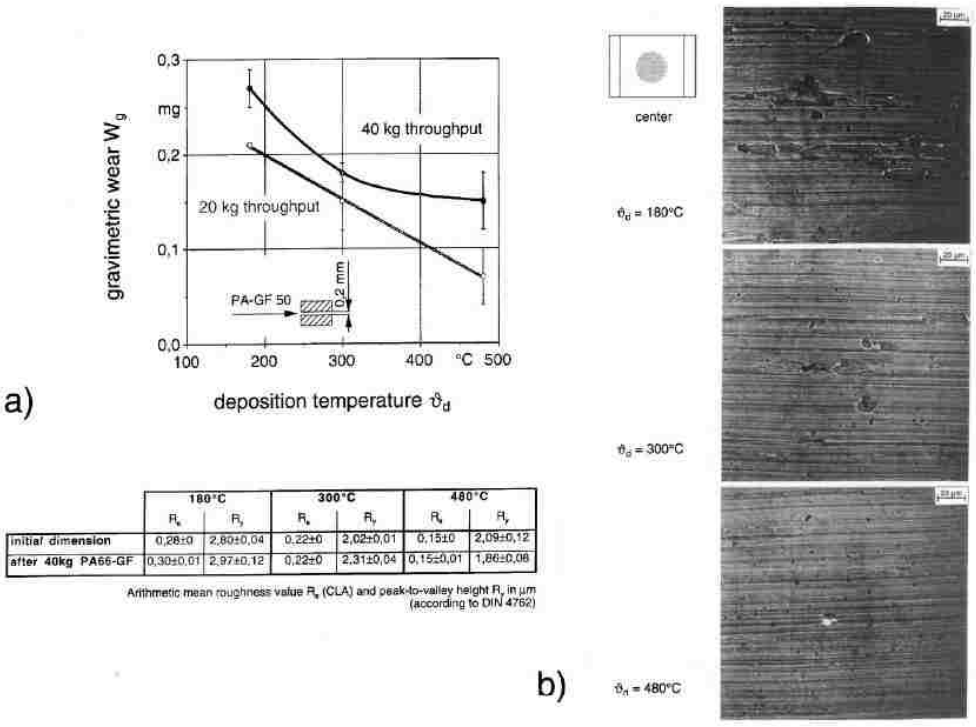

	180°C		300°C		480°C	
	R_a	R_y	R_a	R_y	R_a	R_y
initial dimension	0,28±0	2,80±0,04	0,22±0	2,02±0,01	0,15±0	2,09±0,12
after 40kg PA66-GF	0,30±0,01	2,97±0,12	0,22±0	2,31±0,04	0,15±0,01	1,86±0,08

Arithmetic mean roughness value R_a (CLA) and peak-to-valley height R_y in µm (according to DIN 4762)

Figure 2-14: Wear of TiCN (AEPVD) Coatings due to PA66-GF50 as a Function of the Deposition Temperature [42]

2.6 Selected Coating Processes, Coating Types, and Suppliers

For this study, electrodeposited chromium has been chosen as the standard for comparison. The choice of using electroplated chromium rather than an uncoated steel substrate reflects that hard chrome has evolved into a standard coating process for injection mold tooling, and the fact that a chrome plated steel is far more wear resistant than uncoated steel is already well documented. All coatings evaluated are deposited onto H13 steel substrates, which is a commonly employed steel for injection mold tooling

The second deposition process for this study is PVD. The basis for using PVD over CVD is the lower required substrate temperature during the deposition process, which minimizes any concerns related to dimensional distortion of the mold during surface treatment. The PVD coating used in this study is Oerlikon Balzers' BALINIT® FUTURA NANO TiAlN coating which is deposited by arc evaporation PVD. The Choice of TiAlN reflects its high hardness and abrasion resistance and superior oxidation resistance at elevated temperatures

The third coating type is Oerlikon Balzers' BALINIT® DLC STAR, which is a DLC coating with an interfacial layer of chromium nitride used as a support material for the amorphous carbon DLC coating. This coating is deposited by a combination of PVD for the chromium nitride and PACVD for the amorphous carbon, DLC.

Oerlikon Balzers is the selected coating provider for the PVD and PVD/PACVD coatings. This choice reflects the fact that Oerlikon Balzers is a reputable supplier offering one of the largest varieties of coatings of all coating

companies examined. This company is a global provider with locations in North and South America, Europe, and Asia, which is an important consideration for injection molding corporations with production facilities located internationally. Since there is not enough scientific studies comparing the performance of commercially supplied coatings from different suppliers, the choice of coating supplier is a function of corporate logistics rather than superiority to other suppliers because the quantity of data available is insufficient to make such a judgment.

Chapter 3 : Testing Methodology

3.1 Overview of Established Procedures for Melt Wear Testing

With regards to wear testing of surface treatments against plasticized polymer melts, most of the work in this field has been developed in Germany. The German-based Kunststoffe-Institute has developed a testing method known as the “DKI platelet method”.[12] A sample schematic of an apparatus used for the DKI platelet method is depicted in Figure 3-1. The apparatus in Figure 3-1 is connected to the injection unit of a molding machine which forces plasticized material through a test slit containing the coatings to be tested. Another adaption of the method uses cylindrical coated samples, which are similar in configuration to a sprue, instead of rectangular samples and injects the plasticized polymer into a mold cavity rather than into open air.[12] This approach is one of the more accurate simulations of the tribological environment experienced by an injection mold since the samples are exposed to similar dynamic changes in pressure and melt velocity, temperature cycling, and solid material removal (demolding) as a coating would experience in an actual molding scenario. Other wear testing methods have been developed by the Kunststoffe-Institute such as the “DKI ring method” which is a testing methods used to emulate the wear conditions occurring in the injection unit of a molding machine between the reciprocating screw and barrel.[12] This can basically be considered a couette-type flow with a stationary outer wall (injection cylinder) and a rotating inner wall (screw) with and flowing polymer melt inside the two boundaries.

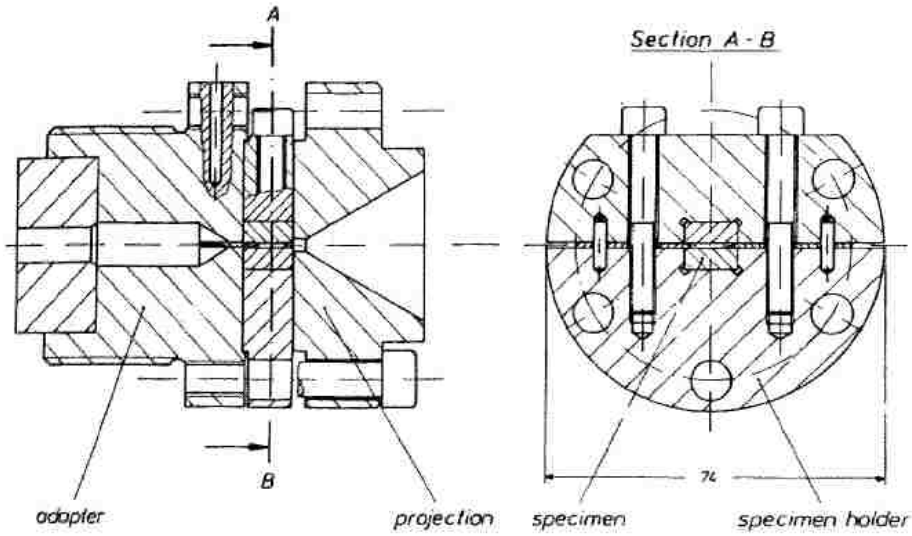

Figure 3-1: Nozzle Apparatus for Investigating Wear Induced by Plasticized Material [11]

Injection molding machines are significant capital investments for a company. The dedication of a molding machine for testing of surface treatments may be economically impractical for an injection molding company; therefore, a method for investigating wear caused by plasticized flows via extrusion has been developed in this thesis. Various concept extrusion test die designs have been developed with the CAD software Solidworks. One of the concept designs will briefly be discussed in the subsequent section of this thesis to highlight the design considerations which led to the final design used in the melt wear testing.

3.2 Melt Wear Testing via Polymer Extrusion

Several considerations exist when utilizing an extrusion die for melt wear testing of surface treatments. One such consideration is the pressure inside the

extrusion die. Of course with the extrusion process, pressure within an extrusion die is relatively static; whereas, with injection molding the pressure is dynamically changing, with injection, packing, and cooling cycles. Monitoring the pressure within the extrusion die with pressure transducer(s) permits comparison between the test pressure conditions of the surface treatments and the actual condition expected during the molding process.

The high wear resistance of many commercially available surface treatments entails that melt wear testing may require a large amount of material throughput and extended testing durations before appreciable wear of the surface treatment is noticeable. High material throughput can be costly due to the cost of material, operators, and overhead. Ultimately, one of the principal considerations for the design of an extrusion test die for surface treatments is to minimize the amount material throughput required while still having the capacity to test numerous samples simultaneously, for statistical purposes.

Additionally, an extrusion test die should ideally provide uniform flow conditions to all samples or be designed in a manner that permits the determination of the amount of flowing material that each samples has been exposed to. Presented in Figure 3-2 is an exploded assembly view of one of the original concept design for the extrusion melt wear testing die. The exploded assembly only contains images of the die block, samples, and sample bolts while the heating components, pressure transducer(s), and thermocouple feedback systems have been omitted for the image. This concept design has the capacity to test 18 coated samples simultaneously but also has many negative

drawbacks. The concept design can be considered a form of sheet extrusion in which the polymer melt exits the extruder and is spread transverse to the direction of flow, forming a thin sheet of flowing material. This flowing sheet of material is then forced through three groups of samples (each group containing six samples and two sacrificial samples, see Figure 3-3. The samples have 0.1 mm grooves on both sided, and when clamped together by the sample clamping bolts, the test gap is 0.2 mm. This narrow restriction in the test gap should induce accelerated wear due to the high shear stresses of the polymer accelerating through this gap.

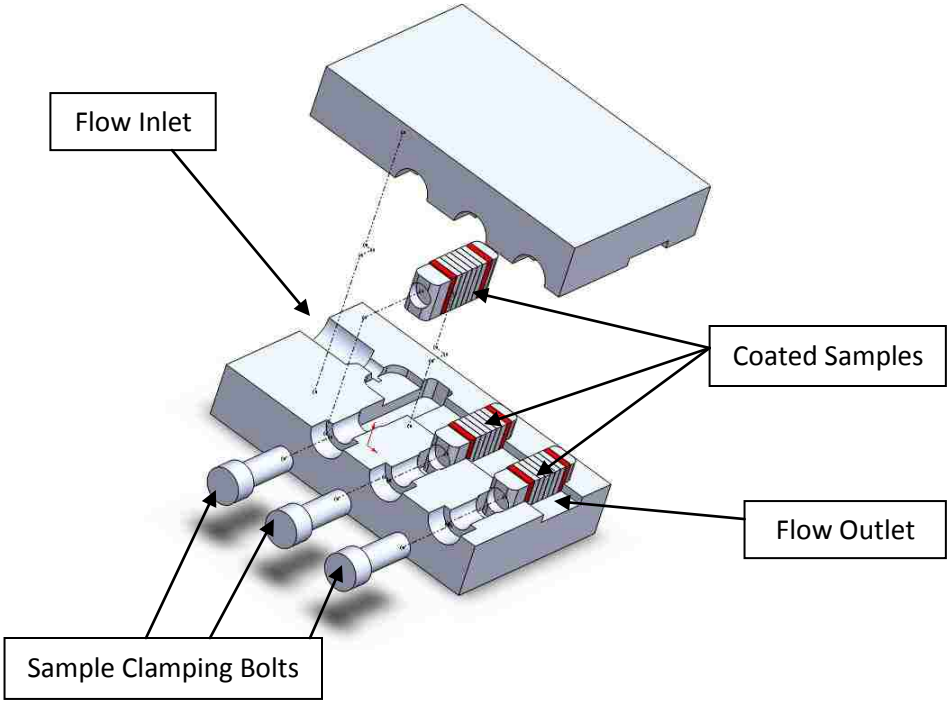

Figure 3-2: Exploded Assembly View of Concept Melt Wear Test Extrusion Die

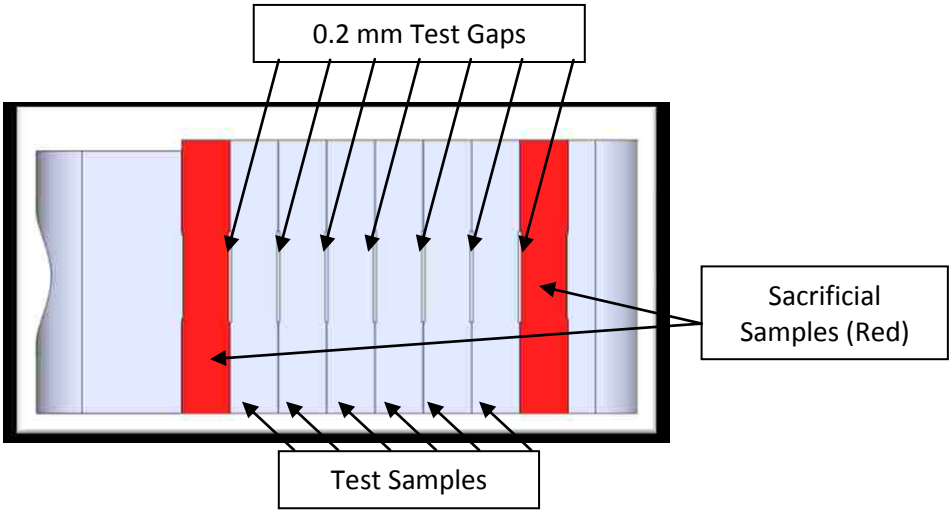

Figure 3-3: Image of Samples for the Concept Die Presented in Figure 3-2, Orientated in a Manner that the Viewer is looking into the Flow Direction

Two major drawbacks are evident with the concept design present in Figure 3-2. The first being the significant pressure drop that would occur after

each group of samples. The second, and perhaps the most significant drawback, is the complexity in providing uniform flow to all samples. Typically, the outer regions of the flow channel possess a higher pressure drop resulting from an increased distance from the pressure source. The lower pressure results in a reduced flow rate of material to these regions. The velocity can be expected to be highest in the center of the flow stream and reduce to a minimum at the edges of the flow stream. The velocity gradient is further accentuated by deflection of the die plates. Deflection can be expected to be highest in the position which is furthest from the supports (i.e. the bolts which hold the die together, which would around the periphery of the flow channel). This position corresponds to the center of the flow stream, which means the height of the flow channel will be greatest in the center of the flow stream and geometrical resistance to flow will be less. Coat hanger manifolds are typically employed in industry to address the inhomogeneous velocity profiles in sheet extrusion dies. Researchers have concluded that the velocity gradient differs between materials. To use the concept die with a coat hanger manifold, the coat hanger manifold design itself would have to be tailored for each material of interest. The complexities of designing the coat hanger manifolds for use in the concept design presented in Figure 3-2 make the use of such a design impractical; therefore, a refined extrusion die design has been developed and fabricated for the melt wear testing in this thesis.

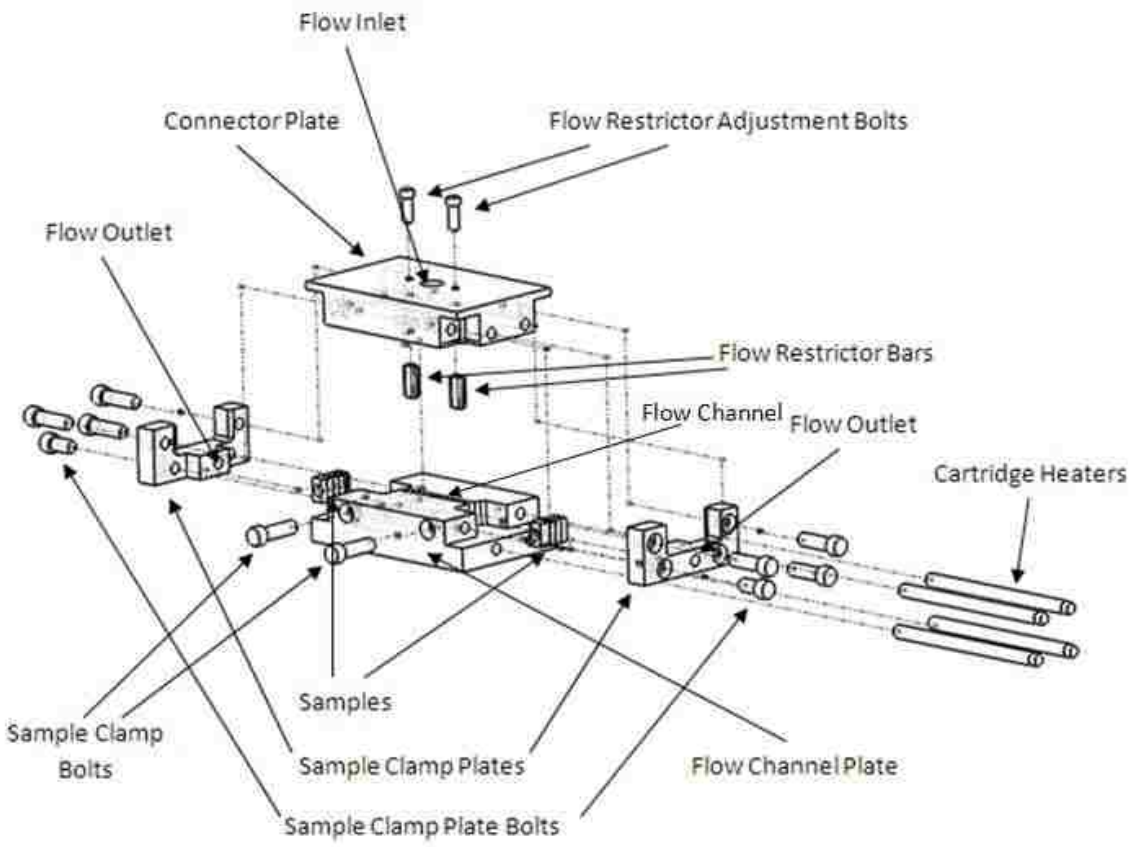

Figure 3-4: Exploded Assembly View of the Extrusion Die Utilized in the Melt Wear Testing

Presented in Figure 3-4 above is an exploded assembly view of the extrusion test die that was designed and fabricated for melt wear testing in this thesis. Not included in the image above is the array of bolts used to hold together the two main die plates, “flow channel plate” and “connector plate”, the pressure transducer that is positioned directly below the flow inlet, and the thermocouple feedback system for the temperature control of the cartridge heaters. This design is center fed from the extruder at the flow inlet. Upon entrance into the flow channel, the flowing polymer melt is subsequently split into two flow directions, both leading to an array of coated samples, with a 0.2mm

test gap that has the ability to be adjusted to provide a larger test gap if necessary. Each group of samples contains only one test gap, eliminating the concerns discussed with the concept extrusion die in Figure 3-2. The throughput material from each group of samples is collected and weighed in order to quantify the degree of polymer melt exposure for each group of samples.

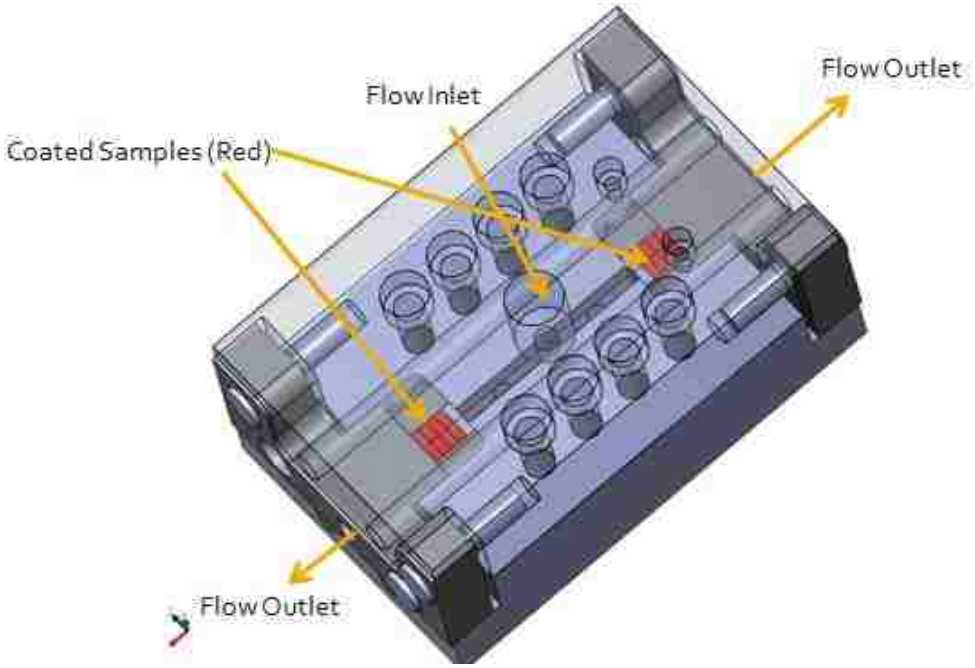

Figure 3-5: Extrusion Test Die for Melt Wear Testing of Surface Treatments

The ability to adjust the test gap proved to be essential for this study. Based on limitations of the extrusion unit, a 0.2 mm test gap is too restrictive. When using a 0.2 mm test gap, the volumetric flow rate is minimal and the material remains in the barrel of the extrusion unit continuously plasticizing rather than flowing through the samples. This extended residence time in the extrusion barrel can cause excessive degradation of the polymer compound which is undesirable; therefore, the test gap employed in this study is 0.6 mm which

provided a greatly increased flow rate more closely simulating the flow conditions in the injection molding process.

3.2.1 Melt Wear Test Procedure

A Brabender extrusion unit is utilized for melt wear testing. Prior to melt wear testing material is dried according the material suppliers recommendations. The material is also processed a temperature corresponding to the middle of the range specified from the material supplier. Screw revolution speed of the Brabender extrusion unit is slowly increased until the pressure reading from the pressure transducer which is position opposite of the melt inlet of the extrusion die generated a signal of approximately 6900 kPa.

The material utilized for melt wear testing is a Celanex® 6407 polybutylene terephthalate (PBT), which is a 30% glass/mineral filled polymer compound. 18.6 kg of the PBT Celanex was forced through the test gap containing the chrome samples and 20.0 kg was forced through the test gap containing the DLC and TiAlN samples.

3.3 Solid-State Wear Testing

A common method employed in scientific research to investigate wear resistance is the “pin-on-plate” method. Pin-on-plate wear testing is a relatively simple method in which a material usually of hemispherical shape is in sliding

contact with the specimen of interest under an applied load normal to the sliding surface. Since mold wear induced during injection molding is both a function of the flowing polymer melt and also the sliding contact of the solidified polymer against the mold steel during ejection, the pin-on-plate method is intended to simulate the wear generated from the demolding cycle.

Figure 3-6: Image of Molded Part for Use in Pin-on-Plate Wear Testing and Friction Testing

To accurately simulate wear caused during the demolding cycle, the material in sliding contact should be the polymeric compound of interest. A mold was fabricated to produce hemispherical geometry on a flat disc for use in pin-on-plate wear testing and also friction testing discussed in the next section of this thesis, refer to Figure 3-6. These molded parts are used in dry sliding contact against the coated H13 steel samples. Excessive wear of the molded plastic parts during pin-on-plate wear testing requires exchange of the molded parts. Based on the geometry of the molded part and the fixture holding the part, sample exchange is not feasible because it is nearly impossible to exchange the

part and resume testing in the exact same location of the original wear track; therefore, results utilizing this test method are not discussed.

Alternatively, copper alloy hemispheres (C51100 – H04) are used to conduct pin-on-plate wear testing. The use of copper alloy hemispheres is not an accurate representation of the tribological environment experienced by the cavity and core geometry during demolding, yet the alloy-to-coating sliding contact provides some insight into the performance these coatings in coating-to-metal contact such as mold components like ejector pins and mechanically activated slides used in molding undercuts.

3.3.1 Testing Procedure for Pin-on-Plate Wear Test with Copper Alloy Hemisphere

Prior to testing, the coated samples and the copper alloy hemispheres are ultrasonically cleaned, and a 12 hour delay between ultrasonic cleaning and testing is given to allow all cleaning solution to evaporate. Motion of the copper alloy hemispheres relative to the test specimen is a sinusoidal velocity with an acceleration of 50 revolutions/second^2 up to a velocity of 50 revolutions/second. High and low loads of approximately 500 grams and 200 grams respectively are applied normal to the sliding surface for each type of coated sample (refer to Figure 3-7 for exact applied loads). The test is programmed to slide a certain number of repetitions over a certain travel distance. The configuration of repetitions and travel distance is presented in Figure 3-7. This configuration permits the inspection of wear at different number of repetitions because every

two millimeters of the wear track is exposed to an additional 4000 repetitions. Also, each repetition count represents a forward and backward slide of the copper alloy hemisphere; for example, for the 2 mm wear track exposed to 32,000 repetitions, the total number of slides across the surface is 64,000. All friction testing is performed at room temperature.

Coating Type	High Load (grams)	Low Load (grams)
Chrome	494.9	205.1
DLC	512.3	202.3
TiAlN	487.0	200.0

Figure 3-7: Loading Conditions for Pin-on-Plate Wear Test against Copper Alloy Hemisphere

Total Number of Repetitions	Sliding Travel Distance (mm)
4000	16
8000	14
12000	12
16000	10
20000	8
24000	6
28000	4
32000	2

Figure 3-8: Configuration of Repetitions and Sliding Travel Distance for Pin-on-Plate Wear Test against Copper Alloy Hemisphere

3.4 Friction Testing

The apparatus used for friction testing is depicted in Figure 3-9. The methodology of the friction test is similar to the pin-on-plate wear test. Samples are ultrasonically in isopropyl alcohol for one minute and given a 12 hour delay for the solvent to evaporation prior to friction testing. The coated substrates are

clamped to a table. Sinusoidal, harmonic motion is imposed on the table by an eccentric cam which is powered by a DC motor. The rotational speed is approximately 0.5454 cycles/second for a track length of approximately 5.5 mm. A one kilogram load cell, calibrated before testing, is attached to the table. This load cell records the lateral force at a frequency of 100 hertz. Normal weight of 281.3 grams and 94.1 grams are used during the test. With recorded lateral force and known normal load known, the coefficient of friction can be calculated. Both Zytel® HTNFR52G30NH NC010, which is a 30% glass filled, flame retardant polyamide resin, (referred to as Nylon for the rest of this document) and Celanex® 6407 PBT (the same polymer compound used for melt wear testing, referred to as PBT for the rest of this document) molded specimens, see Figure 3-6, are used to generate the coefficient of friction data.

Figure 3-9: Friction Testing Apparatus [43]

3.5 Surface Profilometry

An optical surface profilometer, Micromeasure model # C1717/ 100, with a 100µm probe is utilized to calculate the surface roughness of the uncoated H13

steel substrate and also the surface roughness of the different coated samples. Calculating surface roughness prior to and after coating deposition is a good quantitative method to determine how well the coating mirrors the surface finish of the substrate. Surface roughness measurements were taken along two paths of the samples in the location of the machined groove which forms the test gap in the melt wear test. Along each path two test procedures are used. The first test procedure records the altitude of the sample's surface every 2 μm over a length of 4 mm. The second test procedure records the altitude of the sample's surface every 20 μm over a length of 6 mm. This results in a total of four altitude measurements for each sample. Surface roughness measurements of ten samples from each group (i.e. uncoated H13 steel and DLC, TiAlN, and Chrome coated steel) are averaged and presented in Chapter 4. The reported surface roughness is the arithmetic average surface roughness (Ra) given by [44]:

$$\bar{z}$$

The optical surface profilometer is also employed to measure the gap height of the test groove, where the flowing polymer melt is exposed during melt wear testing. The intention of measuring the gap height of the test groove is to compare the measurements prior to and after melt wear testing in order to quantify the amount of material removal (i.e. induced wear) during the melt wear test. Difficulty with obtaining reliable measurements of the coated samples' gap height after exposure to the polymer melt is discussed in Chapter 4.

3.6 Scanning Electron Microscopy and Energy Dispersive X-Ray Spectroscopy

Scanning electron microscopy (SEM) is utilized in this study to examine the surface topography of the uncoated H13 steel substrate and the coated samples. SEM images of the pristine coatings, as supplied from the commercial coating corporations, are extensively used for inspection of coating defects. Additionally, acquired images of the pristine coatings are compared with images of the worn coatings after melt wear testing and solid state wear testing to evaluate the amount of wear incurred during testing and the dominant wear mechanisms.

The analytical technique for elemental analysis is energy dispersive X-ray spectroscopy (EDS). Through the use of EDS, the elements present in the base H13 substrate and the in surface treatments are obtained. EDS also aids in characterization of defects present in the pristine coating and the wear mechanisms occurring after melt wear testing, such as surface oxidation.

3.7 Focused Ion Beam

A focused ion beam (FIB) is used in this study for ablation of the coating surface to achieve a localized cross section of the coating for evaluation of coating thickness. The FIB technique is similar to SEM, except that the beam utilized is a focused beam of gallium ions as opposed to a beam of electrons in SEM imaging. Focusing a high current beam of gallium ions at the surface of a coating vaporizes/sputters the surface atoms. Gallium ions, which are

considerably larger than electrons, impact the surface with much greater momentum aiding in ablation. Prior to ablation of the coating surface, a protective layer of platinum is deposited on the surface of the coating. Then, a FIB is directed at the surface, micro-milling the surface by vaporizing the atoms. The FIB is used in conjunction with SEM and EDS to aid in characterization of the coating.

3.8 Porosity Testing

The presence of defects or pinholes in functional hard coatings is detrimental to the performance in an environment such as injection molding, especially when processing polymers prone to emission of corrosive decomposition by-products. Such pinholes are direct passages for the corrosive environment to the substrate. With the high susceptibility of steel to oxidation, coating porosity results in accelerated, localized corrosion at the substrate-coating interface leading to deterioration of the base substrate and undercutting of the surface treatment at the interface. Such undercutting weakens adhesion to the substrate material and can promote coating delamination

Electrochemical testing is used to determine the porosity of the pristine coatings in this study. Specifically, potentiodynamic polarization testing is the applied electrochemical process. Conducting this test requires the use of an electrolytic cell with a cathode, anode, electrolytic solution providing the ionic conduction path, and an electrical conduction path provided by the potentiostat. The coated substrate serves as the anode in the electrolytic cell (i.e. electrons flow from the anode to the cathode). The electric potential provided by the

potentiostat is the driving force for the electrochemical reactions occurring in the cell. Additionally, the magnitude of the applied voltage dictates the type of reactions occurring in the cell. The anodic scan begins at the open circuit potential where sum of the cathodic and anodic reaction rates is zero. As the potential applied from the potentiostat increases, the scan enters the “active region” where the prevailing chemical reaction is metal oxidation. In the anodic scan, the current represents the rate at which the reaction are occurring at the anode, typically expressed as current per unit area. (Reference for this paragraph is provided in [45])

The active region, low applied potential in the anodic scan, is the region of interest for porosity testing in this thesis. Here the assumption is that iron oxidation is the dominant reaction, which is governed by the equation:

A higher current density implies that a higher degree of oxidation is occurring at the surface of the anode (coated sample). Based on the assumption of iron oxidation being the dominant reaction occurring in the cell, a higher current density indicates a greater degree of porosity of the coated sample.

For the potentiodynamic polarization testing in this thesis, the electrolytic solution is a 3.5% weight NaCl solution. A precisely controlled area of the coated sample is exposed to the NaCl solution. Once the exposed area of the coated specimen is submerged in the solution at room temperature, ample time is given until the open circuit potential (OCP) is reached. Care is taken to ensure that no air bubble or contaminants are present on the surface of the exposed area. The

anodic scan begins slightly below the OCP, which in this case is approximately -0.3 volts to -0.5 volts for the samples tested; hence, the anodic scan is started at a potential of -0.6 volts. The end potential of the anodic scan is set to the low value of .25 volts to ensure that the anodic scan is being conducted in the “active region” where metal oxidation prevails. The anodic scan rate is 10 mV/second. To ensure consistency in the testing procedure, the NaCl solution is replaced after every two anodic scans and the distance and orientation of the anode and cathode is kept constant.

Chapter 4 : Results and Discussion

4.1 Evaluation of Pristine Coatings

4.1.1 Scanning Electron Microscopy, Energy Dispersive X-Ray Spectroscopy, & Focused Ion Beam

A typical SEM image of the uncoated H13 steel substrate is presented below in Figure 4-1, and an EDS spectrum of the steel substrate is presented in Figure 4-2. Along with the expected spectral peaks for iron, trace amounts of the alloying elements carbon, copper, silicone, molybdenum, and manganese are apparent as well as a slight degree of oxidation.

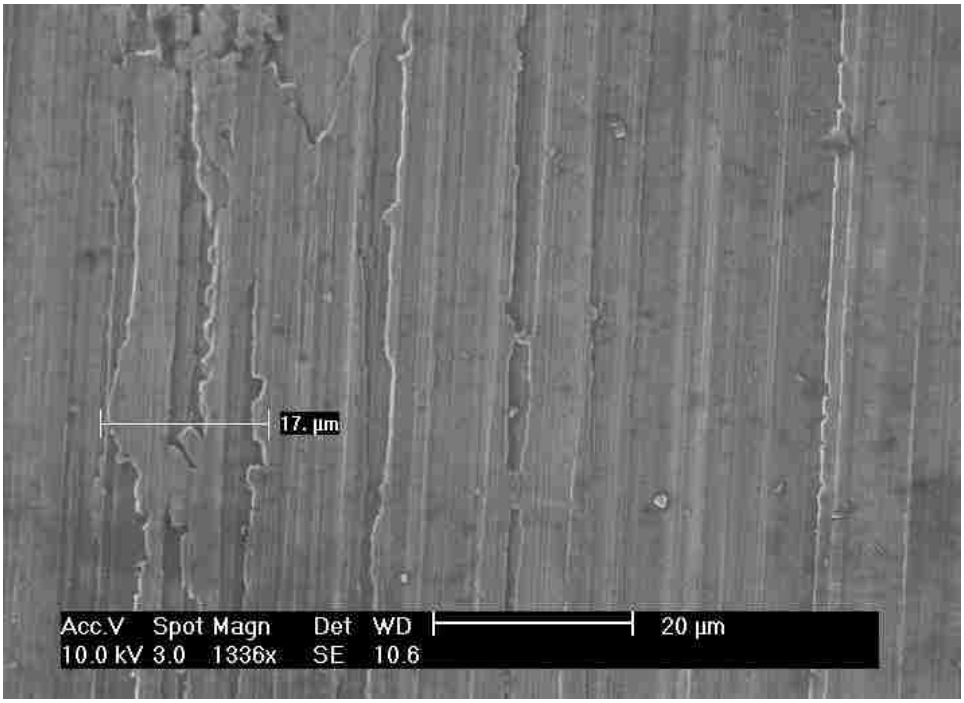

Figure 4-1: SEM Image of Uncoated H13 Steel Substrate

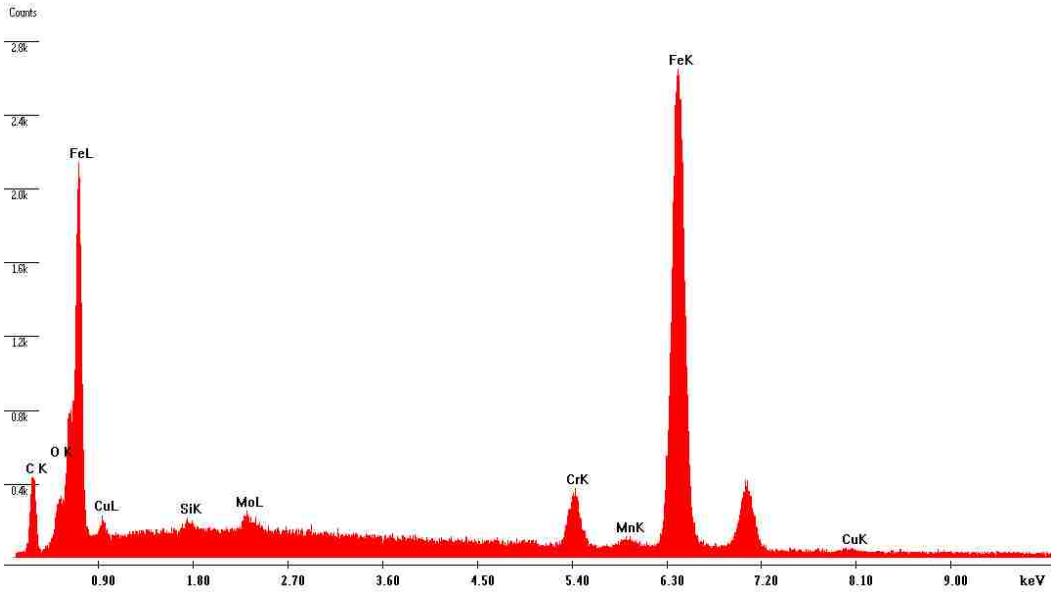

Figure 4-2: EDS Elemental Spectrum of Uncoated H13 Substrate

Figure 4-3 depicts an image of the TiAlN coated sample. This image is representative of the typical topography of this type of surface treatment. Methodical inspection with both SEM and EDS of numerous TiAlN coated samples reveals no exposure of the base substrate.

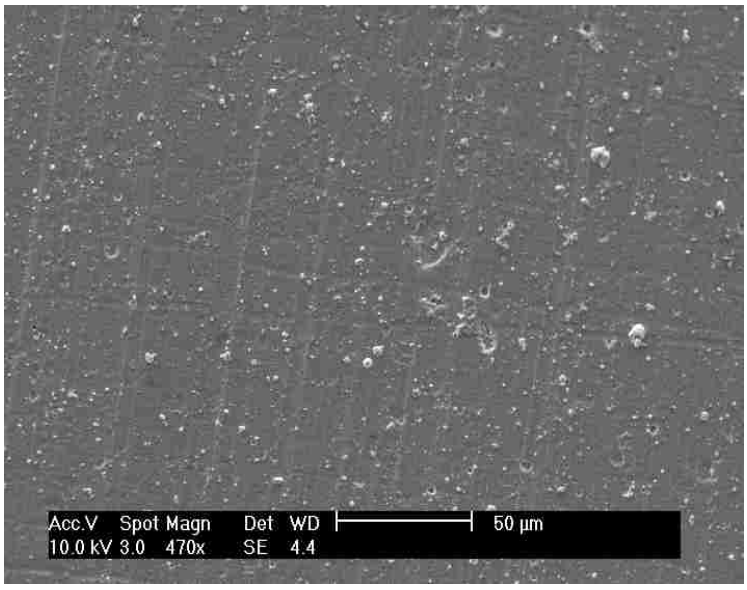

Figure 4-3: Typical SEM Surface Image of TiAlN Coated Sample

Only spectral peaks corresponding to the elements which comprise the coating; titanium, aluminum, and nitrogen, appear in the EDS spectrum, refer to Figure 4-4 below.

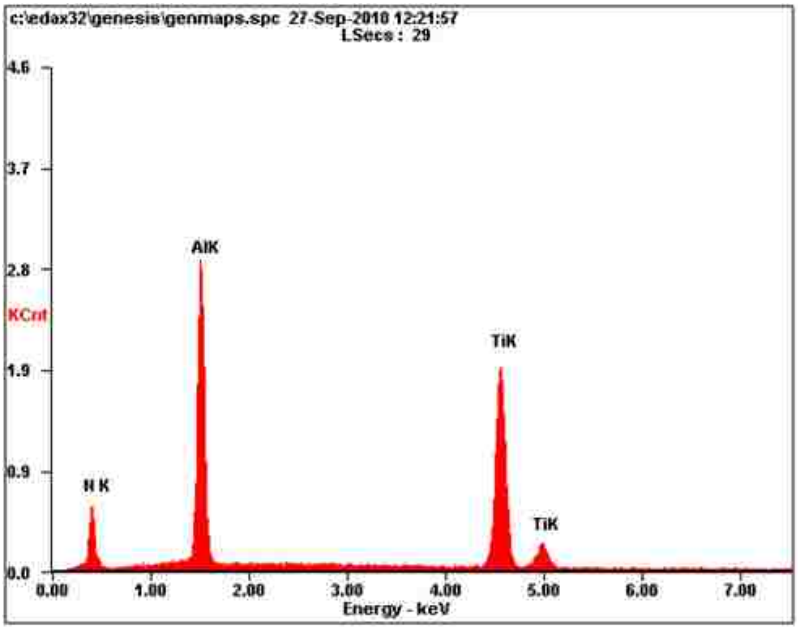

Figure 4-4: EDS Elemental Spectrum of TiAlN

The characteristic surface defect evident in all TiAlN coatings examined is the “crater-like” depression depicted in Figure 4-5. These depressions at the surface of the coating range in size from approximately less than 1μm and up to 20μm in diameter. EDS does not detect any spectral traces of the substrate material when focused into these depressions. The dimensioned FIB cross-section, shown in Figure 4-6, of the relatively large defect in Figure 4-5 clearly demonstrate a bulk coating thickness of approximately 6.6μm, while coating thickness at the base of the depression is nearly 5μm less than the bulk coating thickness. The reduction in thickness at these defects is adverse since the

barrier protecting the substrate is reduced and the uneven terrain induces increased friction forces, which is evident in the friction results.

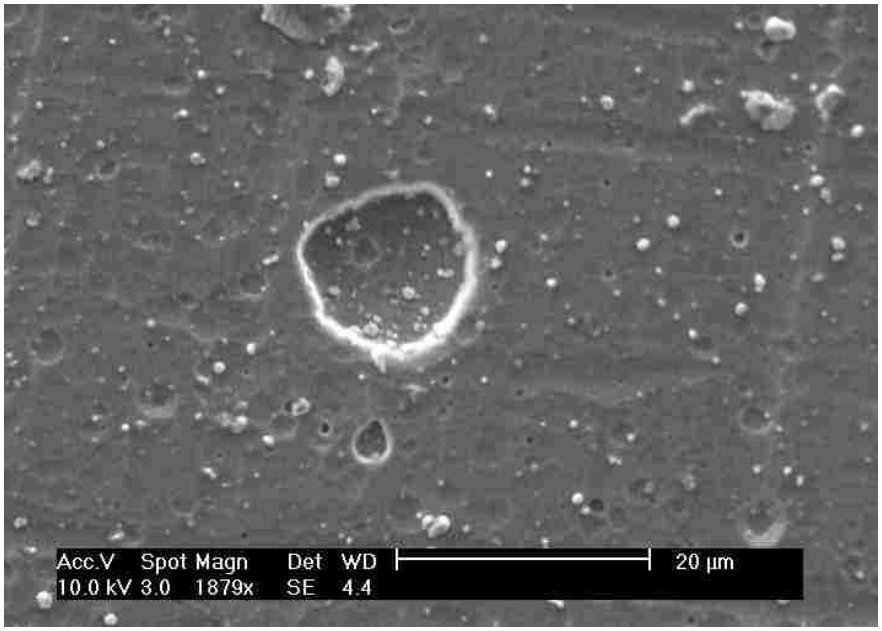

Figure 4-5: SEM Image of a Characteristic Defect for the TiAlN Coated Samples

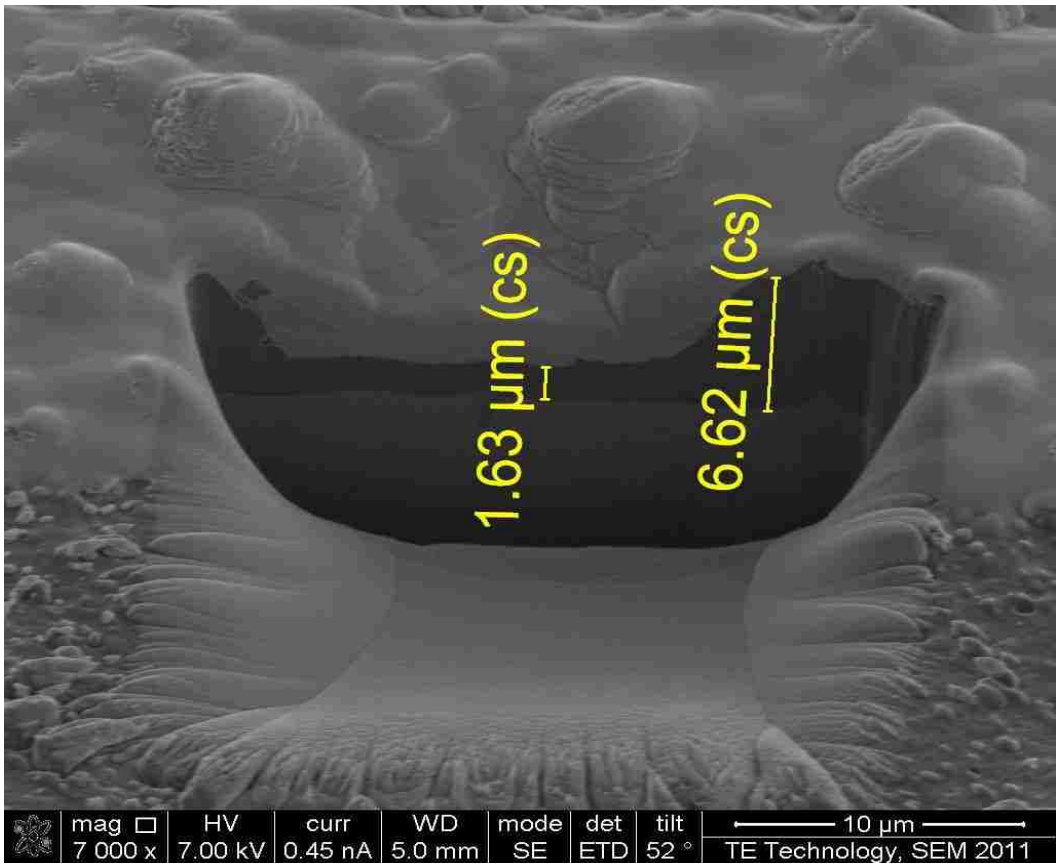

Figure 4-6: FIB Dimensioned Cross Section of the TiAlN Defect Presented in Figure 4-5

The EDS spectrums shown below in Figure 4-7 confirms that the darker layer at the surface is indeed the TiAlN coating since a spot spectrum collected at this layer consists of the corresponding titanium, aluminum, and nitrogen elements. In the same figure a spectrum of the base H13 steel is also depicted showing the expected iron peak with residual traces of the gallium from the gallium ions used to ablate the coating's surface.

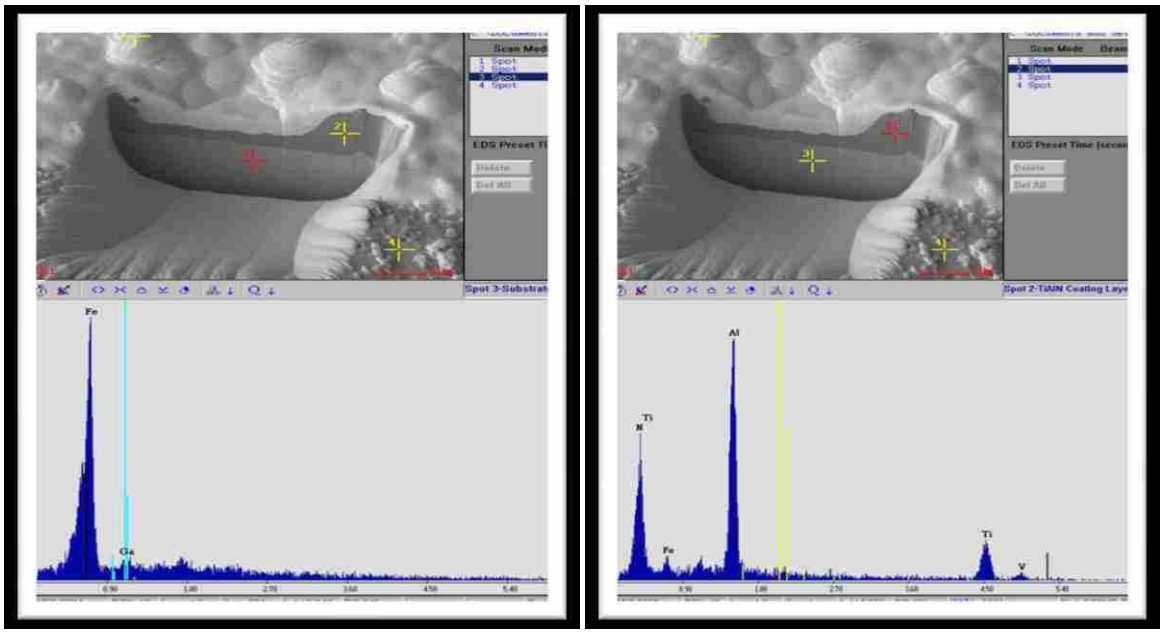

(A) **(B)**

Figure 4-7: EDS Elemental Spectrum of the FIB Cross Sectioned TiAlN Coating Defect Corresponding to (A) the Substrate Material and (B) the Surface Treatment

Of the three surface treatments under inspection, the DLC coating appears to most closely mirror the surface finish of the substrate. A characteristic SEM image of the surface of the DLC coating is presented in Figure 4-8. The surface finish resulting from the milling process of the uncoated H13 steel substrate is clearly still visible after DLC deposition.

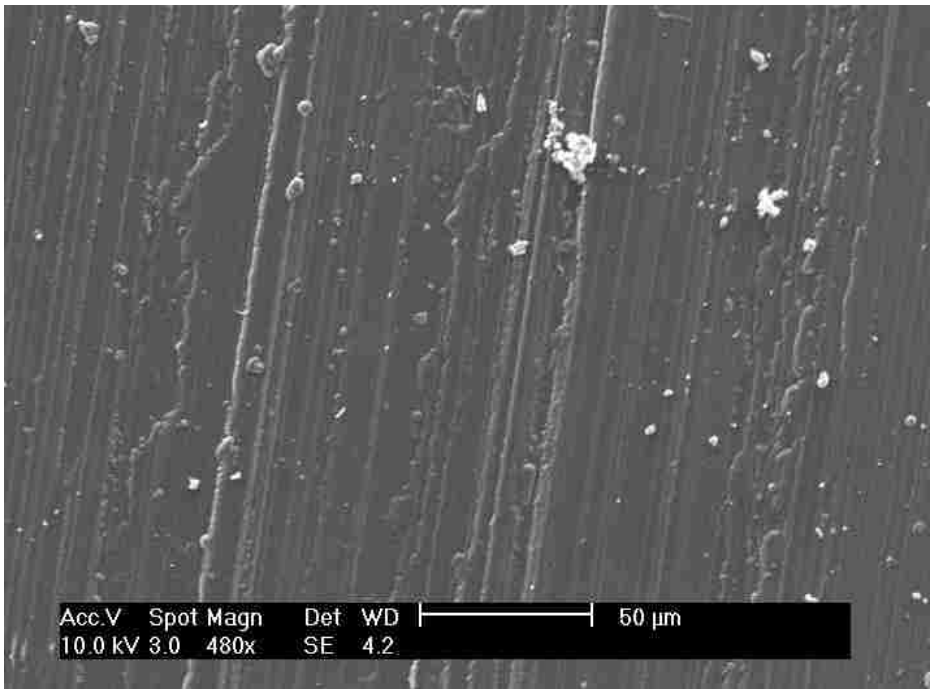

Figure 4-8: Characteristic Surface SEM Image of the DLC Coating

The FIB cross-sectional ablation of the DLC coating, refer to Figure 4-9, reveals a coating thickness of approximately 1.25µm with an approximately 370nm interfacial layer of chromium nitride which acts as a support layer for the amorphous carbon. This support layer is typically used in load bearing applications, which is exactly the case for an injection mold tool experiencing compression during clamping and pressurization of the cavity and melt delivery system. EDS spectrums presented in Figure 4-10 show the coating is strictly comprised of carbon with trace iron peaks resulting from charged particle penetration through the coating to the base material causing a slight collection of emitted x-rays characteristic of the iron in the steel substrate. Additionally, this figure shows the elemental spectrum of the interfacial layer of chromium nitride which contains evident chromium peaks and also has peaks corresponding to the

carbon coating and base substrate because the collected EDS contains some x-rays collected from the adjacent materials.

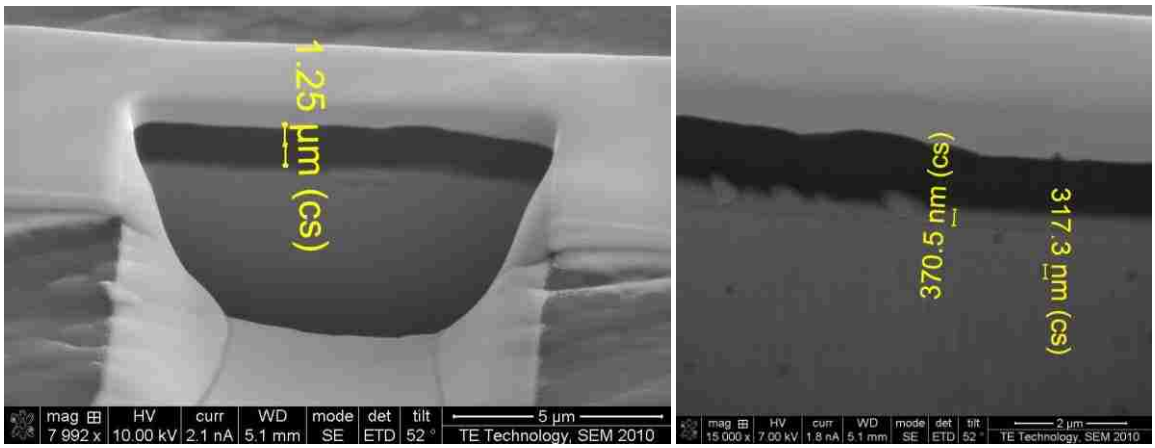

(A) **(B)**

Figure 4-9: FIB Dimensional Cross Section of (A) DLC Coating and (B) Interfacial Layer of Chromium Nitride

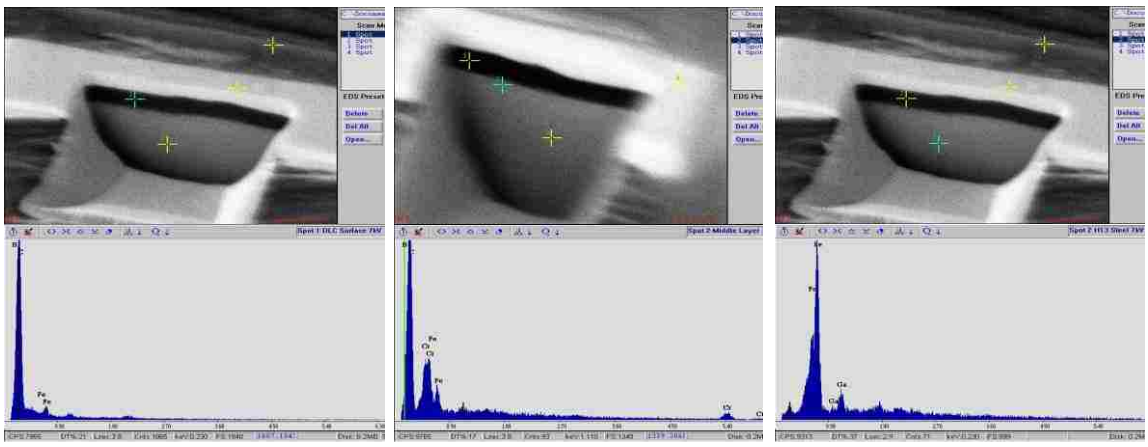

(A) **(B)** **(C)**

Figure 4-10: EDS Elemental Spectrums of (A) the Amorphous Carbon Layer of the DLC Coating, (B) the Interfacial Chromium Nitride Support Layer of the DLC Coating, and (C) the Base H13 Substrate.

For the DLC coating, localized exposure of the substrate is clearly evident on numerous DLC specimens, see to Figure 4-11. This result is unexpected

because the amorphous carbon portion of the coating is deposited by PACVD which is a conformal coating process. Exposure of the substrate material is undesirable as accelerated wear and corrosion will occur at the localized exposure and leading to corrosive pitting at the substrate potentially undercutting the coating and reducing adhesion. The general expectation is that coating deterioration will initiate and propagate from the localized regions of exposed substrate when subject to the injection molding tribological environment.

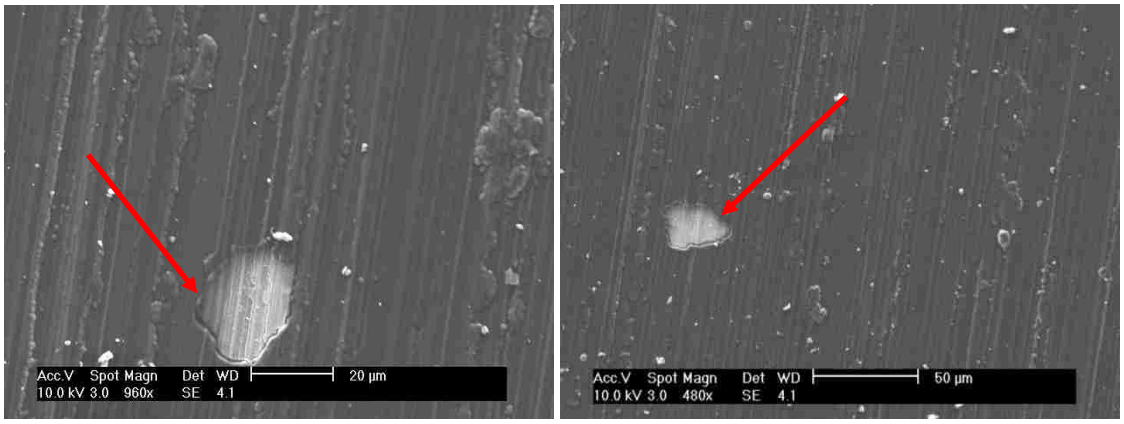

Figure 4-11: Characteristic Defect, Exposed Substrate, of the DLC Coating

Inspection of one DLC coated H13 sample via SEM reveals a relatively large concentration of the exposed substrate defect near an elevation change corresponding to the groove machined into the sample, for melt wear test gap, prior to coating deposition. The images, (A) and (B) in Figure 4-12, are images acquired in the SEM with a backscattering detector. Backscattering images have the advantage of clearly contrasting features composed of different elemental compositions. In the backscattered images, the bright white regions correspond to exposed substrate or residual H13 steel particles which landed on the coatings

surface during a post deposition grinding operation imposed on the coated samples to enable proper seating in the extrusion test die. The region highlighted in the red box in, Figure 4-12, is definitely exposed substrate from thorough inspection of this region with the scanning electron detector. The EDS spectrum presented in (C) of Figure 4-12 confirms that the elements at the surface of the bright white region indeed match the typical composition of the H13 substrate.

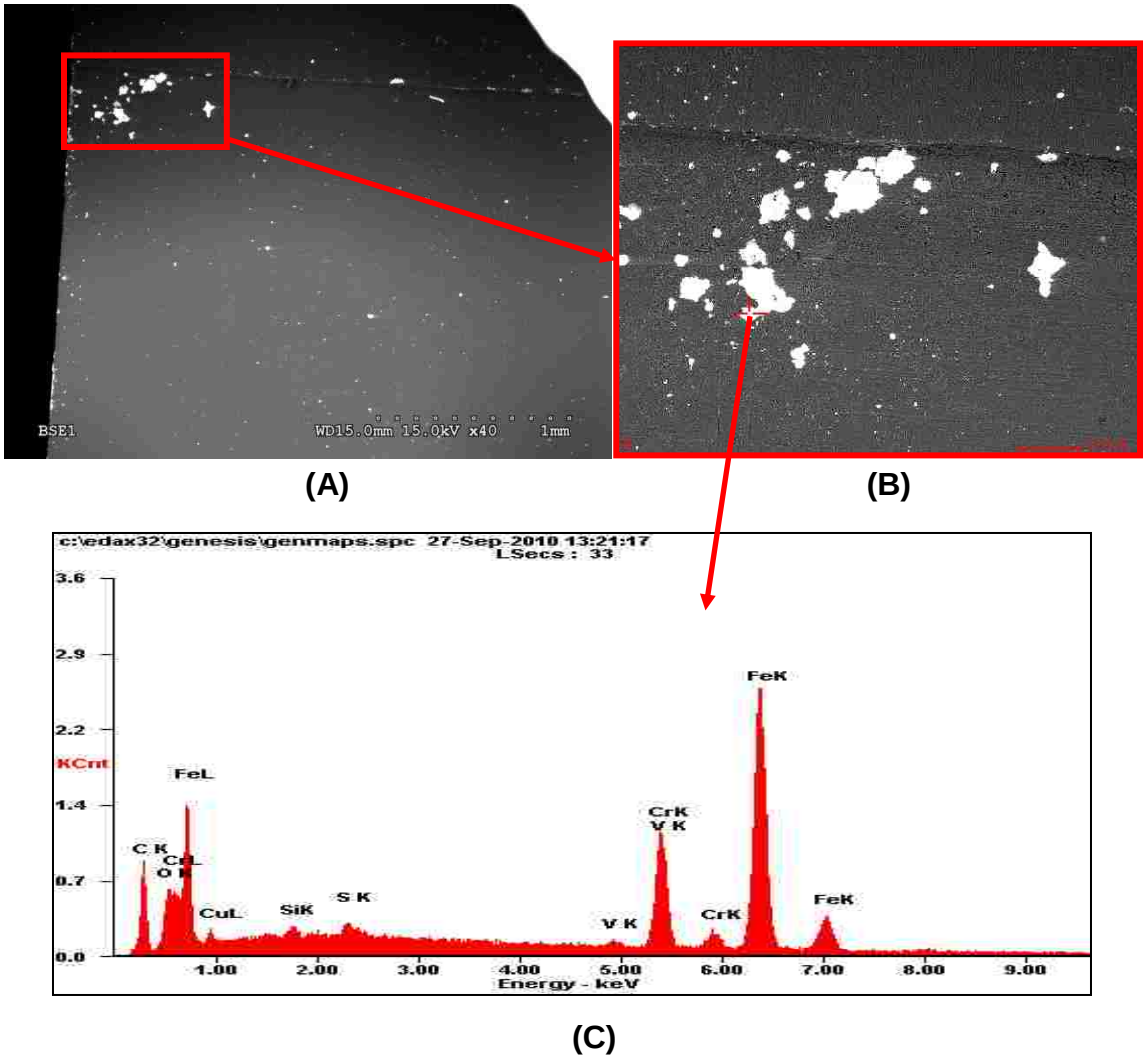

Figure 4-12: (A) Low Magnification Backscatter Image of DLC Coated Specimen, Clearly Showing Large Area of Exposed Substrate in Top Left Corner, (B) Increased Magnification Backscatter Image of Top Left Corner, (C) EDS Spot Spectral Image of Exposed Substrate

A characteristic SEM image of the chrome coated substrate is shown in Figure 4-13 with the EDS spectrum presented in Figure 4-14. In general, the electrodeposited chromium appears to mirror the condition of the substrate material prior to deposition with a slight smoothing effect. The EDS spectrum is composed of strictly chromium peaks with some carbon appearing in the spectrum. The chrome electroplating supplier states that the thickness of the chromium coating is approximately 50µm. An FIB cross-section of the chrome coating is not presented because the FIB employed is limited to surface ablation of less than 50µm penetration depth.

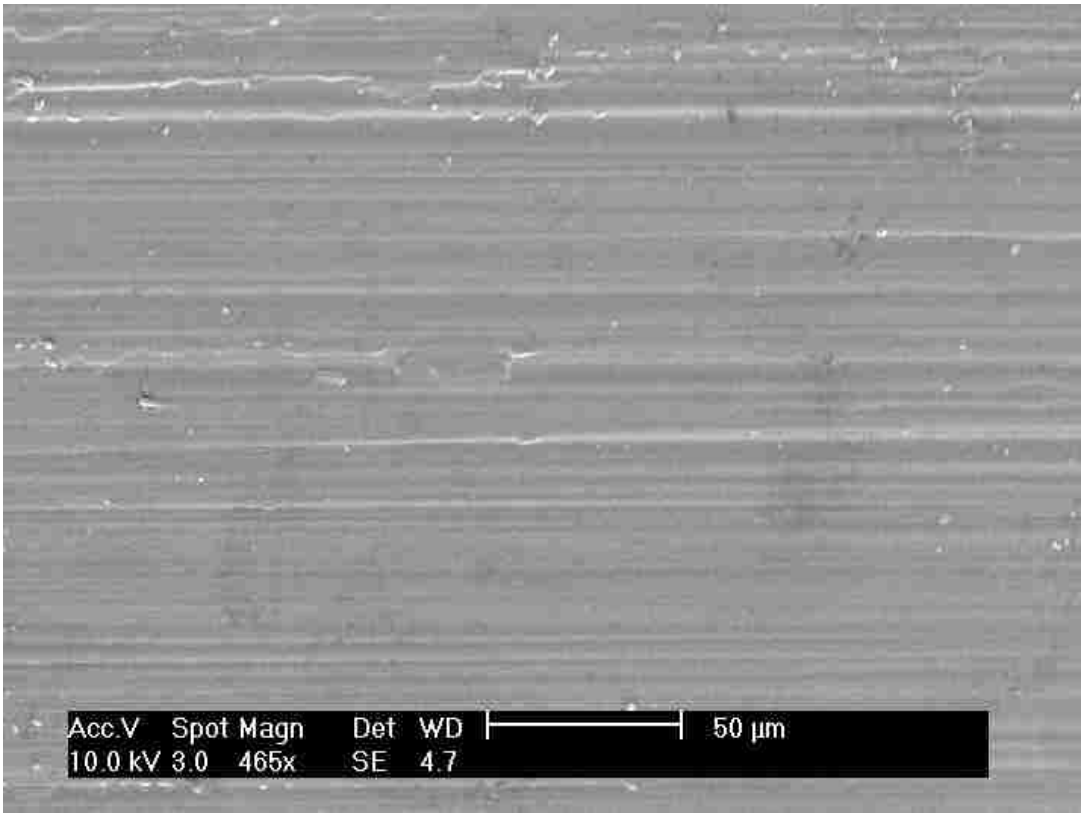

Figure 4-13: Characteristic SEM Surface Image of Coated Chrome Sample

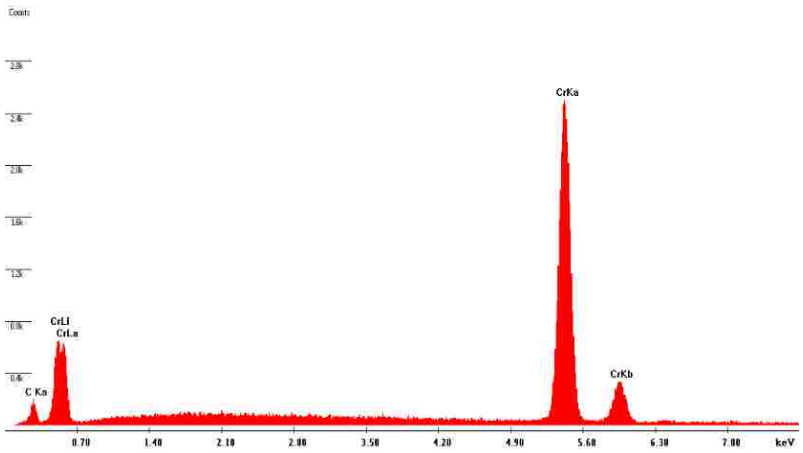

Figure 4-14: EDS Elemental Spectrum of Pristine Chrome Coated Specimen

The major defect evident in the electrodeposited chromium is the presence micro-cracking at the surface, see Figure 4-15. SEM observation of the surface of the chrome coated specimens shows that in general large regions of the surface are void of these micro-cracks, while some localized regions contain a heavily micro-cracked structure. The micro-cracking seems to dominantly occur at sharp exterior or interior corners of the coated specimens with inward propagation of these cracks.

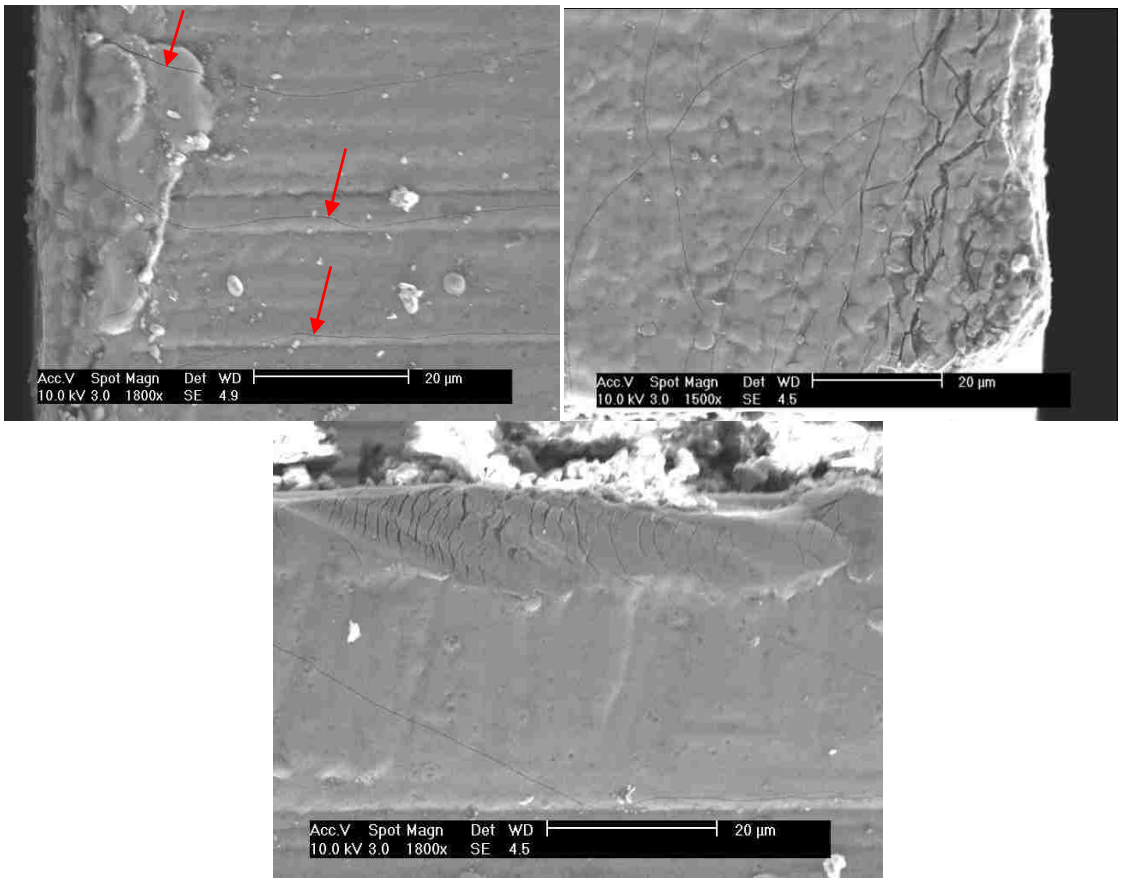

Figure 4-15: SEM Images of the Electrodeposited Chrome Revealing a Structure Containing a High Level of Micro-Cracks

4.1.2 Surface Roughness

Surface roughness measurements with the optical profilometer indicate that the deposited coatings examined in this study tend to mirror the surface topography of the uncoated H13 steel substrate to varying degrees. The average surface roughness of the uncoated samples is .506779µm with a standard deviation of .074371µm, which is an expected surface roughness value for the milling process. The average surface roughness of the DLC coated samples is .498721µm with a standard deviation of .103675µm showing a highly

mirrored surface topography compared to the base substrate likely resulting from the PACVD of the DLC. The average surface roughness of the TiAlN samples is .569164µm with a standard deviation of .059954µm. The higher surface roughness values of the TiAlN samples can be contributed to the "crater-like" defects discussed earlier. The average surface roughness of the chrome samples is .458328µm with a standard deviation of .132651µm, quantitatively confirming the SEM observed smoothing effect at the surface of the electroplated chrome specimens.

4.1.3 Porosity

The plot depicted in Figure 4-16 summarizes the results obtained via the anodic potentiodynamic polarization scans for the H13 substrate and substrates coated with electroplated chrome, DLC, and TiAlN. The key parameter for the plotted anodic scans is the integral of the scans, i.e. area under the curves, over the potential (voltage) range. A larger integral value indicates a higher degree of induced oxidation from the electrochemical processes. In the case of the coated substrates, a higher integral value entails a higher degree of porosity to the base substrate, considering that iron oxidation is assumed to be the dominant reaction occurring at the low applied voltages in the anodic scan. The base H13 uncoated substrate is used as a reference for comparison. Since the coatings in this study are highly inert to chemical reaction, the deposited coatings prevent corrosion from occurring at the substrate surface except for where direct passages, i.e. pores, for the electrolytic solution to the base substrate exist. As

the anodic scan curves approach the anodic scan curves of the reference material (the H13 steel), more porosity of the coating can be assumed. Obviously if the coating were to be completely removed from the substrate, 100% porosity would exist, and the anodic scans should be identical to the base material.

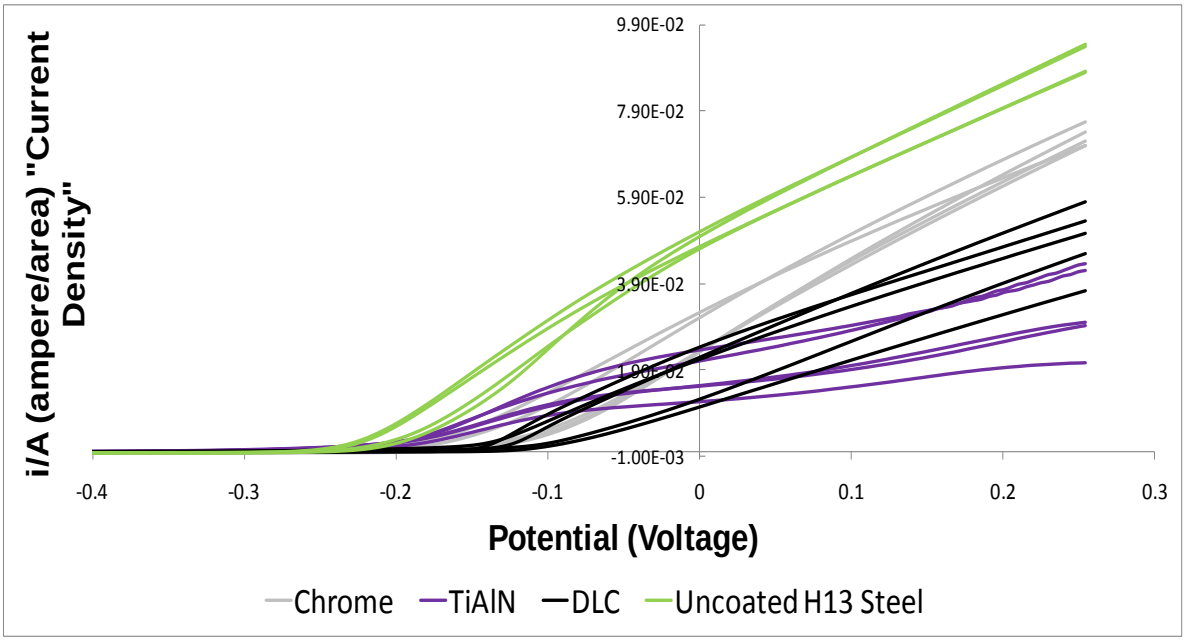

Figure 4-16: Plot of Anodic Potentiodynamic Polarization Scans for Chrome, TiAlN, DLC, and Uncoated H13 Steel

From the anodic scan plot in Figure 4-16, the electrodeposited chrome exhibits the highest degree of porosity, largest area under the plotted curves, of all the surface treatments examined. This finding most likely results from the micro-cracked structure of the hard chrome coating previously discussed in the SEM evaluation of the coatings. Both the TiAlN and DLC specimens exhibit less porosity than the chrome coating but are less conclusive when compared to each other. Some TiAlN samples exhibit less porosity than the DLC samples and vice

versa. In general, the PVD TiAlN and PVD/PACVD DLC specimens possess a higher degree of variability in the plotted anodic scans when compared the reference material and the electrodeposited chrome. This may suggest a higher degree of quality variation resulting from the manufacturing process.

4.1.4 Friction

For the application of surface engineering thermoplastic injection molds, low coefficients of friction (C.O.F) of the surface treatment against polymer is advantageous to reduce the incurred wear during demolding and to reduce the demolding force. A summary of the coefficient of friction results of the coating in sliding contact with a sinusoidal velocity against PBT and Nylon hemispheres with an applied normal load is presented in Figure 4-17, Figure 4-18, Figure 4-19, and Figure 4-20. Vertical error bars in the plots indicate plus or minus one standard deviation. The electrodeposited chrome exhibits the most lubricious properties under both loading scenarios and against both polymer varieties. The second most lubricious coating in these friction tests is the DLC. TiAlN exhibits the highest coefficient of friction for all tests conducted.

The performance of DLC in the friction tests is rather surprising. One major basis for selection of the DLC coating in this study is its extremely low coefficient against steel, approximately 0.1 - 0.2. Obviously, DLC's lubricious performance against steel does not translate to lubricous performance against the polymer compounds studied, nullifying one of the expected key strengths of the DLC coating for use on molds.

Some notable trends are also obvious in the friction plots. First, the variability in the friction data generated is greater under low loading scenarios in general. As the applied normal load increases, the spread in the C.O.F results for the different coatings decreases; in other words, the difference in C.O.F between the different coatings is less at high loads. Additionally, certain trends are evident for each coating type. For TiAlN, the C.O.F decreases with increasing load against both PBT and Nylon. DLC's C.O.F increases with increasing load against Nylon and decreases with increasing load against PBT. Lastly, the C.O.F of electrodeposited chrome increases with increasing load.

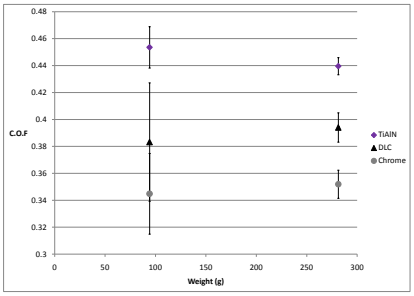

Figure 4-17: Plot of Mean Coefficient of Friction Values for Nylon Hemisphere under Normal Load with TiAlN, DLC, and Chrome

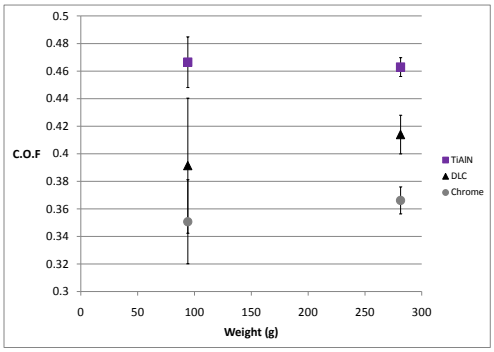

Figure 4-18: Plot of Median Coefficient of Friction Values for Nylon Hemisphere under Normal Load with TiAlN, DLC, and Chrome

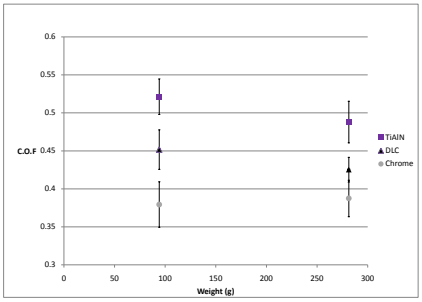

Figure 4-19: **Plot of Mean Coefficient of Friction Values for PBT Hemisphere under Normal Load with TiAlN, DLC, and Chrome**

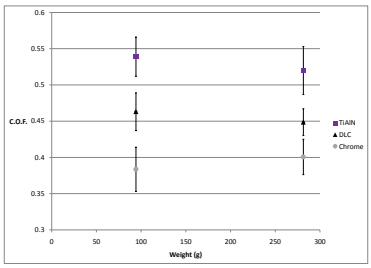

Figure 4-20: Plot of Median Coefficient of Friction Values for PBT Hemisphere under Normal Load with TiAlN, DLC, and Chrome

4.2 Evaluation of Worn Coatings

4.2.1 Pin-on-Plate Wear Testing against Copper Alloy Hemisphere

The results from the pin-on-plate wear test are presented in Figure 4-21-Figure 4-26. Only data obtained from testing at the high load setting is presented because the results do not show any significant wear for any coating type under any of the applied loading schemes. Additionally, since minimal wear is evident in all samples, all results correspond to the highest level of repetitions, 32,000, and the data for the other number of repetitions has been omitted. Considering that each repetition count is a forward and backward motion, the total number of dry slides across the surface is equal to 64,000 slides. SEM wear tracks and with the indicated direction of sliding contact for the electrodeposited chrome, TiAlN,

and DLC are shown in Figure 4-21, Figure 4-23, and Figure 4-25 respectively. Altitude measurements acquired with a surface profilometer across the entire length of the sample, including the wear track, show no indication of trenches/valleys generated by the dry sliding wear contact against the copper alloy hemisphere. The only noteworthy data gathered from the surface profilometer measurements of the wear tracks is a reduced surface roughness along the wear track. The reduction of surface roughness results from the smoothing effect of the surface exposed to sliding contact as the peaks of the surface are abrasively removed.

For the pin-on-plate testing, the weight of the copper hemisphere was recorded before and after testing to determine the amount of material loss due to abrasion. The results indicate a the highest amount of weight loss occurred for the copper alloy in contact with the TiAlN sample, with a weight loss of 0.006 grams at the high load and a weight loss of 0.003 grams at the low load. A weight loss of 0.001 grams of the copper alloy hemisphere occurred under the high load contact against both the chrome and DLC samples. At the low load no measurable copper weight loss is observed for either the DLC or chrome system.

Figure 4-21: Wear Track on Electrodeposited Chrome Sample after 32,000 Repetitions of Sliding Contact against Copper Alloy Hemisphere with Applied Weight of 494.9 g

EDS elemental analysis is employed on the surface of the wear track to determine if spectral elemental peaks from the base substrate are collected. Figure 4-22 shows an EDS spectrum collected from the surface of the wear track of the electrodeposited chrome coating. Surprisingly iron peaks are evident in the spectrum. Considering that the electrodeposited chrome coating possesses a thickness of over 50µm, the presence of iron peaks is totally unexpected because surface profilometer measurements exhibit no elevation change along the wear track. Iron peaks also exist in the EDS spectrum gathered from a region outside the wear track. The reason for the presence of iron peaks in both spectrums is unknown, but this is not an indication of exposed substrate because surface profilometer measurements do not confirm this. The only explanation for the presence of iron peaks is possible penetration of the charged particles

through the substrate or the micro-cracks in the coating and subsequent collection x-rays characteristic of the iron atoms in the base H13 steel, but this seems unlikely considering that the coating is relatively thick in comparison to DLC and TiAlN.

Other than the iron peaks and the expected chromium peaks, copper peaks are also evident due to abrasive material removal of the copper alloy hemisphere onto the wear track. The presence of copper peaks is also evident in the spectrums collected on the wear tracks of the DLC and TiAlN samples, Figure 4-24 and Figure 4-26, respectively.

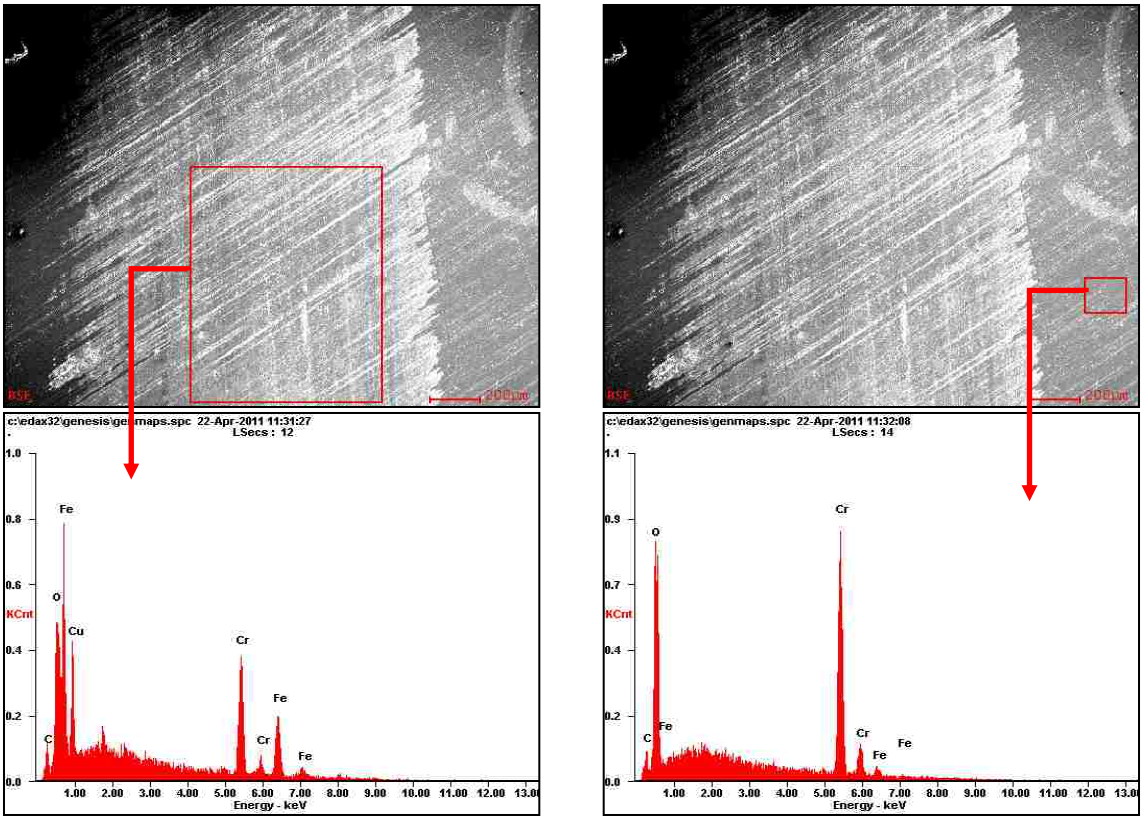

(A) **(B)**

Figure 4-22: EDS Spectrums of Regions Enclosed by Red Box in SEM Image of (A) Region of Wear Track Exposed to 32,000 Repetitions of Sliding Contact with Copper Alloy Hemisphere and (B) Pristine Portion of Coating

The temperature at the surface of the sample is increased from ambient temperature during the pin-on-plate sliding contact because of frictional heating. The presence of oxygen in the collected spectrums of the chrome sample is perhaps due to oxidation of the coating during the pin-on-plate test. This oxidation may result from the reduced oxidation resistance at the elevated temperatures. This hypothesis is somewhat unlikely considering the superb oxidation resistance of chromium.

A more likely justification for the presence of oxygen only on the chromium sample is that the frictional heat generated between the sliding chrome-copper

contact system is greater than that generated in the other coating-copper contact systems. Considering that DLC is a very lubricious coating in sliding contact against metal, less frictional heating in the DLC-copper sliding contact system is certainly plausible. Although the friction of the TiAlN sliding contact system is higher than that of the DLC system, a higher degree of abrasion in the copper alloy hemisphere is noted, as previously discussed. The higher induced abrasion results in a larger area of the copper hemisphere in contact with the TiAlN coating, thus reducing the applied pressure and localized frictional heat generation. The abrasion of the copper in the chrome-copper contact system is minimal; thus, the contact pressure is greater than in the TiAlN system because of a smaller area in contact with the sample. With the greater contact pressure, the localized frictional heating of the copper hemisphere should be higher in the chrome-copper system, resulting in temperature induced oxidation of the abraded copper particles.

This hypothesis is also substantiated by the color of the abraded copper particles in the case of the chrome-copper system. In this system, the color of the abrade particles is black which is indicative of copper oxide. The abraded copper particles in the other system maintain the original color of the copper specimen prior to testing.

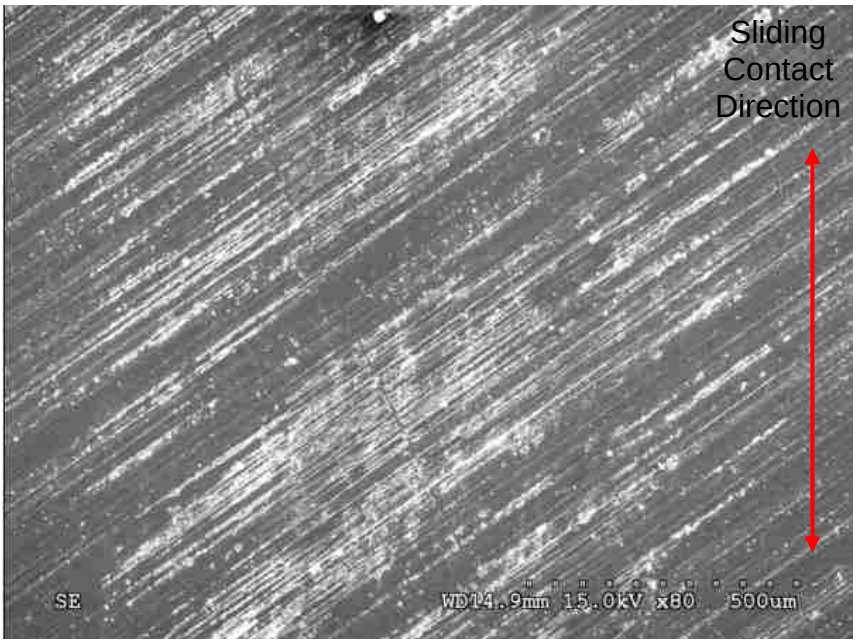

Figure 4-23: Wear Track on PACVD DLC Sample after 32,000 Repetitions of Sliding Contact against Copper Alloy Hemisphere with Applied Weight of 512.3 g

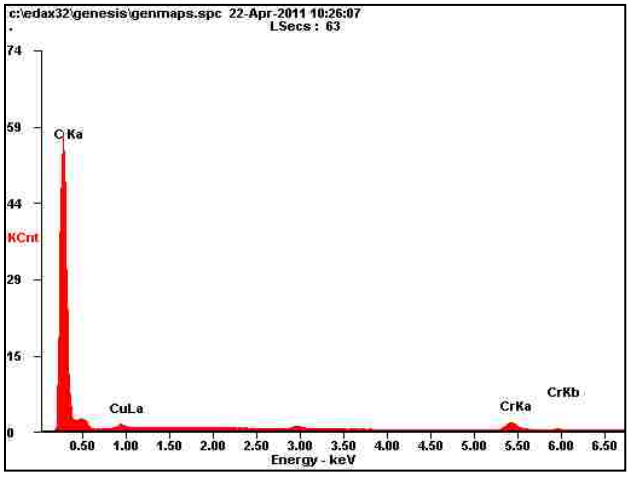

Figure 4-24: EDS Spectrum Focused on Portion of DLC Wear Track Exposed to 32,000 Repetitions against Copper Alloy Hemisphere

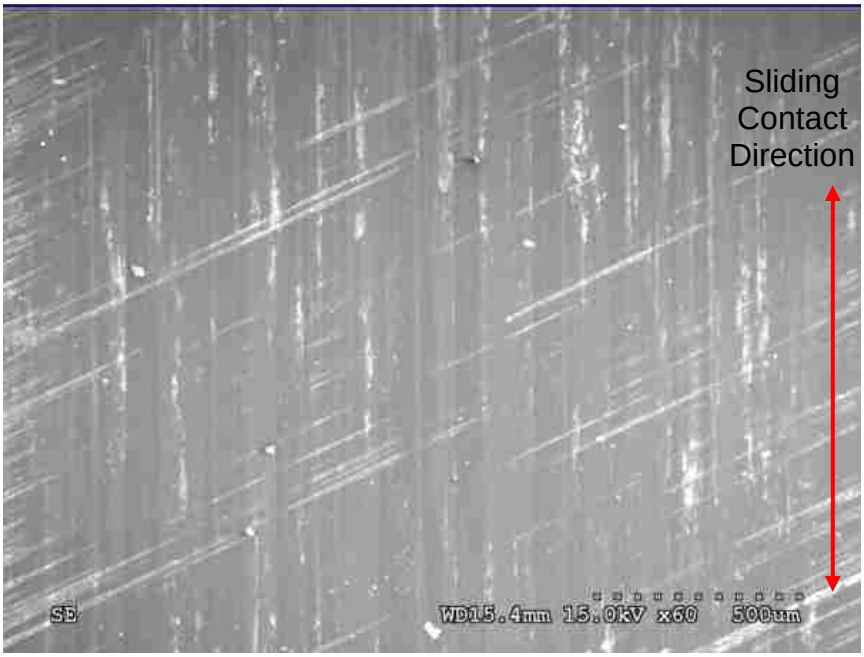

Figure 4-25: Wear Track on PVD TiAlN after 32,000 Repetitions of Sliding Contact against Copper Alloy Hemisphere with Applied Weight of 487.0 g

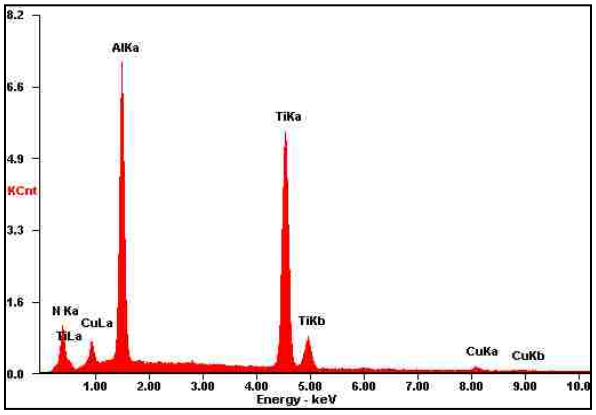

Figure 4-26: EDS Spectrum Focused on Portion of TiAlN Wear Track Exposed to 32,000 Repetitions against Copper Alloy Hemisphere

4.2.2 Melt Wear Testing via Extrusion

To quantify the amount of wear incurred during the melt wear testing, comparison of surface profilometer measurements of the groove which forms the test gap before and after melt wear testing was the intended method. This

method is found to be unfeasible for the extrusion process and the polymer compound employed in this study. The major issue is removal of the polymer compound from the surface of the sample after melt wear testing. PBT is heavily resistant to solvent attack. After testing of the polymer compound against an array of solvents, only extremely aggressive solvents dissolved the polymer compound. Subjecting the coated samples to an aggressive solvent is undesirable as these solvents could also attack the coatings and substrate material. Oxygen plasma cleaning of the samples after melt wear testing also proved to be unfeasible. Exposure to oxygen plasma can also induce corrosion of the samples; therefore, exposure time must be minimized. Even after extended periods of exposure to oxygen plasma residual polymer remains on the sample.

The optical surface profilometer requires a reflective surface to record measurements. Residual polymer on the surface of the coated samples is found to obstruct the reflective properties of the coating, resulting in an inability to record reliable measurements on the surface profilometer after melt wear testing via extrusion. This phenomenon is depicted in Figure 4-27. Reliable measurements of the surface topography can be recorded prior to melt wear testing, yet after exposure to the polymer melt in the extrusion die the measurements obtained with the surface profilometer contain an extremely large number of erroneous spikes. These erroneous spikes make any reasonable quantification of incurred wear impossible; therefore, qualification of the incurred wear is done by SEM inspection of the surface after melt wear testing.

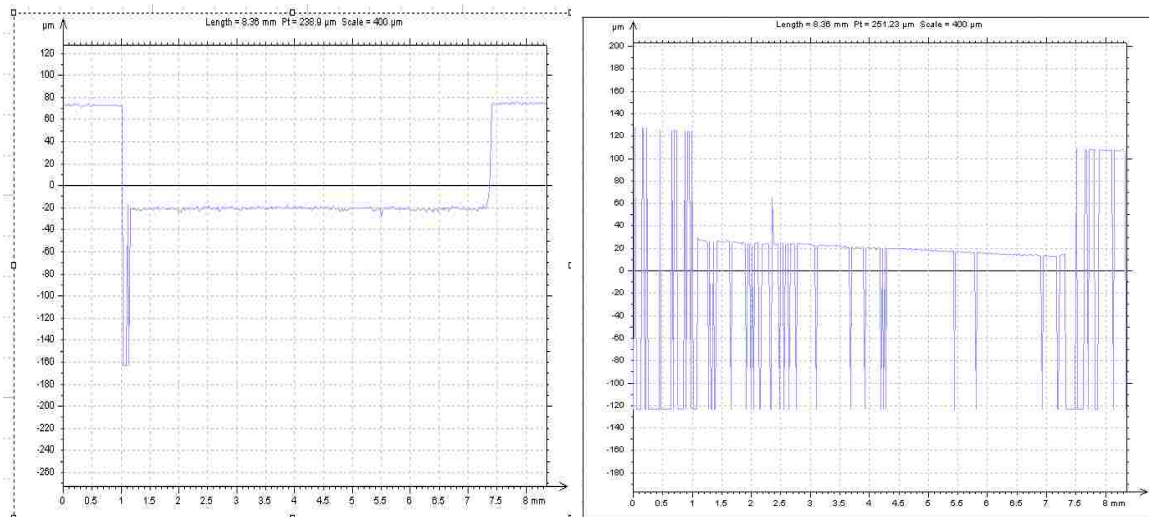

(A) **(B)**

Figure 4-27: Typical Surface Profilometer Data Sample (A) before Melt Wear Testing and (B) after Melt Wear Testing

The dominant wear is found to occur at the leading corner of the sample which serves as the entrance to the test gap. This position is illustrated in Figure 4-28. This finding is unique in comparison to the DKI platelet method, which does not position samples in a manner such that flow is accelerated around a corner.

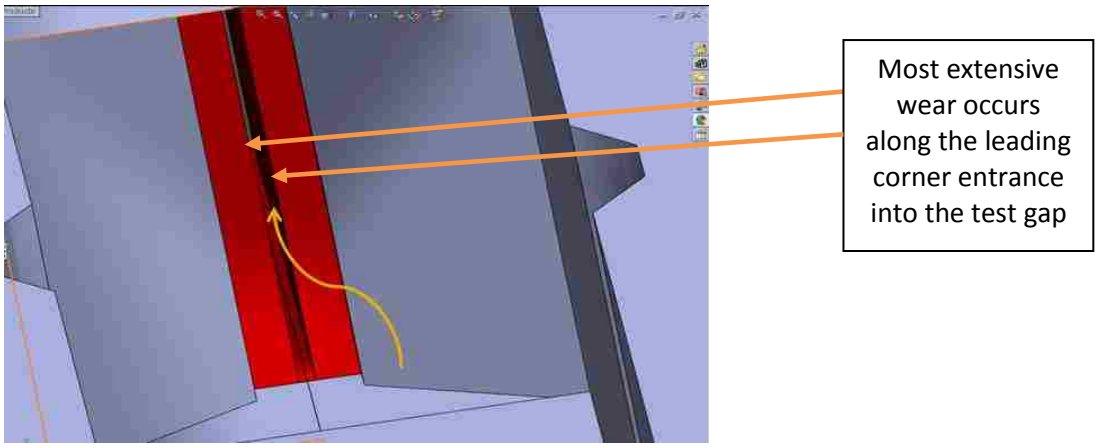

Figure 4-28: Solid Works Image Depicting Wear the Highest Degree of Wear is Occurring (Test samples are indicated by the color red)

An image of the worn electrodeposited chrome sample after exposure to 18.6 kg of PBT is shown in Figure 4-29. The major wear mechanisms appear to be both micro-milling due to the high filler content of the PBT and also corrosion. The leading corner of the chrome sample which served as the entrance into the test gap exhibits a rounded geometry. Prior to melt wear testing, the corner was relatively sharp. Corrosive pitting of the chrome samples is illustrated in Figure 4-30, as well as noticeable oxygen peaks in EDS spectrums corresponding to oxidation of the samples. The images of the worn surface shown in both figures are characteristic of all chrome samples inspected after the PBT polymer throughput.

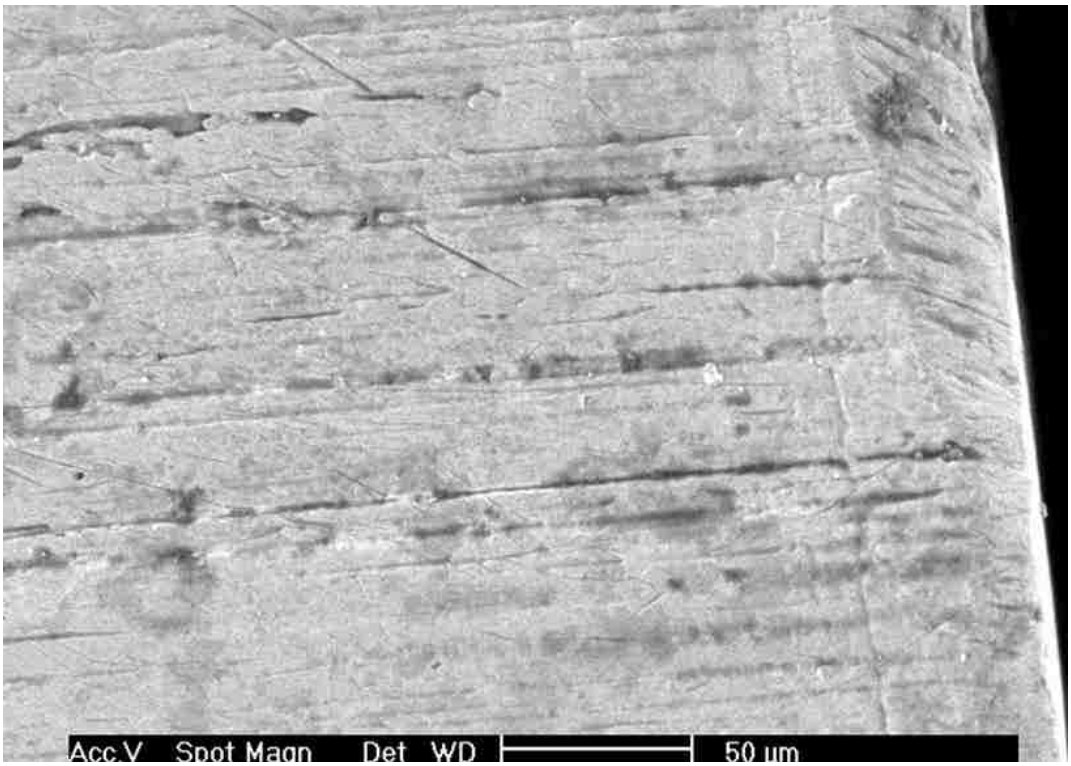

Figure 4-29: SEM Image of Chrome Showing a High Degree of Wear at the Leading Corner Entrance into the Test Gap after Melt Wear Testing with 18.6 kg Throughput

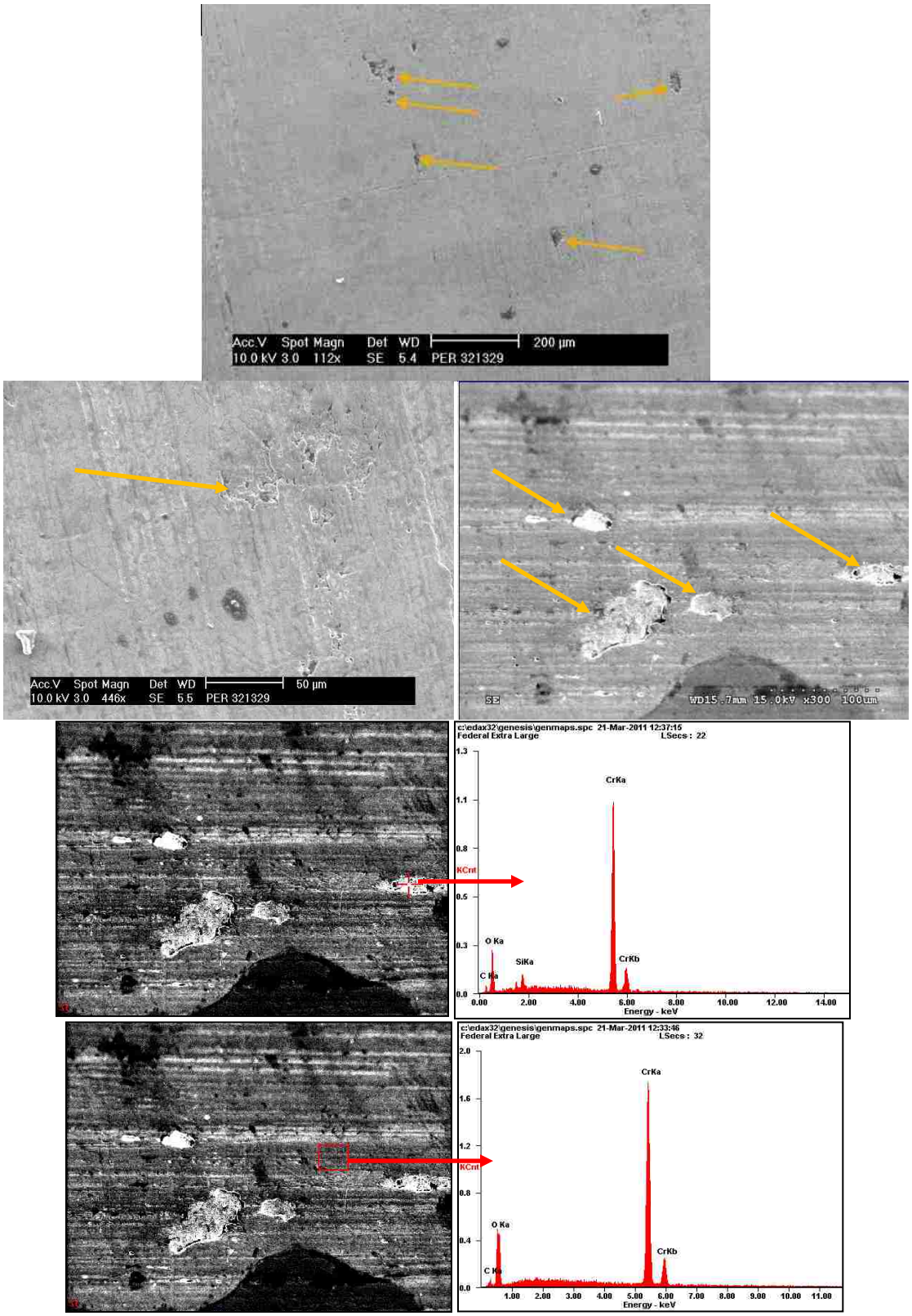

Figure 4-30: SEM Images and EDS Spectrums Highlighting the Corrosive Pitting Evident in the Electroplated Chrome Samples after Melt Wear Testing

The major wear mechanism evident in the DLC coated samples after melt wear testing is localized delamination of the coating from the substrate material. Both the DLC and TiAlN samples were exposed to 20 kg of PBT throughput. Figure 4-31 depicts an SEM image of the DLC coating after PBT melt wear testing, which possesses no observable wear. This is characteristic much of the DLC surfaces inspected by SEM after the melt wear test, yet localized regions of coating delamination are certainly evident. Corrosion of the coating is not observable with

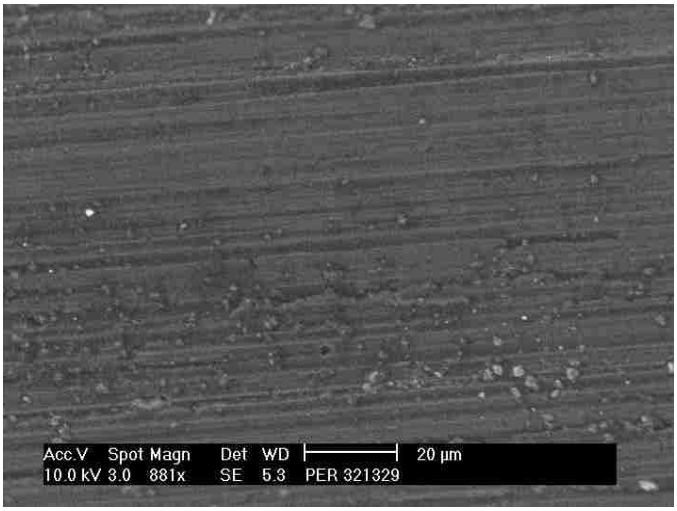

Figure 4-31: SEM Image of Region of DLC Coating Exhibiting no Wear after the Melt Wear Test with 20 kg Throughput

Figure 4-32 shows severe corner wear at the leading edge of the DLC sample forming the entrance into the test gap. These images clearly show delamination of the coating and exposure of the base substrate. This finding is confirmed by EDS analysis at the apparent delamination region, which provides

an elemental spectrum corresponding to the base H13 steel. Accelerated abrasive wear and micro-milling of the steel substrate is also palpable.

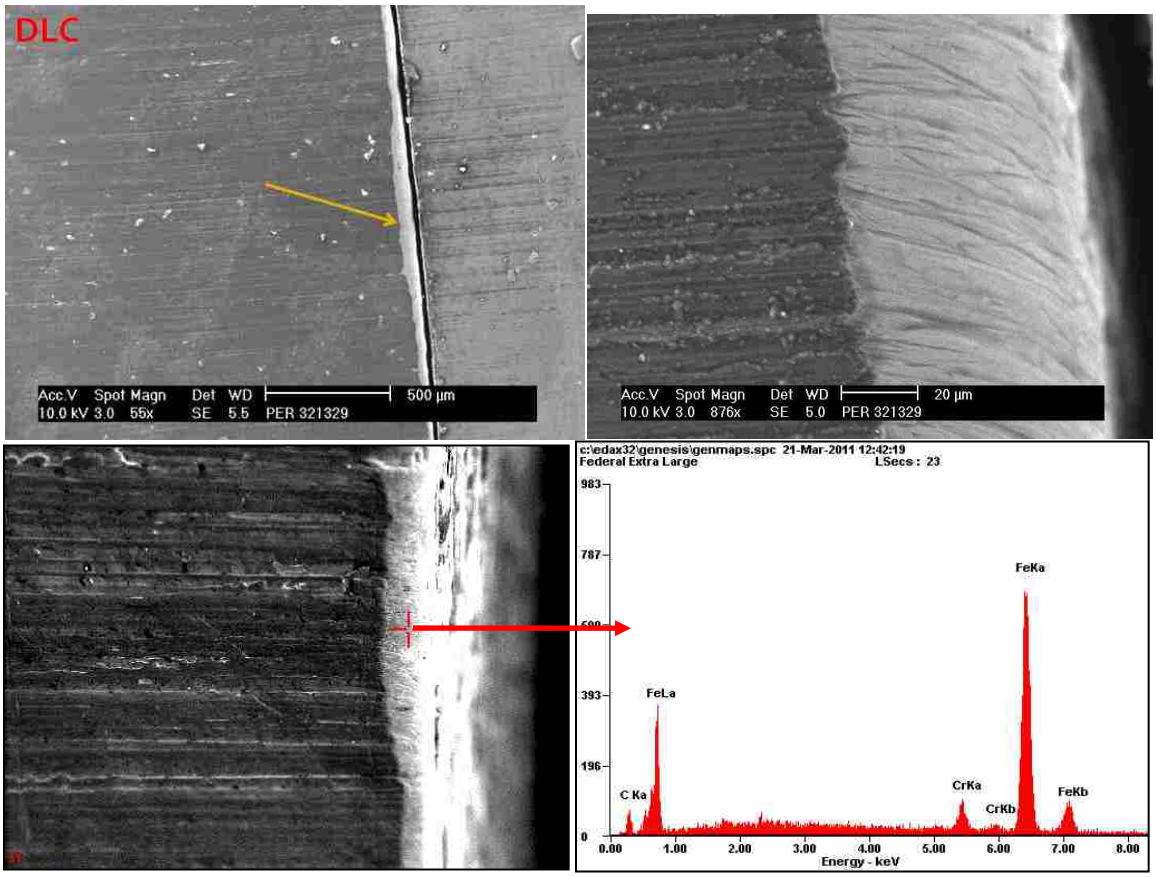

Figure 4-32: High and Low Magnification SEM Images and EDS Spectrum of TiAlN Sample Showing Delamination at the Leading Corner Entrance into the Test Gap after Melt Wear Testing with 20 kg Throughput

Delamination of the coating is not limited to the leading corner forming the entrance to the test gap. The rear corner of the DLC sample also exhibits delamination. This is perhaps due to compression of the DLC sample in the extrusion die during assembly, which is necessary for the extrusion die design utilized in this study. Such compression of a coating possessing a thickness of

only 1.25 µm can induce cracking of the coating and subsequent delamination of the coating after exposure to the flowing polymer melt.

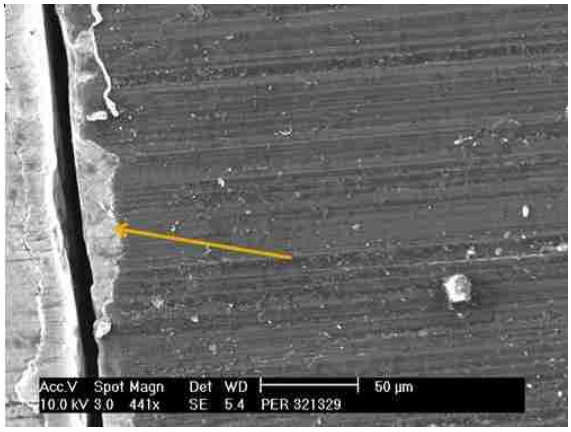

Figure 4-33: SEM Image Showing Coating Delamination at Rear Edge of DLC Sample

Delamination of the DLC coating in the direction of flow is also manifest in the localized interior regions of the samples. Figure 4-34 illustrates such coating removal. In some regions of the coated DLC samples, an extremely large amount of localized delaminations are observable. As the number of these localized delaminations increase, it is expected that the subsequent coating removal with further polymer throughput will be accelerated.

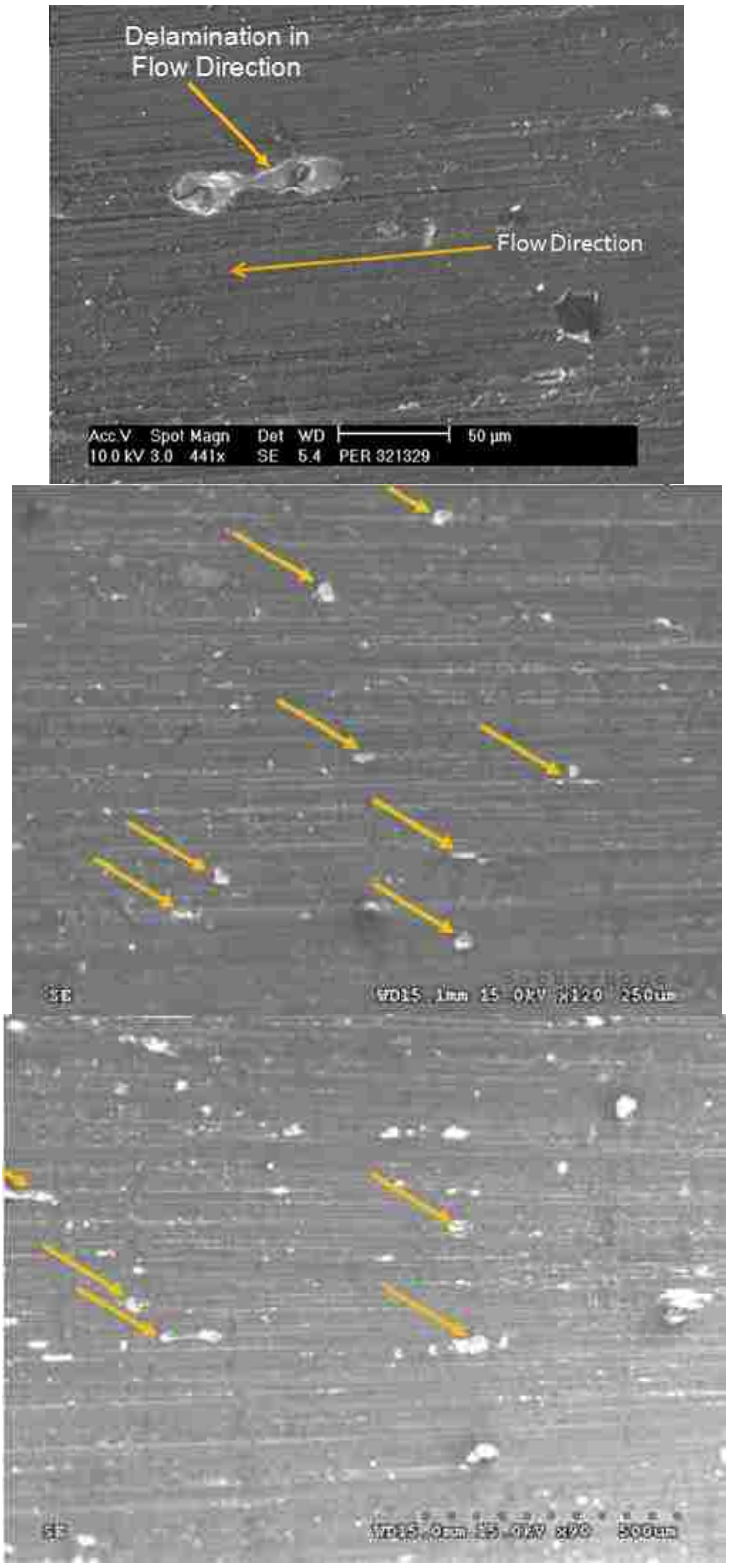

Figure 4-34: SEM Images Showing Localized Delamination of the DLC Coating in the Flow Direction after Melt Wear Testing with 20 kg Throughput

The TiAlN surface treatment exhibited the highest level of wear and corrosion resistance of all the samples examined in this study. SEM images of the characteristic condition of the TiAlN surface after PBT melt wear testing are presented in Figure 4-35. After meticulous inspection with a SEM and EDS, no wear or oxidation is of the coating is observable. The leading corner of the TiAlN sample which formed the entrance into the test gap also displays no observable wear, refer to Figure 4-36.

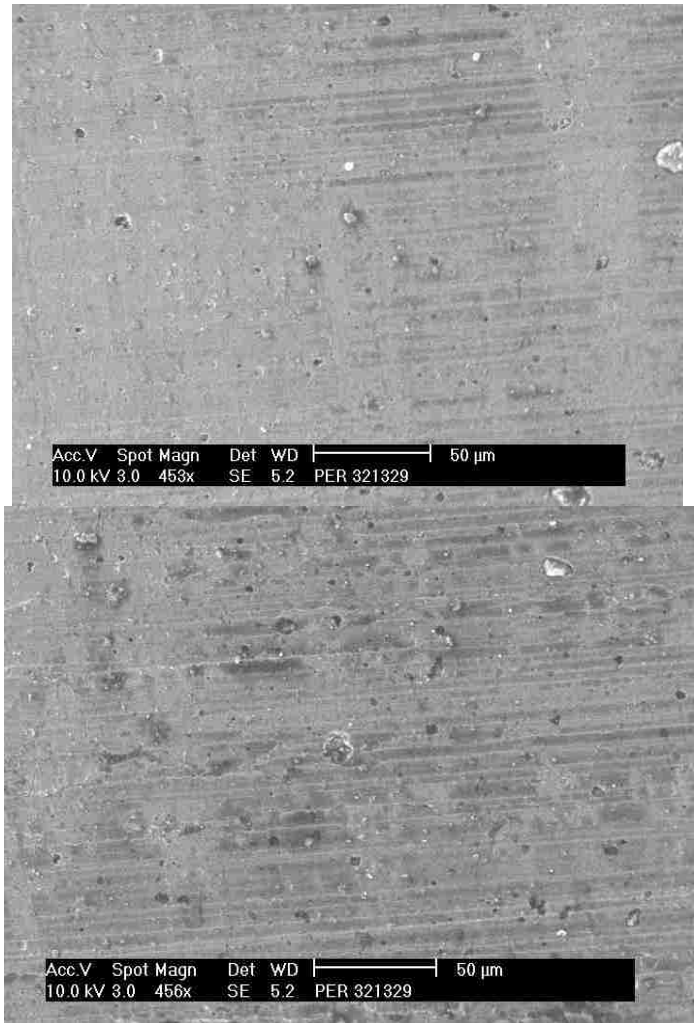

Figure 4-35: SEM Images Showing Seemingly no Wear of the TiAlN Samples after Melt Wear Testing

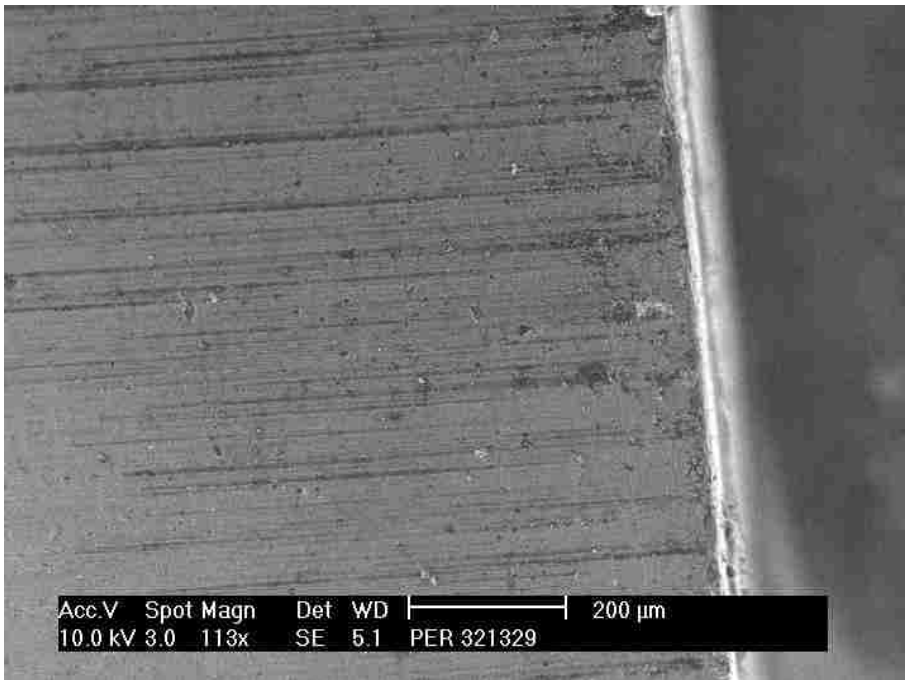

Figure 4-36: SEM Image Showing Superior Performance of the Leading Corner of TiAlN Sample at Entrance to Test Gap after Melt Wear Testing with 20 kg Throughput

Chapter 5 : Conclusion and Recommendations for Future Work

5.1 Conclusion

Surface engineering for injection mold tooling is vital for the economic feasibility of the injection molding process. Indeed, proper selection and application of surface treatments can give an injection molding corporation a competitive edge. The selection of surface treatments for mold tooling is not a trivial task. Many factors must be considered before selection of a mold coating. These factors include the industrial supplier, chemical composition and mechanical properties of the coating, deposition process, restrictions imposed by the injection mold, and the polymer compound being processed.

The deposition temperature of the selected coating process is of paramount concern. This temperature must be below the original tempering temperature of the mold steel to ensure dimensional stability and to ensure that the hardness of the substrate material is preserved, providing a solid foundation for the selected functional hard coating, especially considering the compressive stresses endured by an injection during the mold clamping and pressurization of the mold cavity. Often the best wear resistant coatings are deposited at the highest temperatures, yet such depositions processes are not feasible for injection mold tooling.

Additionally, the mechanical properties and structure of the coating itself must be considered. Surface treatments should inherently possess high hardness to provide abrasion resistance, yet also be chemically inert to prevent corrosion. The deposition process selected should provide strong adhesion strength at the coating-substrate interface. The inherent mechanical properties of the coating itself are of little concern if delamination of the coating subsequently leaves the base substrate exposed to the harsh tribological environment of the molding process. Coatings will not last forever; therefore, coatings that are chemically strippable are preferred because the base substrate will remain relatively unaffected. After chemically stripping the worn coating, the mold substrate can be recoated with little complication, providing a pristine mold. Mechanical stripping is an invasive process which can damage the base substrate leading to timely and costly mold repair. Ideally, minimal porosity is present in the mold coating to ensure isolation of the substrate from the polymer

compound. Also, chemical inertness of the coating is desirable to prevent corrosion at the coating's surface. To ensure minimal demolding force and wear incurred during the demolding cycle, coatings should be lubricious against the polymer compound being molded. Coating thickness and uniformity needs to be considered when designing and fabricating the mold, especially when narrow dimensional tolerances exist in the part to be manufactured, especially with micromolding. Conformal deposition processes which deposit coatings of homogenous thickness are preferred over line-of-sight processes which have limitations in coating complex geometry.

With the wide variety of coating processes available, the selection of coatings and deposition processes can be narrowed by eliminating the processes and coating varieties that violate the key considerations of importance for the specific injection mold being fabricated. Although, even after narrowing down the possible coatings and coating processes, a wide array of coating types will still remain. This is problematic because enough scientific information is not available to properly specify the optimal mold coating; therefore, injection molding companies should implement testing procedures, which emulate the tribological environment of the injection molding process, to evaluate coatings of interest.

This thesis evaluates three commercially supplied surface coatings for use in wear and corrosion resistance in injection mold tooling. The three coatings evaluated are each deposited via different coating technologies. The three

coatings evaluated are electrodeposited chrome, PVD TiAlN, and PVD/PACVD DLC with a CrN interfacial layer.

Results indicate that all three coating types mirror to surface topography of the substrate to varying degrees. The topography of the DLC coating most closely conforms to the base substrate likely due to the PACVD of the amorphous carbon which is a conformal coating technique, yet the DLC coating shows localized regions of exposed substrate. The electrodeposited chrome shows a reduction in surface roughness when compared to the base substrate. A network of surface micro-cracks is evident on the surface of the electrodeposited chrome coated specimens, which are generally located at sharp corners of the samples and propagate inwards. PVD TiAlN shows increased surface roughness due to “crater-like” defects existing on the surface.

Porosity testing is conducted via potentiodynamic polarization. Results of the porosity test reveal that electrodeposited chrome possesses the highest degree of porosity of the three coatings examined. TiAlN and DLC exhibit reduced porosity in comparison to electrodeposited chrome. Some TiAlN coated substrates exhibit more porosity than some DLC coated substrates and vice versa. A higher degree of variability in porosity is revealed for both the TiAlN and DLC coated samples in comparison to electrodeposited chrome, indicative of a higher degree of variation in coating quality from the deposition process.

Friction testing of the samples against PBT and Nylon polymer compounds shows that the electrodeposited chrome has superior lubricious properties against the two polymer compounds. TiAlN exhibits the highest

coefficient of friction against both plastics. The coefficient of friction values for the DLC coating falls in between the TiAlN and the hard chrome specimens.

Focused ion beam cross-sections of the DLC and TiAlN coatings are conducted to analyze coating thickness and inspect coating defects in the case of TiAlN. The FIB cross-section of the DLC coating reveals a coating thickness of approximately 1.25µm with an interfacial layer chromium nitride, approximately 370.5 nm thick. TiAlN exhibits a bulk coating thickness of approximately 6.62 µm with nearly a 75% reduction of coating thickness at the surface defect inspected.

Pin-on-plate wear testing of the three coatings in sinusoidal sliding contact with a copper alloy hemisphere shows no appreciable wear on the surface of the coatings even after 64,000 translations. Surface profilometer measurements along the wear track indicate no valley creation, only a reduction in surface roughness in the test region is noticeable. The results of the pin-on-plate wear test show outstanding performance of all coatings tested and suggest that higher applied loads should be used in future work. During pin-on-plate wear testing loss of weight of the copper alloy hemisphere is greatest when in contact with TiAlN and is comparable for both the DLC and electrodeposited chrome.

To simulate the tribological environment experienced by injection molds during polymer processing, a novel test extrusion die has been developed and is employed in this study. Results of melt wear testing indicate that wear can be observed with minimal polymer throughput, relative to that experienced by an injection mold in constant production. The highest level of induced wear occurs on regions of the sample that form the entrance to the test gap where the

polymer melt is accelerated around a sharp corner, which is similar to the tribological environment of a gate in an injection mold. Melt wear testing of the coated samples against the flowing molten PBT compound reveals superior wear and corrosion resistance of the TiAlN coating in comparison to the chrome and DLC coatings. No appreciable wear or corrosion is evident in the TiAlN samples. Both the DLC and chrome coatings show a high degree of wear along the corners forming the entrance to the test gap. The dominant wear mechanism for the DLC coating is delamination of the coatings from the substrate. Although PACVD generates strong adhesion from chemical bonding with the substrate, the PVD/PACVD BALINIT® DLC STAR has PACVD DLC applied on top of a PVD CrN interfacial support layer; therefore; attachment to the substrate is merely maintained by mechanically. Corrosion of the DLC coating is not evident. Corrosive pitting and micro-milling on the surface of the electrodeposited chrome are the dominant wear mechanisms in the melt wear test.

Considering that wear is a function of the tribological environment, the degree and type of wear induced on surface treatments will vary depending on substrate material, processing conditions, mold design, and material being processed; therefore, a no general recommendation for mold surface treatments can be realistically specified. TiAlN does exhibit promising results for the replacement of electroplated chrome for use on injection mold tooling. Although appreciable wear is evident in both the DLC and chrome coatings, DLC is not recommended for coating mold geometry in contact with flowing polymers because the thickness is extremely small and coating delamination quickly

initiates and accelerates. This delamination exposes the substrate material, which possesses inferior wear and corrosion resistance, to the harsh tribological environment of the flowing polymer compound leading to accelerated wear resulting in timely and costly mold repairs, especially if the wear is noticed by the operator in a timely fashion. DLC does exhibit good lubricity in metal-to-coating contact, and is probably best employed on components used in sliding metal contact such as mechanically actuated slides, guide pins, and ejection rods.

The general recommendation is for injection molding companies to actively implement their own testing procedures for evaluation of surface treatments. The testing methodology in this thesis provides a good basis for such tribological evaluation of surface treatments.

5.2 Directions for Future Work

Since the best technique to evaluate wear and corrosion resistance is to subject the coating to conditions that most closely match those seen in its intended application, refinement of the melt wear testing apparatus used in this study is a logical next step. The test apparatus in this study exposes the samples to relatively constant uniform velocities with static pressures and constant temperatures. Injection molds experience dynamically changing velocities and pressures as well as rapid temperature cycling and solidification and ejection of a polymer; therefore, creation of a test apparatus that can effectively induce all these parameters is desirable. Such a test apparatus also

needs to be able to induce wear quickly and provide uniform conditions to all surface treatments being testing for consistency and efficiency.

Since the pin-on-plate wear test did not induce any substantial wear on the coatings, this test should be repeated with much higher applied loads. Additionally, the problem of removing the residual polymer on the coated specimens after melt wear testing is a major setback in this study. Future studies should address this issue to allow quantitative techniques for determining the amount of material loss, like surface profilometry, to be utilized.

An obvious direction for future work is using a wider array of surface treatments. TiN and TiCN PVD coatings which already have gained much commercial success are recommended for future studies. The future of the coating industry seems to be moving in the direction of multilayer and superlattice coatings. These coatings possess interesting properties such as providing stiffness gradients from extreme hardness at the surface tailored throughout the thickness of the coating to match the mechanical properties of the substrate at the interface, which provides superior adhesion to the substrate. Additionally, multilayer coatings inhibit crack propagation by altering the direction of the crack from the normal direction to the substrate to a direction that is parallel with the substrate at the subsequent interfacial layers of the coating. Also the combination of different coating processes is gaining attention, such as applying an electroless nickel coating to the substrate which provides excellent corrosion resistance and then electrodepositing chrome onto the layer of nickel which provides the high hardness required for abrasion resistance. Aside from

researching different coating types, evaluation of the same coatings from different commercial suppliers can aid those in industry with selection of the best supplier.

An expansion of the selected polymer compounds used for wear testing is recommended. Perhaps with a wide array of polymer compounds tested, different polymers can be subcategorized into distinct groups which impose similar wear mechanisms on the surface treatments. Categorizing the polymer compounds by the characteristic induced wear on the coatings may enable testing of one polymer compound type to accurately be applied to a much larger family of plastics.

The focus of this study is injection mold tooling, but other components of the injection molding machine are also exposed to harsh tribological environments such as: reciprocating screws and check valves. Evaluation of surface treatments and creation of testing methods to emulate the tribological environment of these components, which has been done to a certain degree by the Kunststoffe-Institute in Germany, is a promising future direction. Wear of these components also results in significant financial losses resulting from the cost and production downtime associated with repair/replacement of the worn components.

To determine the functional relationship between the demolding force and the surface engineering technique, a novel experimental setup is proposed. The setup should include modular cores which can be coated and inserted into a test mold. Molten polymer compounds of interest can be injected around these

cores, solidified, and ejected, like in the typical molding process. Pressure transducers mounted at the back of the ejection rods can be used to monitor the required ejection force.

In general, tribological evaluation of surface treatments for polymer processing has received little attention from the scientific community. Many opportunities exist to further the scientific knowledge base in this field.

Works Cited

[1] The Society of the Plastics Industry Website, “A Few Facts on… Plastics and the Economy.” 02 Aug. 2010. <http://www.plasticsindustry.org/AboutPlastics/content.cfm>.

[2] Chen, Z., and Turng, L., 2005, "A Review of Current Developments in Process and Quality Control for Injection Molding," Advances in Polymer Technology, **24**(3) pp. 165-182.

[3] Kazmer, D., Rowland, J., and Sherbelis, G., 1997, "Foundations of Intelligent Process Control for Injection Molding," Journal of Injection Molding Technology, **1**(1) pp. 44-56.

[4] PLASTICSTECH. “Injection Molding Machine & Tooling.” 23 Aug. 2010. < http://www.plasticstech.info/equipment/injection-molding-machine/>.

[5] FIMMTECH Inc. “Screw and Check Ring….,” 2007. 3 Aug. 2010. < http://www.fimmtech.com/mold5.htm>.

[6] Beaumont, J., 2004, "Runner and Gating Design handbook: Tools for Successful Injection Molding," Hanser Gardner Publications, Cincinnati.

[7] Beaumont, J., Nagel, R., and Sherman, R., 2002, "Successful Injection Molding," Hanser Gardner Publications, Inc., Cincinnati.

[8] “Plastics Injection Molding Machine.” 9 July 2006. 23 Aug. 2010. <http://rookieelite.spaces.live.com/blog/cns!3701B849D212CC3!151.entry>.

[9] Kenplas Industry Limited, 2010, “Plastics Molds.” 23 Aug. 2010. <http://www.kenplas.com/mold/injectionmold/moldtype.aspx>.

[10] Van Stappen, M., Stals, L. M., Kerkhofs, M., 1995, "State of the Art for the Industrial use of Ceramic PVD Coatings," Surface and Coatings Technology, **74-75**(Part 2) pp. 629-633.

[11] Paller, G., Matthes, B., Herr, W., 1991, "Tribological Properties of r.f.-Sputtered Titanium-Based Hard Coatings and their Behaviour Under Plastics-Processing Conditions," Materials Science and Engineering: A, **140**pp. 647-654.

[12] Mennig, G., and Peter Volz, D., 1980, "Methods of Investigating Wear Caused in Plastics Processing," Kunststoffe - German Plastics, **70**(7) pp. 6-8.

[13] Koelsch, 1998, "Coatings Put Mold Wear on Hold," Molding Sytems, pp. 14-22.

[14] Volz, P., 1979, "WEAR AND TEAR IN PLASTICS TECHNOLOGY," Kunststoffe - German Plastics, **69**(11) pp. 2-9.

[15] Schlesinger, M., 2002, "Electroplating in Electrochemisty Encyclopedia," **2011**. <http://electrochem.cwru.edu/encycl/>

[16] Lou, H., and Huang, Y., 2006, "Electroplating in Encyclopedia of Chemical Processing,".

[17] Kanani, N., 2004, "Electroplating: Basic Principles, Processes and Practice," Elsevier Ltd.,.

[18] Sabharwal, S., Palit, S., Tokas, R. B., 2008, "Electroless Deposition, Post Annealing and Characterization of Nickel Films on Silicon," Bulletin of Materials Science, **31**(5) pp. 729-736.

[19] Dennis, J., and Such, T., 1993, "Nickel and Chromium Plating," Woodhead Publishing Ltd.,.

[20] Cunha, L., Moura, C., and Vaz, F., 2003, "Functional coatings - a look into the state of the art of hard and decorative coatings," Achievments in Mechanical & Materials Engineering, Anonymous pp. 171-174.

[21] Montgomery, S., Kennedy, D., and O'Dowd, N., 2010, "PVD and CVD Coatings for the Metal Forming Industry," Anonymous .

[22] Pochet, L. F., Howard, P., and Safaie, S., 1997, "CVD Coatings: From Cutting Tools to Aerospace Applications and its Future Potential," Surface and Coatings Technology, **94-95**pp. 70-75.

[23] Grainger, S., and Blunt, J., 1998, "Engineering Coatings: Design and Application," Woodhead Publishing Ltd., Cambridge,.

[24] Sproul, W. D., 1996, "Physical Vapor Deposition Tool Coatings," Surface and Coatings Technology, **81**(1) pp. 1-7

[25] Navinšek, B., Panjan, P., and Milošev, I., 1999, "PVD Coatings as an Environmentally Clean Alternative to Electroplating and Electroless Processes," Surface and Coatings Technology, **116-119**pp. 476-487.

[26] Anonymous 2009, "PVD Technology: A Tutorial," Coating Material News, **19**(3) pp. 1-3.

[27] Rauscher, H., Perucca, M., and Buyle, G., 2010, "Plasma Technology for Hyperfunctional Surfaces: Food, Biomedical, and Textile Applications," Wiley-VCH,.

[28] Groves, J., 1998, "Directed Vapor Deposition," Ph.D Dissertation, University of Virginia.

[29] Eden, T., "Cathodic Arc Deposition," **2011**(2/17) . <http://www.arl.psu.edu/capabilities/mm_mp_ct_cad.html>.

[30] Takikawa, H., Izumi, K., Miyano, R., 2003, "DLC Thin Film Preparation by Cathodic Arc Deposition with a Super Droplet-Free System," Surface and Coatings Technology, **163-164**pp. 368-373.

[31] Lugscheider, E., Barimani, C., Wolff, C., 1996, "Comparison of the Structure of PVD-Thin Films Deposited with Different Deposition Energies," Surface and Coatings Technology, **86-87**(Part 1) pp. 177-183.

[32] Takikawa, H., and Tanoue, H., 2007, "Review of Cathodic Arc Deposition for Preparing Droplet-Free Thin Films," Plasma Science, IEEE Transactions on, **35**(4) pp. 992-999.

[33] Anonymous "MEMS Thin Film Deposition Processes," **2010** (10/13). <http://www.memsnet.org/mems/processes/deposition.html>.

[34] Anonymous 2004, "Vacuum Deposition Processes," **2011**(1/17) pp. 10. <www.kolser.com>.

[35] Rodríguez, R. J., García, J. A., Medrano, A., 2002, "Tribological Behaviour of Hard Coatings Deposited by Arc-Evaporation PVD," Vacuum, **67**(3-4) pp. 559-566.

[36] Su, Y. L., Yao, S. H., Leu, Z. L., 1997, "Comparison of Tribological Behavior of Three films—TiN, TiCN and CrN—grown by Physical Vapor Deposition," Wear, **213**(1-2) pp. 165-174.

[37] Reiter, A. E., Brunner, B., Ante, M., 2006, "Investigation of several PVD Coatings for Blind Hole Tapping in Austenitic Stainless Steel," Surface and Coatings Technology, **200**(18-19) pp. 5532-5541.

[38] Polcar, T., Kubart, T., Novák, R., 2005, "Comparison of Tribological Behaviour of TiN, TiCN and CrN at Elevated Temperatures," Surface and Coatings Technology, **193**(1-3) pp. 192-199.

[39] Han, J. G., Yoon, J. S., Kim, H. J., 1996, "High Temperature Wear Resistance of (TiAl)N Films Synthesized by Cathodic Arc Plasma Deposition," Surface and Coatings Technology, **86-87**(Part 1) pp. 82-87.

[40] PalDey, S., and Deevi, S. C., 2003, "Single Layer and Multilayer Wear Resistant Coatings of (Ti,Al)N: A Review," Materials Science and Engineering A, **342**(1-2) pp. 58-79.

[41]Diebel, J R. 2001 "Evaluation of Four Commercially Produced Surface Treatments." Journal of Materials Engineering and Performance 10(3) pp. 263-269.

[42]Heinze, M., 1998"Wear Resistance of Hard Coatings in Plastics Processing." Surface & Coatings Technology, 105(1) pp. 38-44.

[43] Corman, N., Myers, M., and Copper, C. 2003, “Friction Behavior of Press-Fit Applications: Test Apparatus and Methodology.” Proceedings of the 49th IEEE Holm Conference on Electrical Contacts.

[44] Degarmo, E.P., Black, J.T., and Kohser, R.A., 2003, "Materials and Processes in Manufacturing," Wiley, pp. 223.

[45] Enos, David G., Scribner, Louie L.1997, ”The Potentiodynamic Polarization Scan,” Solartron Instruments, Issue 2(0) pp.1-19.

Vita

Tyler Skiba, born to Brenda Goughler and Kevin Skiba, grew up in the rural town of Clarion, PA. He received his Bachelors of Science Degree in Plastics Engineering Technology from the Pennsylvania State University in 2008. He plans to pursue a Ph.D. in Mechanical Engineering and Mechanics at Lehigh University after completion of his Masters of Science degree in the same field.